

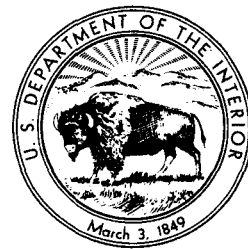
# Short Papers in the Geological Sciences

## Geological Survey Research 1960

---

GEOLOGICAL SURVEY PROFESSIONAL PAPER 400-B

*Scientific notes and summaries of investigations  
prepared by members of the Geologic Division in  
the fields of geology and allied sciences*



---

UNITED STATES GOVERNMENT PRINTING OFFICE, WASHINGTON : 1960

**UNITED STATES DEPARTMENT OF THE INTERIOR**

**FRED A. SEATON, *Secretary***

**GEOLOGICAL SURVEY**

**Thomas B. Nolan, *Director***

---

For sale by the Superintendent of Documents, U.S. Government Printing Office  
Washington 25, D.C. - Price \$4.25 (paper cover)

# CONTENTS

**Foreword** (see chapter A)

**Preface** (see chapter A)

## **Geology of metalliferous deposits**

	Page
1. An hypothesis for origin of ore-forming fluid, by J. Hoover Mackin and Earl Ingerson.....	B1
2. Varieties of supergene zinc deposits in the United States, by A. V. Heyl, Jr., and C. N. Bozion.....	2
3. Lithofacies of the Copper Harbor conglomerate, northern Michigan, by Walter S. White and James C. Wright.....	5
4. Relation of the Colorado mineral belt to Precambrian structure, by Ogden Tweto and P. K. Sims.....	8
5. Pre-ore age of faults at Leadville, Colorado, by Ogden Tweto.....	10
6. Pre-ore propylitization, Silverton caldera, Colorado, by Wilbur S. Burbank.....	12
7. Ring-fractured bodies in the Silverton caldera, Colorado, by Robert G. Luedke and Wilbur S. Burbank.....	13
8. Relation of mineralization to caldera subsidence in the Creede district, San Juan Mountains, Colorado, by Thomas A. Steven and James C. Ratté.....	14
9. Alinement of mining districts in north-central Nevada, by Ralph J. Roberts.....	17
10. Mineral assemblage of a pyrometasomatic deposit near Tonopah, Nevada, by R. A. Gulbrandsen and D. G. Gielow.....	20
11. Sedimentary iron-formation in the Devonian Martin formation, Christmas quadrangle, Arizona, by Ronald Willden.....	21
12. Early Tertiary volcanic geology of an area north and west of Butte, Montana, by Harry W. Smedes.....	23
13. Tectonic setting of the Coeur d'Alene district, Idaho, by Robert E. Wallace, Allan B. Griggs, Arthur B. Campbell, and S. Warren Hobbs.....	25
14. Bleaching in the Coeur d'Alene district, Idaho, by P. L. Weis.....	27
15. Origin of the Main period veins, Coeur d'Alene district, Idaho, by Verne C. Fryklund, Jr.....	29
16. Geologic and economic significance of some geochemical results obtained from stream sediment samples near Nome, Alaska, by C. L. Hummel and Robert M. Chapman.....	30
17. Structural geology and structural control of mineral deposits near Nome, Alaska, by C. L. Hummel.....	33
18. Structural control in five quicksilver deposits in southwestern Alaska, by C. L. Sainsbury and E. M. MacKevett, Jr.....	35
19. Three areas of possible mineral resource potential in southeastern Alaska, by Henry C. Berg.....	38
20. A study of rhenium and molybdenum in uranium ore from the Runge mine, Fall River County, South Dakota, by means of a spectrographic and concentration method, by A. T. Myers, J. C. Hamilton, and V. R. Wilmarth.....	39
21. A study of uranium migration in sandstone-type ore deposits, by John N. Rosholt, Jr.....	41
22. Distribution and lithologic characteristics of sandstone beds that contain deposits of copper, vanadium, and uranium, by R. P. Fischer and J. H. Stewart.....	42
23. Lead-isotope age studies in Carbon County, Pennsylvania, by T. W. Stern, L. R. Stieff, Harry Klemic, and M. H. Delevaux.....	45
24. Uranium at Palangana salt dome, Duval County, Texas, by Alice D. Weeks and D. Hoyer Eargle.....	48
25. Paragenesis of uranium ores in Todilto limestone near Grants, New Mexico, by Alfred H. Truesdell and Alice D. Weeks.....	52
26. Pitchblende identified in a sandstone-type uranium deposit in the central part of the Ambrosia Lake district, New Mexico, by Harry C. Granger.....	54
27. Metamorphic grade and the abundance of ThO <sub>2</sub> in monazite, by William C. Overstreet.....	55

## **Geology of light metals and industrial minerals**

28. Concentrations of "ilmenite" in the Miocene and post-Miocene formations near Trenton, New Jersey, by James P. Owens, James P. Minard, Donald R. Wiesnet, and Frank J. Markewicz.....	57
29. Bloating clay in Miocene strata of Maryland, New Jersey, and Virginia, by Maxwell M. Knechtel and John W. Hosterman.....	59
30. Significance of unusual mineral occurrence at Hicks Dome, Hardin County, Illinois, by Robert D. Trace.....	63
31. Phosphate and associated resources in Permian rocks of southwestern Montana, by Roger W. Swanson.....	65
32. Hugo pegmatite, Keystone, South Dakota, by J. J. Norton.....	67
33. A new beryllium deposit at the Mount Wheeler mine, White Pine County, Nevada, by H. K. Stager.....	70
34. Pre-mineralization faulting in the Lake George area, Park County, Colorado, by C. C. Hawley, W. N. Sharp, and W. R. Griffiths.....	71
35. Bertrandite-bearing greisen, a new beryllium ore, in the Lake George district, Colorado, by W. N. Sharp and C. C. Hawley.....	73

## **Geology of fuels**

36. Regional aeromagnetic surveys of possible petroleum provinces in Alaska, by Isidore Zietz, G. E. Andreasen, and Arthur Grantz.....	75
--	----

**Geology of fuels—Continued**

37. Studies of helium and associated natural gases, by Arthur P. Pierce.....	B77
38. The interpretation of Tertiary swamp types in brown coal, by Gerhard O. W. Kremp and Anton J. Kovar.....	79
39. Coal reserves of the United States, January 1, 1960, by Paul Averitt.....	81
40. Relation of the minor element content of coal to possible source rocks, by Peter Zubovic, Taisia Stadnichenko, and Nola B. Sheffey.....	82
41. The association of some minor elements with organic and inorganic phases of coal, by Peter Zubovic, Taisia Stadnichenko, and Nola B. Sheffey.....	84
42. Comparative abundance of the minor elements in coals from different parts of the United States, by Peter Zubovic, Taisia Stadnichenko, and Nola B. Sheffey.....	87

**Exploration and mapping techniques**

43. Field application of ion-exchange resins in hydrogeochemical prospecting, by F. C. Canney and D. B. Hawkins.....	89
44. Geochemical prospecting for beryllium, by Wallace R. Griffiths and U. Oda.....	90
45. Variations in base-metal contents of monzonitic intrusives, by Wallace R. Griffiths and H. M. Nakagawa.....	93
46. Geochemistry of sandstones and related vegetation in the Yellow Cat area of the Thompson district, Grand County, Utah, by Helen L. Cannon.....	96
47. Geochemical prospecting for copper in the Rocky Range, Beaver County, Utah, by R. L. Erickson and A. P. Marranzino.....	98
48. Soil and plant sampling at the Mahoney Creek lead-zinc deposit, Revillagigedo Island, southeastern Alaska, by Hansford T. Shacklette.....	102
49. Geochemical exploration in Alaska, by Robert M. Chapman and Hansford T. Shacklette.....	104
50. Thermoluminescence and porosity of host rocks at the Eagle mine, Gilman, Colorado, by Carl H. Roach.....	107
51. Usefulness of the emanation method in geologic exploration, by Allan B. Tanner.....	111
52. Polar charts for evaluating magnetic anomalies of three-dimensional bodies, by Roland G. Henderson.....	112
53. Magnetic evidence for the attitude of a buried magnetic mass, by Gordon E. Andreassen and Isidore Zietz.....	114
54. Use of aeromagnetic data to determine geologic structure in northern Maine, by John W. Allingham.....	117
55. Correlation of aeroradioactivity data and areal geology, by Robert B. Guillou and Robert G. Schmidt.....	119
56. Mapping conductive strata by electromagnetic methods, by F. C. Frischknecht and E. B. Ekren.....	121
57. Electrical properties of sulfide ores in igneous and metamorphic rocks near East Union, Maine, by L. A. Anderson.....	125
58. Electrical properties of zinc-bearing rocks in Jefferson County, Tennessee, by G. V. Keller.....	128
59. Terrain corrections using an electronic digital computer, by Martin F. Kane.....	132
60. Application of gravity surveys to chromite exploration in Camagüey Province, Cuba, by W. E. Davis, W. H. Jackson, and D. H. Richter.....	133
61. Spectral reflectance measurements as a basis for film-filter selection for photographic differentiation of rock units, by William A. Fischer.....	136
62. Technique for viewing moon photographs stereoscopically, by Robert J. Hackman.....	139

**Geology applied to engineering and public health**

63. Some thermal effects of a roadway on permafrost, by Gordon W. Greene, Arthur H. Lachenbruch, and Max C. Brewer.....	141
64. Tentative correlation between coal bumps and orientation of mine workings in the Sunnyside No. 1 mine, Utah, by Frank W. Osterwald and Harold Brodsky.....	144
65. Review of the causes of subsidence, by Alice S. Allen.....	147
66. A sample of California Coast Range landslides, by M. G. Bonilla.....	149
67. Alteration of tuffs by Rainier underground nuclear explosion, Nevada Test Site, Nye County, Nevada, by V. R. Wilmarth, Theodore Botinelly, and R. E. Wilcox.....	149
68. Distribution of gamma radioactivity, radioactive glass, and temperature surrounding the site of the Rainier underground nuclear explosion, Nevada, by C. M. Bunker, W. H. Diment, and V. R. Wilmarth.....	151
69. Gravity and seismic exploration at the Nevada Test Site, by W. H. Diment, D. L. Healey, and J. C. Roller.....	156
70. Maximum ground accelerations caused by nuclear explosions at distances of 5 to 300 kilometers, by W. H. Diment, S. W. Stewart, and J. C. Roller.....	160
71. Cation exchange with vermiculite, by Marian M. Schnepfe.....	161
72. Preparation of stable gelatin-montmorillonite clay extrusions, by Irving May.....	163
73. Variation of aluminum, sodium, and manganese in common rocks, by James R. Burns.....	164

**Geology of Eastern United States**

74. Pre-Silurian stratigraphy in the Shin Pond and Stacyville quadrangles, Maine, by Robert B. Neuman.....	166
75. A comparison of two estimates of the thorium content of the Conway granite, New Hampshire, by F. J. Flanagan, W. L. Smith, and A. M. Sherwood.....	168
76. Possible use of boron, chromium, and nickel content in correlating Triassic igneous rocks in Connecticut, by P. M. Hanshaw and P. R. Barnett.....	170
77. Coral faunas in the Onondaga limestone of New York, by William A. Oliver, Jr.....	172
78. Geophysical and geological interpretation of a Triassic structure in eastern Pennsylvania, by Isidore Zietz and Carlyle Gray.....	174
79. Preliminary interpretation of aeromagnetic data in the Allentown quadrangle, Pennsylvania, by Randolph W. Bromery.....	178

**Geology of Eastern United States—Continued**

	Page
80. Taconic and post-Taconic folds in eastern Pennsylvania and western New Jersey, by Avery A. Drake, Jr., Robert E. Davis, and Donald C. Alvord.....	B180
81. Late Paleozoic orogeny in eastern Pennsylvania consists of five progressive stages, by Harold H. Arndt and Gordon H. Wood, Jr.....	182
82. Differential subsidence of the southern part of the New Jersey Coastal Plain since early Late Cretaceous time, by James P. Minard and James P. Owens.....	184
83. Drowned valley topography at beginning of Middle Ordovician deposition in southwest Virginia and northern Tennessee, by Leonard D. Harris.....	186
84. A synthesis of geologic work in the Concord area, North Carolina, by Henry Bell III.....	189
85. Aeromagnetic and aeroradioactivity survey of the Concord quadrangle, North Carolina, by Robert W. Johnson, Jr., and Robert G. Bates.....	192
86. A major topographic lineament in western North Carolina and its possible structural significance, by John C. Reed, Jr., and Bruce H. Bryant.....	195
87. Geologic relations inferred from the provisional geologic map of the crystalline rocks of South Carolina, by William C. Overstreet and Henry Bell III.....	197
88. Determination of structure in the Appalachian basin by geophysical methods, by Elizabeth R. King and Isidore Zietz.....	199
89. Residual origin of the "Pleistocene" sand mantle in central Florida Uplands and its bearing on marine terraces and Cenozoic uplift, by Z. S. Altschuler and E. J. Young.....	202
90. A tropical sea in central Georgia in late Oligocene time, by Esther R. Applin.....	207
91. Significance of changes in thickness and lithofacies of the Sunniland limestone, Collier County, Florida, by Paul L. Applin.....	209
92. Significance of loess deposits along the Ohio River valley, by Louis L. Ray.....	211
93. Magnetization of volcanic rocks in the Lake Superior geosyncline, by Gordon D. Bath.....	212

**Geology of Western Conterminous United States**

94. Measurements of electrical properties of rocks in southeast Missouri, by C. J. Zablocki.....	214
95. Interpretation of aeromagnetic anomalies in southeast Missouri, by John W. Allingham.....	216
96. Some aftershocks of the Hebgen Lake, Montana, earthquake of August 1959, by S. W. Stewart, R. B. Hofmann, and W. H. Diment.....	219
97. Depth soundings in Hebgen Lake, Montana, after the earthquake of August 17, 1959, by W. H. Jackson.....	221
98. Correlation of alpine and continental glacial deposits of Glacier National Park and adjacent high plains, Montana, by Gerald M. Richmond.....	223
99. The late Quaternary age of obsidian-rhyolite flows in the western part of Yellowstone National Park, Wyoming, by Gerald M. Richmond and Warren Hamilton.....	224
100. Distribution of corals in the Madison group and correlative strata in Montana, western Wyoming, and northeastern Utah, by William J. Sando.....	225
101. Middle Tertiary unconformity in southwestern Montana, by G. D. Robinson.....	227
102. Configuration of the 10N pluton, Three Forks, Montana, by Isidore Zietz.....	229
103. Metamorphism and thrust faulting in the Riggins quadrangle, Idaho, by Warren Hamilton.....	230
104. Diverse interfingering Carboniferous strata in the Mackay quadrangle, Idaho, by Clyde P. Ross.....	232
105. Progressive growth of anticlines during Late Cretaceous and Paleocene time in central Wyoming, by William R. Keefer.....	233
106. The "break-away" point of Heart Mountain detachment fault in northwestern Wyoming, by William G. Pierce.....	236
107. Regional geologic interpretation of aeromagnetic and gravity data for the Rowe-Mora area, New Mexico, by Gordon E. Andreasen, Martin F. Kane, and Isidore Zietz.....	238
108. Southwestern edge of late Paleozoic landmass in New Mexico, by George O. Bachman.....	239
109. New information on the areal extent of some Upper Cretaceous units in northwestern New Mexico, by Carle H. Dane.....	241
110. Lithologic subdivisions of the Redwall limestone in northern Arizona—their paleogeographic and economic significance, by Edwin D. McKee.....	243
111. Pliocene sediments near Salida, Chaffee County, Colorado, by Ralph E. Van Alstine, and G. Edward Lewis.....	245
112. Some Late Cretaceous strand lines in northwestern Colorado and northeastern Utah, by A. D. Zapp and W. A. Cobban.....	246
113. Stratigraphy and structure of the Precambrian metamorphic rocks in the Tenmile Range, Colorado, by A. H. Koschmann and M. H. Bergendahl.....	249
114. Salt anticlines and deep-seated structures in the Paradox basin, Colorado and Utah, by H. R. Joesting and J. E. Case.....	252
115. Distribution and physiographic significance of the Browns Park formation, Flaming Gorge and Red Canyon areas, Utah-Colorado, by Wallace R. Hansen, Douglas M. Kinney, and John M. Good.....	257
116. Probable late Miocene age of the North Park formation in the North Park area, Colorado, by W. J. Hail, Jr., and G. E. Lewis.....	259
117. Paleocene and Eocene age of the Coalmont formation, North Park, Colorado, by W. J. Hail, Jr., and Estella B. Leopold.....	260
118. Pre-Cutler unconformities and early growth of the Paradox Valley and Gypsum Valley salt anticlines, Colorado, by D. P. Elston and E. R. Landis.....	261
119. Structure of Paleozoic and early Mesozoic rocks in the northern part of the Shoshone Range, Nevada, by James Gilluly.....	265

**Geology of Western Conterminous United States—Continued**

	<b>Page</b>
120. Structural features of pyroclastic rocks of the Oak Spring formation at the Nevada Test Site, Nye County, Nevada, as related to the topography of the underlying surface, by F. N. Houser and F. G. Poole.....	B266
121. Origin of the Amargosa thrust fault, Death Valley area, California: a result of strike-slip faulting in Tertiary time, by Harald Drewes.....	268
122. Bedding-plane thrust faults east of Connors Pass, Schell Creek Range, eastern Nevada, by Harald Drewes.....	270
123. Possible interbasin circulation of ground water in the southern part of the Great Basin, by Charles B. Hunt and T. W. Robinson.....	273
124. Observations of current tilting of the earth's surface in the Death Valley, California, area, by Gordon W. Greene and Charles B. Hunt.....	275
125. Pliocene(?) sediments of salt water origin near Blythe, southeastern California, by Warren Hamilton.....	276
126. Structure in the Big Maria Mountains of southeastern California, by Warren Hamilton.....	277
127. Fossil Foraminifera from the southeastern California deserts, by Patsy Beckstead Smith.....	278
128. Time of the last displacement on the middle part of the Garlock fault, California, by George I. Smith.....	280
129. Welded tuffs in the northern Toiyabe Range, Nevada, by Harold Masursky.....	281
130. Regional gravity survey of part of the Basin and Range province, by Don R. Mabey.....	283
131. Mesozoic age of roof pendants in west-central Nevada, by James G. Moore.....	285
132. Identification of the Dunderberg shale of Late Cambrian age in the eastern Great Basin, by Allison R. Palmer.....	289
133. Intrusive rocks of Permian and Triassic age in the Humboldt Range, Nevada, by Robert E. Wallace, Donald B. Tatlock, and Norman J. Silberling.....	291
134. Regional significance of some lacustrine limestones in Lincoln County, Nevada, recently dated as Miocene, by Charles M. Tschanz.....	293
135. Evidence in the Snake River Plain, Idaho, of a catastrophic flood from Pleistocene Lake Bonneville, by Harold E. Malde.....	295
136. Alkaline lava flow, with fluidity of basalt, in the Snake River Plain, Idaho, by Howard A. Powers.....	297
137. A distinctive chemical characteristic of Snake River basalts of Idaho, by Howard A. Powers.....	298
138. Age and correlation of some unnamed volcanic rocks in south-central Oregon, by George W. Walker.....	298
139. Upper Triassic graywackes and associated rocks in the Aldrich Mountains, Oregon, by T. P. Thayer and C. E. Brown.....	300
140. The John Day formation in the Monument quadrangle, Oregon, by Richard V. Fisher and Ray E. Wilcox.....	302
141. The Republic graben, a major structure in northeastern Washington, by Mortimer H. Staatz.....	304
142. Suggested source of Miocene volcanic detritus flanking the central Cascade Range, Washington, by Leonard M. Gard, Jr.....	306
143. Late Recent age of Mount St. Helens volcano, Washington, by D. R. Mullineaux and D. R. Crandell.....	307
144. Cenozoic volcanism in the Oregon Cascades, by Dallas L. Peck.....	308
145. Rodingite from Angel Island, San Francisco Bay, California, by Julius Schlocker.....	311
146. Gravity anomalies at Mount Whitney, California, by H. W. Oliver.....	313
147. Relations between Abrams mica schist and Salmon hornblende schist in Weaverville quadrangle, California, by William P. Irwin.....	315
148. Evidence for two stages of deformation in the western Sierra Nevada metamorphic belt, California, by Lorin D. Clark.....	316
149. Early Cretaceous fossils in submarine slump deposits of Late Cretaceous age, northern Sacramento Valley, California, by Robert D. Brown, Jr., and Ernest I. Rich.....	318
150. Gravity variations and the geology of the Los Angeles Basin of California, by Thane H. McCulloh.....	320
151. Previously unreported Pliocene Mollusca from the southeastern Los Angeles Basin, by J. G. Vedder.....	326

**Geology of Alaska**

152. Cenozoic sediments beneath the central Yukon Flats, Alaska, by John R. Williams.....	329
153. The Cook Inlet, Alaska, glacial record and Quaternary classification, by Thor N. V. Karlstrom.....	330
154. Surficial deposits of Alaska, by Thor N. V. Karlstrom.....	333
155. Recent eustatic sea-level fluctuations recorded by Arctic beach ridges, by G. W. Moore.....	335
156. Generalized stratigraphic section of the Lisburne group in the Point Hope A-2 quadrangle, northwestern Alaska, by Russell H. Campbell.....	337
157. A marine fauna probably of late Pliocene age near Kivalina, Alaska, by D. M. Hopkins and F. S. MacNeil.....	339
158. Possible significance of broad magnetic highs over belts of moderately deformed sedimentary rocks in Alaska and California, by Arthur Grantz and Isidore Zietz.....	342
159. Stratigraphy and age of the Matanuska formation, south-central Alaska, by Arthur Grantz and David L. Jones.....	347
160. Radiocarbon dates relating to the Gubik formation, northern Alaska, by Henry W. Coulter, Keith M. Hussey, and John B. O'Sullivan.....	350
161. Metasedimentary rocks in the south-central Brooks Range, Alaska, by William P. Brosgé.....	351
162. Slump structures in Pleistocene lake sediments, Copper River Basin, Alaska, by Donald R. Nichols.....	353

**Geology of Hawaii, Puerto Rico, Pacific Islands, and Antarctica**

163. Pahala ash—an unusual deposit from Kilauea Volcano, Hawaii, by George D. Fraser.....	354
164. Sinkholes and towers in the karst area of north-central Puerto Rico, by Watson H. Monroe.....	356
165. Structural control of hydrothermal alteration in some volcanic rocks in Puerto Rico, by M. H. Pease, Jr.....	360

**Geology of Hawaii, Puerto Rico, Pacific Islands, and Antarctica—Continued**

	<b>Page</b>
166. Successive thrust and transcurrent faulting during the early Tertiary in south-central Puerto Rico, by Lynn Glover III and Peter H. Mattson.....	B363
167. Compressional graben and horst structures in east-central Puerto Rico, by R. P. Briggs and M. H. Pease, Jr.....	365
168. Stratigraphic distribution of detrital quartz in pre-Oligocene rocks in south-central Puerto Rico, by Peter H. Mattson and Lynn Glover III.....	367
169. Occurrences of bauxitic clay in the karst area of north-central Puerto Rico, by Fred A. Hildebrand.....	368
170. The stratigraphy of Ishigaki-shima, Ryūkyū-rettō, by Helen L. Foster.....	372
171. Fossil mammals from Ishigaki-shima, Ryūkyū-rettō, by Frank C. Whitmore, Jr.....	372
172. Distribution of molluscan faunas in the Pacific islands during the Cenozoic, by Harry S. Ladd.....	374
173. Geology of Taylor Glacier-Taylor Dry Valley region, South Victoria Land, Antarctica, by Warren Hamilton and Phillip T. Hayes.....	376
174. New interpretation of Antarctic tectonics, by Warren Hamilton.....	379

**Paleontology, geomorphology, and plant ecology**

175. Gigantopteridaceae in Permian floras of the Southwestern United States, by Sergius H. Mamay.....	380
176. Upper Paleozoic floral zones of the United States, by Charles B. Read and Sergius H. Mamay.....	381
177. Fossil spoor and their environmental significance in Morrow and Atoka series, Pennsylvanian, Washington County, Arkansas, by Lloyd G. Henbest.....	383
178. Paleontologic significance of shell composition and diagenesis of certain late Paleozoic sedentary Foraminifera, by Lloyd G. Henbest.....	386
179. Relation of solution features to chemical character of water in the Shenandoah Valley, Virginia, by John T. Hack....	387
180. Some examples of geologic factors in plant distribution, by Charles B. Hunt.....	390

**Geophysics**

181. Rate of melting at the bottom of floating ice, by David F. Barnes and John E. Hobbie.....	392
182. Internal friction and rigidity modulus of Solenhofen limestone over a wide frequency range, by L. Peselnick and W. F. Outerbridge.....	395
183. Physical properties of tufts of the Oak Spring formation, Nevada, by George V. Keller.....	396
184. Magnetic susceptibility and thermoluminescence of calcite, by Frank E. Senftle, Arthur Thorpe, and Francis J. Flanagan.....	401
185. Salt features that simulate ground patterns formed in cold climates, by Charles B. Hunt and A. L. Washburn.....	403
186. Thermal contraction cracks and ice wedges in permafrost, by Arthur H. Lachenbruch.....	404
187. Contraction-crack polygons, by Arthur H. Lachenbruch.....	406
188. Curvature of normal faults in the Basin and Range province of the Western United States, by James G. Moore.....	409
189. Volcanism in eastern California—a proposed eruption mechanism, by L. C. Pakiser.....	411
190. Some relationships between geology and effects of underground nuclear explosions at Nevada Test Site, Nye County, Nevada, by F. A. McKeown and D. D. Dickey.....	415
191. Structural effects of Rainier, Logan, and Blanca underground nuclear explosions, Nevada Test Site, Nye County, Nevada, by V. R. Wilmarth and F. A. McKeown.....	418
192. Brecciation and mixing of rock by strong shock, by Eugene M. Shoemaker.....	423
193. Paleomagnetism, polar wandering, and continental drift, by Richard R. Doell and Allan V. Cox.....	426
194. Preparation of an accurate equal-area projection, by Richard R. Doell and Robert E. Altenhofen.....	427

**Mineralogy, geochemistry, and petrology**

195. Crystal habit of frondelite, Sapucaia pegmatite mine, Minas Gerais, Brazil, by Marie Louise Lindberg.....	429
196. Some characteristics of glauconite from the coastal plain formations of New Jersey, by James P. Owens and James P. Minard.....	430
197. X-ray determinative curve for natural olivine of composition $Fe_{80-90}$ , by Everett D. Jackson.....	432
198. Acidic properties of Fithian "illite", by Dorothy Carroll and Alfred M. Pommer.....	434
199. Carbon dioxide and alumina in the potentiometric titration of H-montmorillonite, by Dorothy Carroll.....	436
200. Changes in thermogravimetric curves of calcium sulfate dihydrate with variations in the heating rate, by Charles A. Kinser.....	438
201. Synthetic bayleyite, by Robert Meyrowitz and Marie Louise Lindberg.....	440
202. Synthetic hydrous boron micas, by Hans P. Eugster and Thomas L. Wright.....	441
203. Recent developments in the crystal chemistry of vanadium oxide minerals, by Howard T. Evans, Jr.....	443
204. Authigenic rhodochrosite spherules from Gardner Creek, Kentucky, by E. C. T. Chao and William E. Davies.....	446
205. Stratigraphic variations in mineralogy and chemical composition of the Pierre shale in South Dakota and adjacent parts of North Dakota, Nebraska, Wyoming, and Montana, by Harry A. Tourtelot, Leonard G. Schultz, and James R. Gill.....	447
206. Summary of chemical characteristics of some waters of deep origin, by Donald E. White.....	452
207. Geochemical investigation of molybdenum at Nevares Spring in Death Valley, California, by F. N. Ward, H. M. Nakagawa, and Charles B. Hunt.....	454
208. The Death Valley salt pan, a study of evaporites, by Charles B. Hunt.....	456

**Mineralogy, geochemistry, and petrology—Continued**

	Page
209. Early stages of evaporite deposition, by E-an Zen.....	B458
210. Spatial relations of fossils and bedded cherts in the Redwall limestone, Arizona, by E. D. McKee.....	461
211. Structurally localized metamorphism of manganese deposits in Aroostook County, Maine, by Louis Pavlides.....	463
212. Migration of elements during metamorphism in the northwest Adirondack Mountains, New York, by A. E. J. Engel and Celeste G. Engel.....	465
213. Chilled contacts and volcanic phenomena associated with the Cloudy Pass batholith, Washington, by Fred W. Cater, Jr.....	471
214. The role of impermeable rocks in controlling zeolitic alteration of tuff, by A. B. Gibbons, E. N. Hinrichs, and Theodore Botinelly.....	473

**Analytical and petrographic methods**

215. Determination of total iron in chromite and chrome ore, by Joseph I. Dinnin.....	476
216. Determination of zinc in basalts and other rocks, by L. F. Rader, W. C. Swadley, H. H. Lipp, and Claude Huffman, Jr.....	477
217. Comparison of three methods for the determination of total and organic carbon in geochemical studies, by I. C. Frost.....	480
218. The determination of lead in iron-bearing materials, by Jesse J. Warr and Frank Cuttitta.....	483
219. Determination of lead in pyrites, by Frank Cuttitta and Jesse J. Warr.....	485
220. Determination of lead in zircon with dithizone, by Frank Cuttitta and Jesse J. Warr.....	486
221. Preparation of lead iodide for mass spectrometry, by Frank Cuttitta and Jesse J. Warr.....	487
222. Determination of small quantities of oxygen adsorbed on anatase, by Frank Cuttitta.....	488
223. Preliminary tests of isotopic fractionation of copper adsorbed on quartz and sphalerite, by Frank Cuttitta, F. E. Senftle, and E. C. Walker.....	491
224. Water-soluble boron in sample containers, by Claude Huffman, Jr.....	493
225. Dilution-addition method for flame spectrophotometry, by F. S. Grimaldi.....	495
226. A spectrophotometric method for the determination of FeO in rocks, by Leonard Shapiro.....	496
227. Spectrochemical analysis using controlled atmospheres with a simple gas jet, by C. S. Annell and A. W. Helz.....	497
228. Combination of gravimetric and spectrographic methods in the analysis of silicates, by Rollin E. Stevens, Arthur A. Chodos, Raymond G. Havens, Elizabeth Godijn, and Sarah T. Neil.....	499
229. Sodium-sensitive glass electrodes in clay titrations, by Alfred M. Pommer.....	502
230. Precipitation of salts from solution by ethyl alcohol as an aid to the study of evaporites, by R. A. Gulbrandsen.....	504
231. A gamma-ray absorption method for the determination of uranium in ores, by Alfred F. Hoyte.....	504
232. Method of grinding cesium iodide crystals, by Prudencio Martinez.....	507
<b>Index</b> .....	509



16. GEOLOGIC AND ECONOMIC SIGNIFICANCE OF SOME GEOCHEMICAL RESULTS OBTAINED FROM STREAM SEDIMENT SAMPLES NEAR NOME, ALASKA

By C. L. HUMMEL and ROBERT M. CHAPMAN, Menlo Park, Calif., and Denver, Colo.

During recent areal geologic investigations, thirty samples of sediments were obtained from streams throughout a 500-square-mile area near Nome, Alaska. They were collected primarily to test the efficacy of this method of geochemical exploration in the part of the metamorphic terrane of the Seward Peninsula that is best known geologically. In general, the sediment samples contained meaningful quantities of a number of metals; anomalously high amounts of copper, zinc, bismuth, and molybdenum in samples collected from Thompson Creek in the Kigluaik Mountains located 30 miles north of Nome are of particular geologic and economic significance as indicators of metalliferous lodes in an area not formerly known to contain them.

The geochemical sediment samples were collected and processed according to procedures developed by the U.S. Geological Survey. The samples were selected to include mainly the finest and lightest stream sediments and some organic material, wherever it was present.

Although sediment sampling was designed as a field method for determining the heavy metal content of sediments by colorimetric techniques, all of the determinations reported here were made in a Survey laboratory as part of a continuing program to develop and improve geochemical exploration methods (Chapman and Shacklette, Art. 49). F. N. Ward was a constant source of advice and assistance.

The amounts of antimony, arsenic, bismuth, copper, lead, molybdenum, tungsten, and zinc were determined in all samples. Useable quantities were obtained of all metals except tungsten, whose level of detection (20 ppm) is still too high to be of value by this method in the Nome area.

All of the bedrock of the Nome area has been regionally metamorphosed; high-grade metamorphic rocks occur only in the Kigluaik Mountains while metamorphic rocks of considerably lower grade form the bedrock of the area between the Kigluaik Moun-

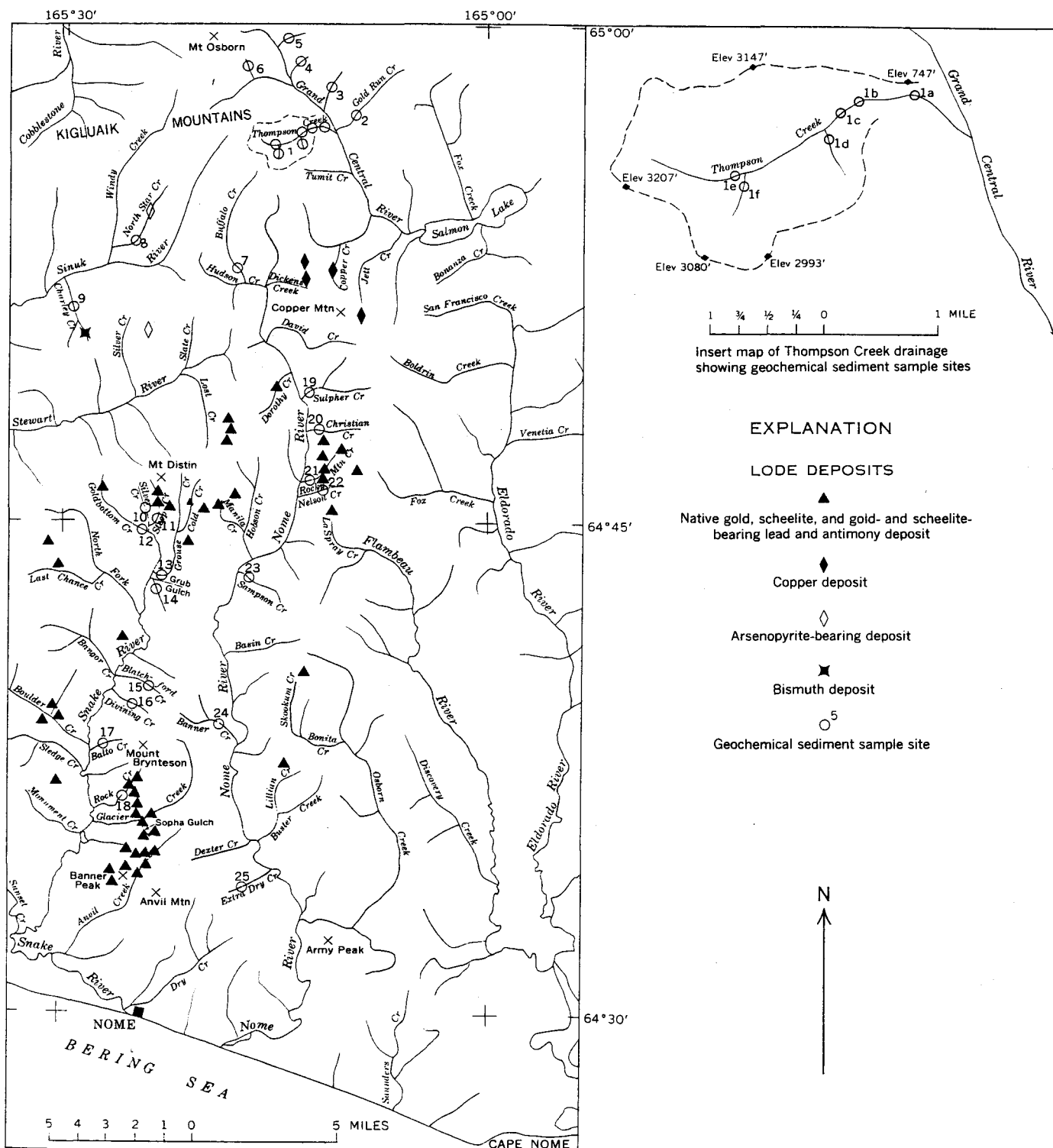


FIGURE 16.1.—Map showing location of lode deposits and geochemical sediment sample sites near Nome, Alaska.

tains and Bering Sea, in which the Nome goldfields lie (Moffit, 1913, p. 140). The bedrock of the goldfields is composed entirely of low grade schists and interbedded marble. Known lodes of the goldfields, of the type from which the gold of the alluvial and beach placers

of the goldfields was derived, are for the most part filling-type deposits in shattered quartz masses (fig. 16.1). Scheelite and native gold are the dominant non-gangue constituents in a few deposits but base metal sulfides predominate in most of them. Except

for a single deposit in which native bismuth and bismuthinite occur and several copper sulfide deposits, most of the lodes are composed of lead and antimony sulfides with minor amounts of scheelite and gold.

The Nome goldfields are bounded on the north by the Kigluaik Mountains. The bedrock of the mountains is composed entirely of very high grade metamorphic rocks into which have been intruded many relatively small sills and dikes of silicic and mafic igneous rocks and granite pegmatites. Although the igneous rocks are thought to be genetically related to the mineral deposits of the goldfields, the only direct evidence of hydrothermal mineralization in the Kigluaik Mountains consists of a single lode on North Star Creek in which arsenopyrite was the only metallic mineral which was recognized.

The results obtained from geochemical sediment samples collected in the Nome goldfields closely reflect the presence or absence, and the composition and proximity to sample sites, of the known lode deposits in the drainage basins of the streams from which the sediments were collected (table 16.1). As might have been expected, most of the samples from the goldfields contained greater quantities of antimony and arsenic. However, in specific cases, anomalously high amounts of other metals were obtained from samples collected from drainage basins where lodes containing those metals crop out, such as lead in sample 11 from Steep Creek and bismuth in sample 9 from Charley Creek.

In marked contrast with the results obtained from sediment samples from the Nome goldfields were those obtained from samples collected from streams in the Kigluaik Mountains. In the absence of known metaliferous lodes, no anomalous quantities of the metals determined could be expected. In general, none were obtained; samples 2 through 8, collected from widely separated localities throughout the part of the Kigluaik Mountains included in the area of this report, had consistently small amounts of all the metals determined and thus provided a basis for estimating the quantities of these metals in sediments derived from the high grade metamorphic rocks. The only exceptions to these general results were some obtained from sediment samples collected from Thompson Creek a western tributary of the Grand Central River. The first sample (1A) was collected by the authors in 1957; other samples of the series (1B-1E) were collected at the request of the authors by D. M. Hopkins in 1959 on the basis of the geochemical results obtained from sample 1A.

Samples from Thompson Creek contained more copper, zinc, molybdenum, and bismuth than those from any other part of the area. The resulting anomalies of

TABLE 16.1.—Content (in ppm) of several metals in sediment samples from streams near Nome, Alaska

[Analysts: W. L. Jones, H. H. Mehnert, H. M. Nakagawa, H. Neiman, L. E. Patten]

Locality	Sample	Pb	Cu	Zn	As	W	Mo	Bi	Sb
Thompson Creek	1A	<20	120	400	<10	<20	10	<5	2
	1B	25	150	600	<10	<20	8	35	1
	1C	25	100	400	10	<20	12	45	2
	1D	25	75	125	10	<20	4	10	1
	1E	25	75	225	<10	<20	4	50	1
	1F	25	100	225	<10	<20	12	10	2
Kigluaik Mountains	2	<20	30	80	<10	<20	10	<5	2
	3	<20	30	100	<10	<20	4	5	2
	4	<20	30	100	10	<20	2	<5	2
	5	<20	30	100	<10	<20	4	<5	1
	6	<20	30	100	<10	<20	2	<5	2
	7	<20	30	100	30	<20	6	10	1
	8	<20	30	100	<10	<20	10	<5	2
Nome goldfields	9	<20	30	80	300	<20	2	20	6
	10	<25	20	50	150	<20	<4	<5	10
	11	50	30	75	60	<20	<4	<5	30
	12	<25	20	100	150	<20	<4	5	8
	13	<25	30	100	150	<20	<4	<5	10
	14	<25	30	125	60	<20	<4	<5	8
	15	<25	20	75	40	<20	<4	5	4
	16	<25	20	75	30	<20	<4	<5	4
	17	<25	20	75	80	<20	<4	<5	6
	18	<25	20	75	300	<20	<4	5	6
	19	<25	20	75	20	<20	<4	<5	4
	20	<25	30	75	60	<20	<4	<5	6
	21	25	30	100	150	<20	<4	<5	10
	22	<25	30	100	150	<20	<4	<5	4
	23	<25	30	75	80	<20	<4	<5	10
	24	<25	20	75	20	<20	<4	<5	4
	25	<20	30	100	10	<20	2	<5	2

these metals were two to six times greater than the background content estimated from samples 2 to 8. Because no lode material has been found in the Thompson Creek drainage, the difference between the results obtained from there and those obtained from drainages with known lode deposits is significant. For example, the Thompson Creek samples contained more bismuth than samples 9 from Charley Creek although a lode containing native bismuth and bismuthinite crops out about half a mile above the sample site and both minerals are present in placer deposits at least as far downstream as the sample site. Similarly, although sphalerite is abundant in a lode cropping out at the head of Steep Creek, a headwater tributary of the Snake River, the quantity of zinc in a sample collected about a mile downstream did not exceed its background content. Individually, the Cu, Zn, Mo, and Bi geochemical anomalies are strong indicators of undiscovered metal-

liferous lodes in the Thompson Creek drainage. Taken together, they indicate that the Kigluaik Mountains, and perhaps other areas in which high-grade metamorphic rocks occur on the Seward Peninsula, contain hydrothermal deposits of base metals, even though they lack the gold-bearing lodes and placer deposits that characterize the Nome goldfields.

Briefly summarized, the conclusions of this report are:

1. Meaningful geochemical results were obtained from stream sediments in the mineralized metamorphic terrane of the Seward Peninsula.
2. The greatest quantities of copper, zinc, bismuth, and molybdenum in all of the sediment samples oc-

curred in those collected from Thompson Creek in the Kigluaik Mountains and strongly indicate the presence of lode deposits containing these metals in the Thompson Creek drainage basin.

3. The indication of metalliferous lodes near Thompson Creek suggests that hydrothermal deposits may occur in the high-grade metamorphic rocks elsewhere in the Kigluaik Mountains and, perhaps, in those exposed at other places on the Seward Peninsula.

#### REFERENCE

- Moffit, F. H., 1913, *Geology of the Nome and Grand Central quadrangles, Alaska*: U.S. Geol. Survey Bull. 533, p. 140.



## 17. STRUCTURAL GEOLOGY AND STRUCTURAL CONTROL OF MINERAL DEPOSITS NEAR NOME, ALASKA

By C. L. HUMMEL, Menlo Park, Calif.

Structures belonging to systems of two ages have been identified and mapped in the bedrock of an area near Nome, Alaska (fig. 17.1). The lode and placer deposits of the Nome goldfields are closely associated with some of the structures of the younger system.

Structures of the older system developed during a period of deep-seated deformation, probably in the Mesozoic era, at which time all the bedrock of the area was regionally metamorphosed. The major structures of this system once formed a series of nearly northward trending folds which may have extended northward for 100 miles across the middle of the Seward Peninsula. Other structures include numerous minor folds of various sizes and several types of axial lineation; all these features are more or less parallel to the major folds. The major folds were greatly modified by later orogenic activity, so that only deformed remnants of two of them are now recognizable in the area—a broad, open syncline about 25 miles wide in the eastern part of the area and a somewhat tighter but still open anticline in the western part.

Structures of the younger system are thought to be related to the eastward-trending uplift, probably of Tertiary age, from which the present Kigluaik mountain range developed. This uplift transected the older northward-trending folds about at right angles, leaving within the area the truncated ends of the two folds mentioned above. Structural features of the uplift are clearly expressed by the present topography. Not only

does the range have the same trend as the uplift, but the uplift is bounded by steeply dipping normal faults, one of which marks the northern limit of the range and the other almost coincides with the southern limit. The highest mountains of the range lie along the axis of an arch, formed during the elevation of the uplift, that plunges eastward and westward from Mount Osborn, the highest peak in the range. Because of the arcuate pattern of the faults that bound it, the uplift is also widest through Mount Osborn. The southern boundary fault marks the contact between the high-grade metamorphic rocks which crop out only in the uplift and those of much lower metamorphic grade which form the bedrock throughout the area to the south. On the basis of this difference of metamorphic grade and on stratigraphic evidence, it is estimated that at least 30,000 feet of vertical movement has taken place in the center of the uplift.

Other structures of the younger system, present only in the area south of the Kigluaik Mountains, are thought to be subsidiary effects of the uplift. These include two folds of considerable size and three sets of faults. The folds, both of them just south of the uplift, are an eastward-plunging syncline in the west-central part of the area and a southwestward-plunging syncline in the northeastern part, superposed upon the eastern and western limbs of the older north-trending syncline. The three sets of faults strike to the north, northeast, and east, respectively. Only the east-west

PRECAMBRIAN(?) PALEOZOIC QUATERNARY  
OR PALEOZOIC(?)

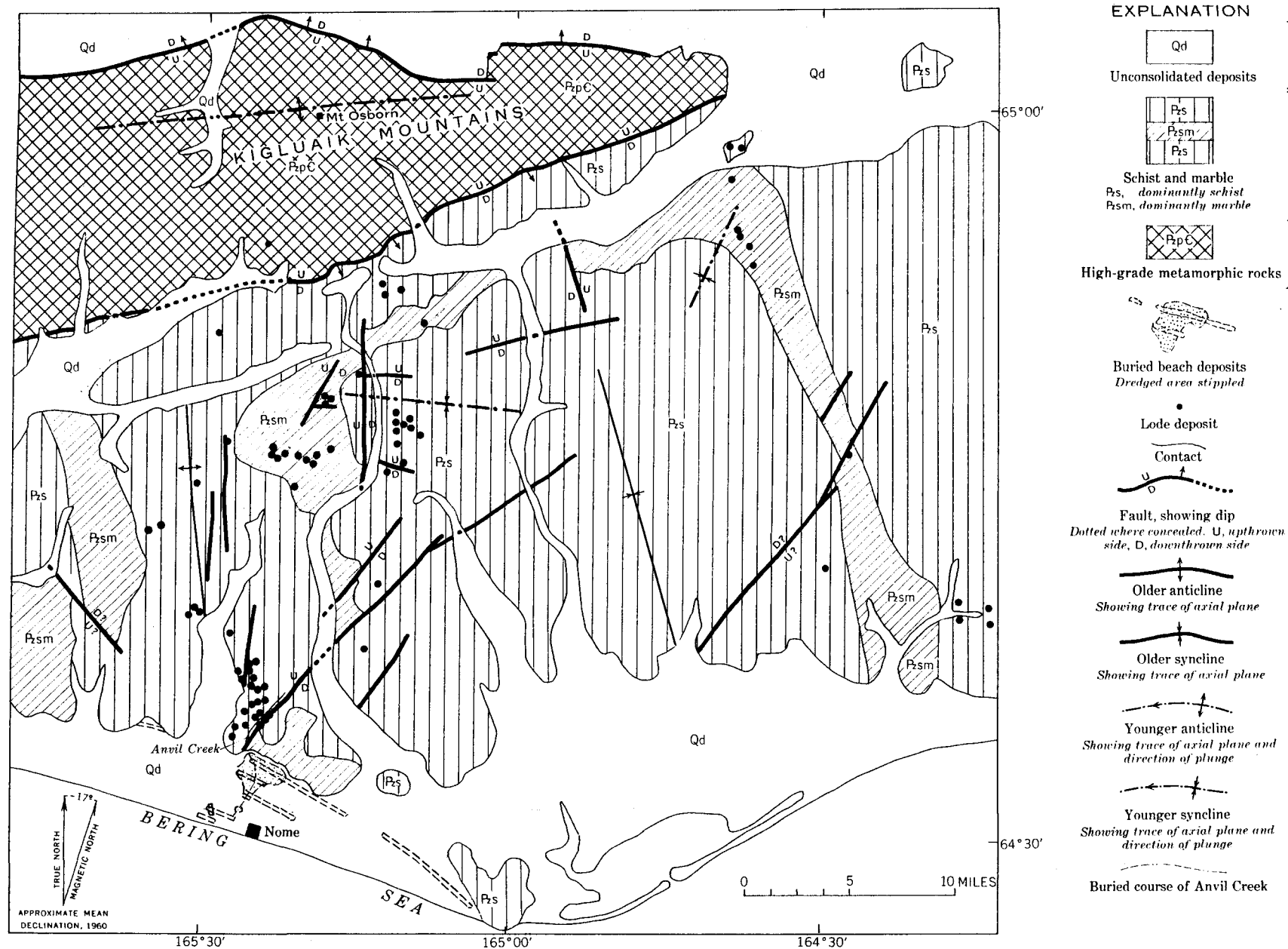


FIGURE 17.1.—Structures and mineral deposits near Nome, Alaska.

faults are obviously related to the uplift; they strike about parallel to the boundary faults, and the north sides of most of them are strongly upthrown.

The lode and placer deposits of the Nome goldfields are closely associated with the younger folds and faults south of the Kigluaik Mountains. The lode deposits, most of which are filling-type deposits composed of varying proportions of base-metal sulfides, scheelite, and native gold in shattered quartz, occur in three areas; two of these extend along the two younger synclines just south of the Kigluaik Mountains, and the third lies between a northward- and a northeastward-striking fault just north of Nome. Within each of these areas the lodes have been further localized along minor faults and disturbed joints.

The areal distribution of the placer deposits is generally related to that of the lodes and thus is indirectly controlled by structure. This indirect control is of particular interest and importance in the case of the northeastward-striking fault which reaches the coastal plain just north of Nome. Numerous lode deposits occur in and near the fault zone where it is exposed in the valley of Anvil Creek, which marks the southwestern end of the fault. Similar lodes in eroded portions of the fault and bedrock were the sources of the gold in the alluvial placer deposits on Anvil Creek, the richest in the goldfields, and of the gold in the richest parts of several buried beaches which have been formed along the ancestral course of Anvil Creek under deposits of the coastal plain.



# 18. STRUCTURAL CONTROL IN FIVE QUICKSILVER DEPOSITS IN SOUTHWESTERN ALASKA

By C. L. SAINSBURY and E. M. MacKEVETT, JR., Menlo Park, Calif.

Most of Alaska's known quicksilver deposits are in the southwestern part of the State. Five of them—the Red Devil, Red Top, Kagati Lake, White Mountain, and Willis—illustrate different types of structural control (fig. 18.1). These deposits were studied during 1958 and 1959 as a part of the U.S. Geological Survey's

investigation of quicksilver deposits in southwestern Alaska.

The quicksilver deposits, which are probably of Tertiary age, are alike in having been mainly formed by the deposition of cinnabar in open fractures in competent rocks, but in detail each deposit has its individual structural control. The cinnabar is commonly accompanied by stibnite, but it also occurs alone, or less extensively with realgar and orpiment. The common gangue minerals are quartz, dolomite, and calcite.

The Red Devil mine, Alaska's largest quicksilver producer, has produced more than 20,000 flasks. The mine is in graywacke and argillaceous rock of the Cretaceous Kuskokwim group, which strike N. 30°–45° W. and dip 45°–60° SW, and in altered dikes that cut these rocks. The ore bodies were formed at and near intersections between northeast-trending dikes that dip 40°–60° SE. and northwest-trending faults that are essentially parallel to the bedding (fig. 18.2). This structural control was first recognized by J. D. Murphy, former manager and resident geologist at the mine. Typical ore bodies are pencil-shaped and plunge about 40° S. The northwest-striking faults have right-lateral displacements that range from a few inches to about 40 feet, and the cumulative right-lateral displacement of the faults is several hundred feet. The mineralized intersections are in a zone that is at least 600 feet wide and 1,500 feet long.

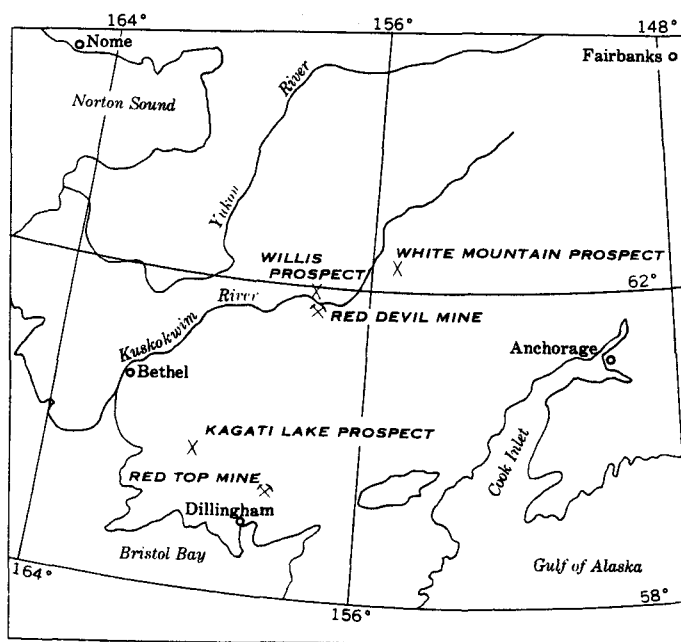


FIGURE 18.1.—Index map showing location of five quicksilver deposits in southwestern Alaska.

The Kagati Lake prospect is in a strongly fractured quartz monzonite and granodiorite stock, probably of Tertiary age (fig. 18.3). The quicksilver deposits are localized along favorable faults and joints, commonly in irregular quartz veins and pods. Most of the well-defined ore bodies are only a few inches wide and are traceable for less than 10 feet along their strikes. Most of the deposits lie in what is called the "main shear zone," which consists of many steep closely spaced fractures that strike about N. 20° W., but some are in sub-parallel fractures west of it. Minor amounts of ore occur in fractures that trend more nearly due northwest.

The Red Top mine has had a small production. The ore occurs along a steep fault zone where it intersects minor folds that plunge southward. The general

strike of the fault zone is N. 70° W., parallel to the regional attitude of the graywackes and siltstones of the Gemuk group, of Carboniferous to Cretaceous age (J. M. Hoare, oral communication, 1960). The differing structures on opposite sides of the fault zone are illustrated in figure 18.4A. On the north side the beds along the line of section are essentially homoclinal, dipping steeply southwestward; on the south side they form small folds that plunge southward. Abundant breccia, shear zones, and divergent fractures occur where the fault intersects the plunging folds. Most of the ore consists of cinnabar in a dolomite gangue that is localized in breccia zones and veinlets along the divergent fractures. The competent graywacke fractured readily and is crossed by wide breccia zones and open fractures, whereas the fractures in the siltstone are tight, contain abundant gouge, and commonly lack ore. The minette dike that is shown in figure 18.4A is unaltered and apparently unrelated to the formation of the ore. The dump at the lower adit contains some

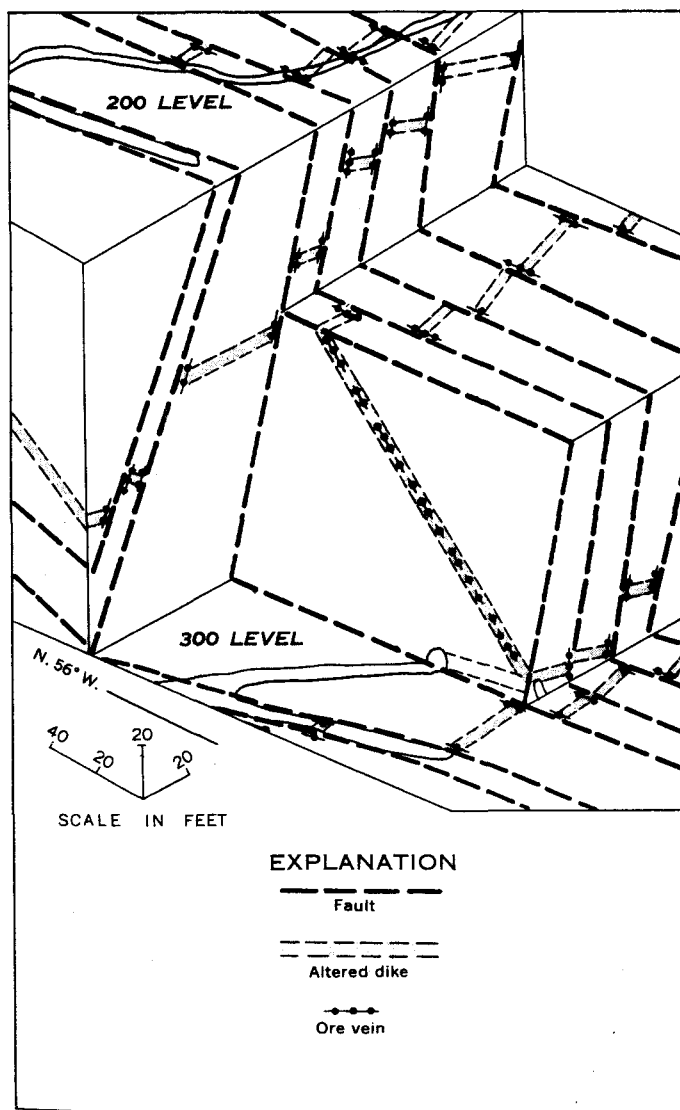


FIGURE 18.2.—Generalized isometric block diagram of part of the Red Devil mine. The dikes and veins cut graywacke and shale of the Kuskokwim group.

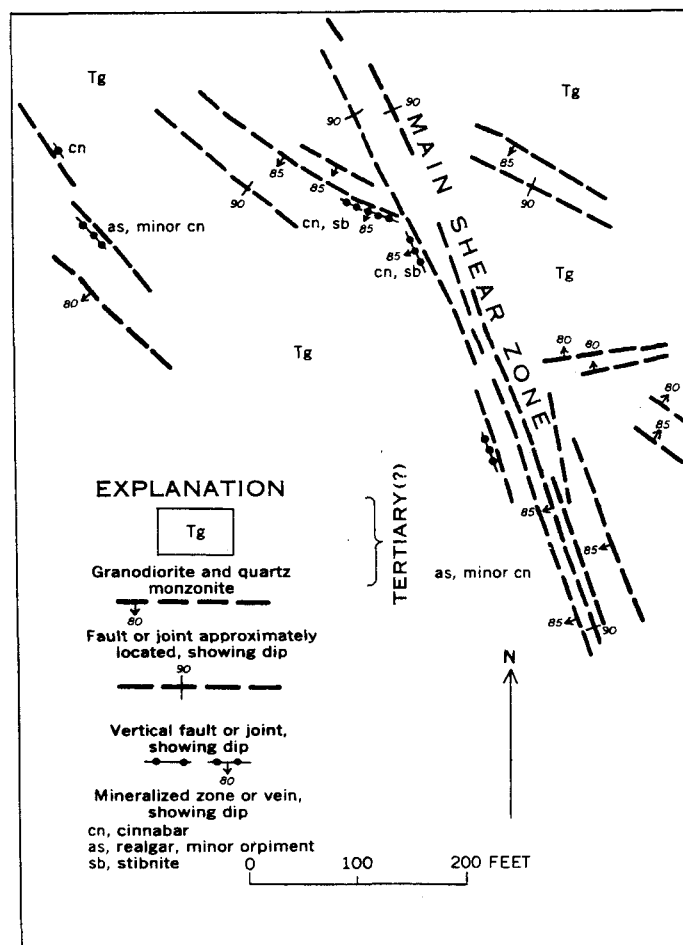
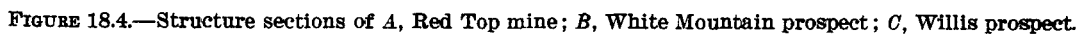


FIGURE 18.3.—Geologic sketch map of the Kagati Lake prospect.





## 19. THREE AREAS OF POSSIBLE MINERAL RESOURCE POTENTIAL IN SOUTHEASTERN ALASKA

By HENRY C. BERG, Menlo Park, Calif.

Reconnaissance geological mapping of Admiralty Island and the Chilkat Range (fig. 19.1) has disclosed three heretofore undescribed areas of higher mineral-resource potential than the surrounding terrain.

About 100 square miles of the central part of Admiralty Island (1, fig. 19.1) is underlain by intrusive, contact-metamorphic, and migmatitic rocks. The area comprises most of the high mountains west and northwest of Hasselborg Lake, and includes the southern end of the lake. It contains numerous outcrops of orange, dark-red, and dark-brown gossan, whose areas range from less than 100 to several thousand square feet. Field and laboratory (chemical, X-ray) studies indicate local concentrations of oxide and sulfide minerals, chiefly rutile, pyrite, pyrrhotite, and chalcopyrite, which contain traces to significant amounts of copper, zinc, titanium, and niobium.

Yttrium, zirconium, niobium, thorium(?), and the rare-earth elements lanthanum, cerium, praseodymium, and neodymium were detected by X-ray spectroscopic analysis of heavy minerals from pegmatite veins on Admiralty Island 5 miles west-southwest of the head of Seymour Canal (2, fig. 19.1). The pegmatite veins are associated with granite, migmatite, and contact-metamorphic rocks, which underlie an area of 50 square miles.

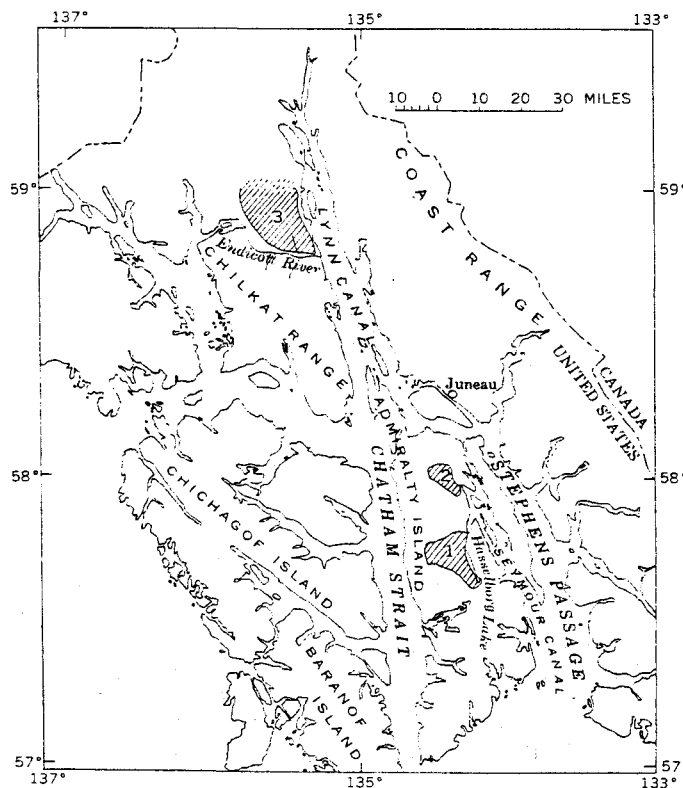


FIGURE 19.1.—Index map of part of southeastern Alaska showing three areas of possible mineral resource potential.

The part of the Chilkat Range north of the Endicott River (3, fig. 19.1) was found to be richer in sulfide minerals than the part south of the river. Orange, red, and brown gossan is widely distributed in the igneous, metamorphic, and volcanic rocks, which underlie an area of more than 200 square miles. The largest outcrops of gossan are several thousand square feet in area, but in general the gossan masses are not so common or extensive here as in central Admiralty Island. Sulfide minerals occur in local concentrations consisting chiefly of veinlets and disseminations of pyrite, pyrrhotite, and chalcopyrite. These minerals contain traces to major amounts of cobalt, copper, zinc, and lead. Magnetite and ilmenite commonly occur in disseminated particles, and in films coating shear surfaces in the rocks. In some places the oxides contain trace quantities of chromium.

Small deposits of secondary copper salts are not uncommon; malachite, azurite, and chrysocolla form stringers and stained patches in the country rocks near some of the sulfide deposits.

The areas have been prospected superficially over a period of many years and several groups recently made reconnaissance mineral surveys of the general region with helicopter support. Little trenching, test pitting, or other physical exploration has been undertaken however, and few claims have been staked. No mineral production has been reported. Thick soil, glacial deposits, and dense vegetation cover much of the areas under consideration; hence geochemical and geophysical techniques, coupled with physical exploration, probably will be necessary to test fully the mineral potential.



#### 49. GEOCHEMICAL EXPLORATION IN ALASKA

By ROBERT M. CHAPMAN and HANSFORD T. SHACKLETTE, Denver, Colo., and Georgetown, Ky.

Field and laboratory studies of the applicability in Alaska of presently known methods of geochemical exploration were begun in 1956; soils, plants, stream sediments, and stream waters were sampled in several regions of Alaska. Although most of the samples were taken over and near known mineral deposits, some were collected in areas that do not contain known deposits. Soil and plant sampling were concentrated in the areas shown on figure 49.1.

Thirty-eight different species of plants were used in evaluating methods of biogeochemical prospecting. Plant samples were collected at soil sample sites in order to relate the amount of metals in the plants to the amount in the soil where they were growing.

Analysis of the data is not fully completed and in some areas more samples are needed, but the following evaluations can be made:

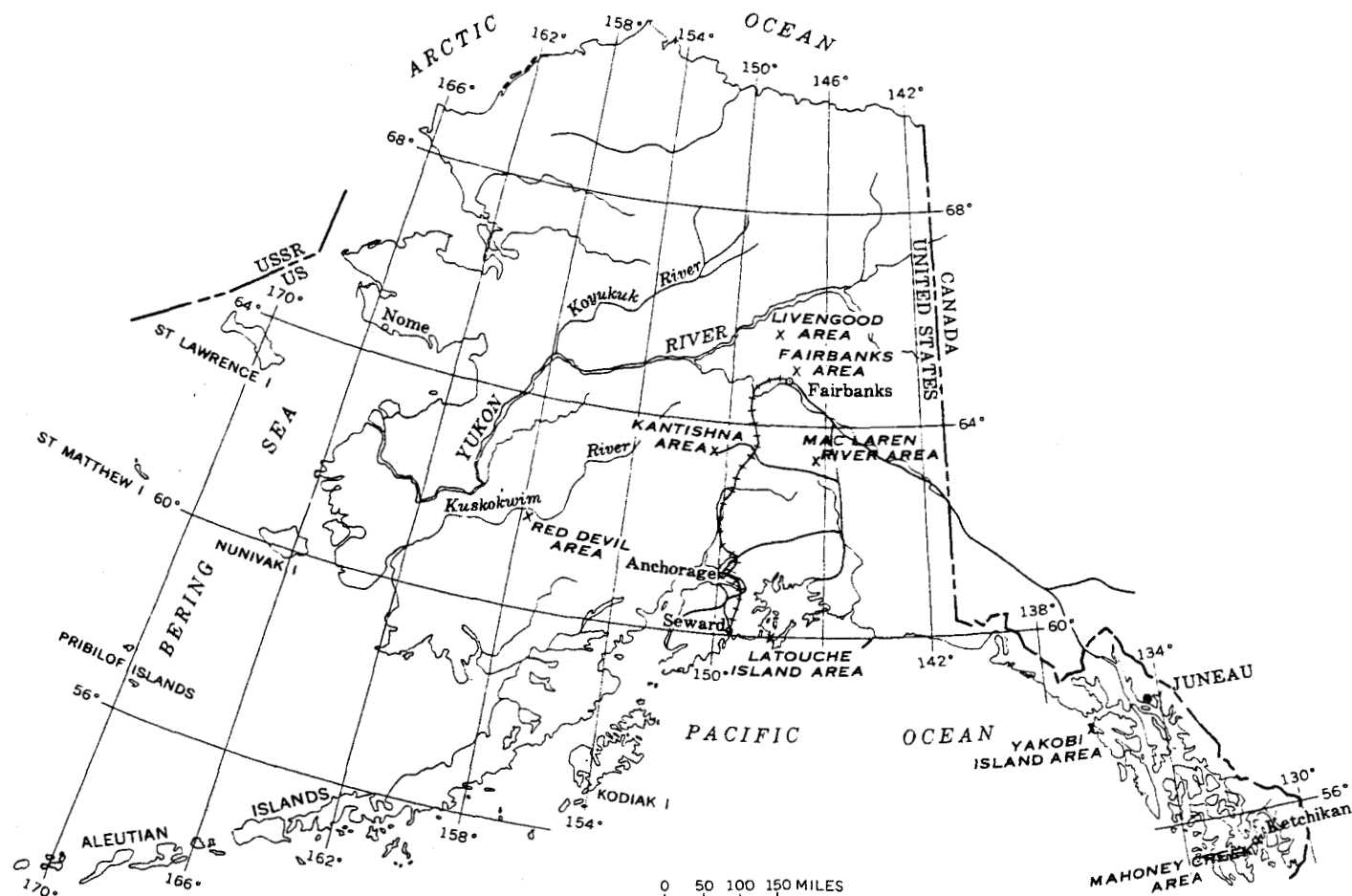


FIGURE 49.1.—Map of Alaska showing areas of detailed geochemical sampling.

1. Soil samples generally give anomaly patterns that assist in locating most of the deposits that were tested. Lead-zinc deposits at Mahoney Creek; lead-, zinc-, copper-, antimony-, and arsenic-bearing deposits in the Kantishna area; and silver-lead and tungsten deposits in the Fairbanks area showed clear-cut anomalies. Less distinct, but at least in part definitive, anomalies were obtained from samples taken over copper-nickel deposits on Yakobi Island, copper-bearing pyrite deposits on Latouche Island, mercury deposits at Red Devil, a copper deposit along the upper Maclaren River, and several sulfide-mineral deposits and a serpentine body near Livengood (table 49.1).
2. In general, samples from the C soil horizon near bedrock give the most reliable and useful sample and the largest metal content. Many of the A horizon samples show lower anomaly values and do not always reflect anomalies that are present in the underlying C horizon or bedrock and, owing to the humus content, are more difficult to process chemically.
3. Many plant and soil analyses show close correlation in the upper range of anomalous metal content, whereas the relationship is often obscure in the lower range of values.
4. On some sampling traverses the high metal values in plant ash do not occur at the sample site having

TABLE 49.1.—Metal content, in parts per million, of soils in several areas of Alaska, based on approximately 1,060 samples

[Analyses of —80 mesh material by rapid wet chemical field tests by staff of Geochemical Exploration Section laboratory. Soil C horizon may in places include some B horizon.]

Area	Rock type	Soil A <sub>1</sub> horizon											
		Background (ppm)						Anomalous (ppm)					
		Pb	Zn	Cu	Ni	As	Sb	Pb	Zn	Cu	Ni	As	Sb
Mahoney Creek	Slate												
Yakobi Island	Amphibole schist			<20	<20								
Yakobi Island	Gabbro and some diorite			<20-20	<20-20					>100-400	>50-400		
Yakobi Island	Norite			20-100	20-50					>100-400	>50-400		
Latouche Island	Graywacke and slate	<20-50	10-80+	10-50				100-1, 250	100-200	>50-200			
Red Devil	Graywacke and shale												
Kantishna	Quartz-mica schist	<20-100(?)	<20-100(?)	10-50(?)		10-150(?)	?	>100-1, 000 or 2, 000	120(?)—180	60-100		200-1, 200	?
Maclaren River	Basaltic rocks			30-70						>70-400			
Livengood	Ultramafic and mafic rocks												
Livengood	Chert and metasedimentary rocks												
Fairbanks	Quartz-mica schist and some granitic rocks	<20-40	20-100			<10-20(?)		50-80	>100-180				

Area	Rock type	Soil C horizon													
		Background (ppm)							Anomalous (ppm)						
		Pb	Zn	Cu	Ni	As	Sb	Hg	Pb	Zn	Cu	Ni	As	Sb	Hg
Mahoney Creek	Slate	<20-50	<20-50	80-100(?)					>50- >3, 000	>50- 2, 000	>100- 300				
Yakobi Island	Amphibole schist			<20	<20										
Yakobi Island	Gabbro and some diorite			50-70	20-50						100- 1, 500	100-600			
Yakobi Island	Norite			20-100	20-70						>100- 1, 500	100-600			
Latouche Island	Graywacke and slate	10-50	10-80+	10-50					80-200	100(?)— 4, 000	80-800				
Red Devil	Graywacke and shale					<10- 150(?)	<1-6(?)	<2.5- 6.5					>150- 3, 600	>6-900	9-160+
Kantishna	Quartz-mica schist	<20- 100(?)	<20- 100(?)	10- 100(?)		<10- 200(?)	1-10(?)		>100- 4, 000	>100- 3, 000	>100- 300		>200- 2, 400 or 4, 000	>10- 1, 100	
Maclaren River	Basaltic rocks			40-200							>200- 1, 200				
Livengood	Ultramafic and mafic rocks	<20-50	25-120	20-80	50-400			<2.5- 3(?)							
Livengood	Chert and metasedimentary rocks	<20-20	20-120(?)	10-80	<25- 100(?)			<2.5- (?)							>6(?)— 15(?)
Fairbanks	Quartz-mica schist and some granitic rocks	<20-40	20-150(?)	10-(?)			<1-4		50-8, 000	>150(?)— 7, 000					

high soil values, but at an adjacent site. The direction of root growth of the plant in response to other soil factors having a physiological effect may cause this displacement.

5. Plant roots do not extend to great depths in Alaska, owing to (a) the general abundance of water in the upper soil horizons, (b) the thin soil mantle that usually overlies bedrock, and (c) the occurrence of permafrost or late-thawing cold subsoil which limits downward root growth. This growth characteristic restricts the usefulness of plants in indicating deeply buried metal deposits.
6. The ability of plants to indicate anomalous metal occurrence in the substratum on which they are growing varies with the species of plant and kind of metal. A species that accurately indicates anomalous amounts of one metal may be useless for indicating another metal.
7. The average metal content of all species for all areas studied varied with the different metals, and ranked in descending order as follows: zinc, iron, nickel, copper, lead, and molybdenum (table 49.2). High, low, and median values for these elements are also given.

TABLE 49.2.—Mean metal content of 38 species of Alaskan plants, based on 5,126 analyses. Values expressed as percent in ash

[Analyses by rapid wet chemical field tests by staff of U.S. Geological Survey laboratory]

Value	Metal content in number of analyses indicated					
	Lead (1,439)	Copper (1,502)	Zinc (1,439)	Nickel (396)	Iron (338)	Molybdenum (12)
High.....	0.500	0.300	4.00	0.600	7.50	0.003
Low.....	.002	.001	.02	.002	.04	.001
Mean.....	.012	.027	.32	.034	.28	.001
Median.....	.010	.022	.15	.015	.25	.001

8. There is commonly a great variation in amounts of a particular metal absorbed by different species of plants growing at the same site. This may represent the inherent limitations of the species in their range of metal absorption. Some species show a ratio of high to low metal content as great as 200:1, whereas others cover a range of only 5:1 to 10:1. Ratios of high to low percentages of several plants, which are considered to be representative of the total species analyzed, are given in table 49.3. Plants with high ratios have the capacity to indicate anomalous metal concentrations, whereas species with low ratios may be limited in this respect. These ratios may vary within a species, depending on the metal.

9. No definite geobotanical indicator species of flowering plants were observed in Alaska, although some of the species found on soil derived in part from serpentine may be included in this category. Several species of mosses and liverworts, however, were found which are generally recognized as occurring only on metal-rich substrata. The Alaskan specimens were found only on substrata containing, or presumed to contain, anomalous metal concentrations.

TABLE 49.3.—Ratios of high to low content of metals in selected species of Alaskan plants

[Analyses by rapid wet chemical field tests by staff of U.S. Geological Survey laboratory]

	Ratio of high to low metal content (number of analyses in parentheses)				
	Lead	Copper	Zinc	Nickel	Iron
Alder ( <i>Alnus crispa</i> (Alt.) Pursh.)	(122) 200:1	(122) 20:1	(122) 14:1	(17) 5:1	-----
Crowberry ( <i>Empetrum nigrum</i> L.)	(38) 40:1	(65) 8:1	(38) 3:1	(7) 30:1	(14) 8:1
Deer cabbage ( <i>Fauria Cristagalli</i> (Menz.) Makino)	(73) 15:1	(73) 10:1	(73) 10:1	(17) 10:1	(56) 7:1
Dwarf blueberry ( <i>Vaccinium uliginosum</i> L.)	(166) 20:1	(195) 40:1	(166) 25:1	(40) 150:1	(14) 3:1
False hellebore ( <i>Veratrum Eschscholtzii</i> A. Gray)	(44) 10:1	(44) 100:1	(44) 10:1	(21) 50:1	(23) 5:1
Menziesia ( <i>Menziesia ferruginea</i> Smith)	(76) 60:1	(76) 20:1	(76) 8:1	(15) 25:1	(26) 16:1
Mountain hemlock ( <i>Tsuga Mertensiana</i> (Bong.) Sarg.)	(66) 200:1	(66) 20:1	(66) 2:1	(7) 20:1	(56) 8:1
White birch ( <i>Petula resinifera</i> Britton)	(51) 200:1	(51) 15:1	(51) 27:1	(47) 32:1	-----

10. Stream sediments that were collected from 0.5 mile to as much as 2 or 3 miles downstream from deposits bearing one or more metals other than gold, generally showed an anomalous content of at least one metal (table 49.4). Lead, zinc, copper, antimony, arsenic, nickel, and chromium all give identifiable anomalies. Tests for tungsten, cobalt, molybdenum, titanium, manganese, and several other metals did not appear to be as useful, although these metals were not tested as extensively as the former group of metals.
11. Stream sediment derived chiefly or entirely from loessial mantle generally gives no clue to mineral deposits in the watershed.
12. Stream sediment sampling failed to detect placer deposits that lie beneath a relatively thick muck and gravel cover, which in most localities in interior Alaska is frozen. Apparently such deposits do not yield detrital or dissolved metal to the surficial stream sediment.
13. Stream water samples do not consistently give reliable leads to metalliferous deposits in the drain-

TABLE 49.4.—*Metal content of stream sediments in several areas of Alaska, based on approximately 455 samples*

[Analyses of -80 mesh material, after grinding it to -200 mesh, by rapid wet chemical field tests, by staff of U.S. Geological Survey laboratory]

Area and rock types	Background metal content (in ppm)								Anomalous metal content (in ppm)							
	Pb	Zn	Cu	Ni	Cr	As	Sb	W	Pb	Zn	Cu	Ni	Cr	As	Sb	W
Southeastern Alaska Many rock types.	<20- 40(?)	<20- 80(?)	<10- 50(?)	<20- 80(?)	20-150 (?)	-----	<1-4 (?)	-----	50(?) - 4,000+	80(?) - 4,000	>50(?) - 400	>80(?) - 1,200	>150(?) - 1,500	-----	5(?) -15	-----
Yakobi Island. Gabbro, norite, diorites and schist.	-----	-----	30- 50(?)	20- 80(?)	-----	-----	-----	-----	-----	-----	60(?) - 400	100(?) - 400	-----	-----	-----	-----
Latouche Island. Gray- wacke and slate.	<10- 40(?)	50- 100(?)	10- 60(?)	-----	-----	10- 80(?)	3- 10(?)	-----	-----	-----	-----	-----	-----	-----	-----	-----
Interior Alaska. Many rock types.	<20- 60(?)	<20- 100(?)	<10- 50(?)	-----	-----	<10- 120(?)	<1- 5(?)	<20(?)	>60(?) - 300(?)	120(?) - 700	60(?) - 80	-----	-----	>120(?) - 300	6(?) -45	20-40
Kantishna. Quartz-mica and chlorite schist.	10- 80(?)	20- 120(?)	20- 50(?)	-----	-----	<10- 120(?)	1- 12(?)	-----	>80(?) - 1,500	>120(?) - 2,500	>50(?) - 150	-----	-----	>120(?) - 3,200	>12(?) - 600	-----

age basins. Some base metal deposits were detected by anomalously high amounts of copper, lead, or zinc in water 0.5 mile downstream. Although this condition seemed to be detectable for as much as 3 miles downstream, it diminished to indefiniteness at that distance. In contrast, some other streams draining areas having similar deposits showed only normal metal content.

14. Apparently no useful correlation can be made between pH and metal content of stream waters, or

between sulfide deposits and the sulfate content of waters draining from such deposits.

The analytical values given in tables 49.1 through 49.4 were determined by rapid wet chemical field tests that have a precision of -50 to +100 percent. Due consideration should also be given to the distance of the sample from the source deposit and to the rock type from which the sample material is derived. Thus, it is impossible to give an exact figure that divides background from anomalous values.



## **GEOLOGY APPLIED TO ENGINEERING AND PUBLIC HEALTH**

---

### **63. SOME THERMAL EFFECTS OF A ROADWAY ON PERMAFROST**

By GORDON W. GREENE, ARTHUR H. LACHENBRUCH, and MAX C. BREWER, Menlo Park, Calif.

---

*Work done in cooperation with the Bureau of Public Roads, Office of Naval Research, Air Force Cambridge Research Center, and the Bureau of Yards and Docks*

---

The effects of a roadway on the thermal regime of the ground constitute one of the more important problems in permafrost engineering. A sizeable portion of the highway maintenance effort in permafrost terrain is directed toward repairing the results of differential settling and heaving in the subgrade materials. These thermal problems have been under study for several years by the U.S. Geological Survey in various places in Alaska.

The most conspicuous thermal effect of building a roadway is probably the increase in variability of ground temperature, that is, the increased sensitivity of ground temperature to changes in air temperature and surface radiation from summer to winter and from year

to year. The effect is illustrated with data from the Richardson Highway in figure 63.1. It is seen that the total range of temperature from summer to winter at each depth is much greater beneath the roadway than beneath the nearby undisturbed ground. In the summer roadways are generally warmer than surrounding ground because of greater net absorption of radiation by their dark unshaded surfaces, and the absence of the cooling effect of evaporating moisture. In the winter roadways are generally cooler than the surrounding ground because snow, which serves as an insulator, is removed by plows or wind, or the insulating quality is destroyed by compaction under vehicular traffic. A larger seasonal range of temperature at the surface

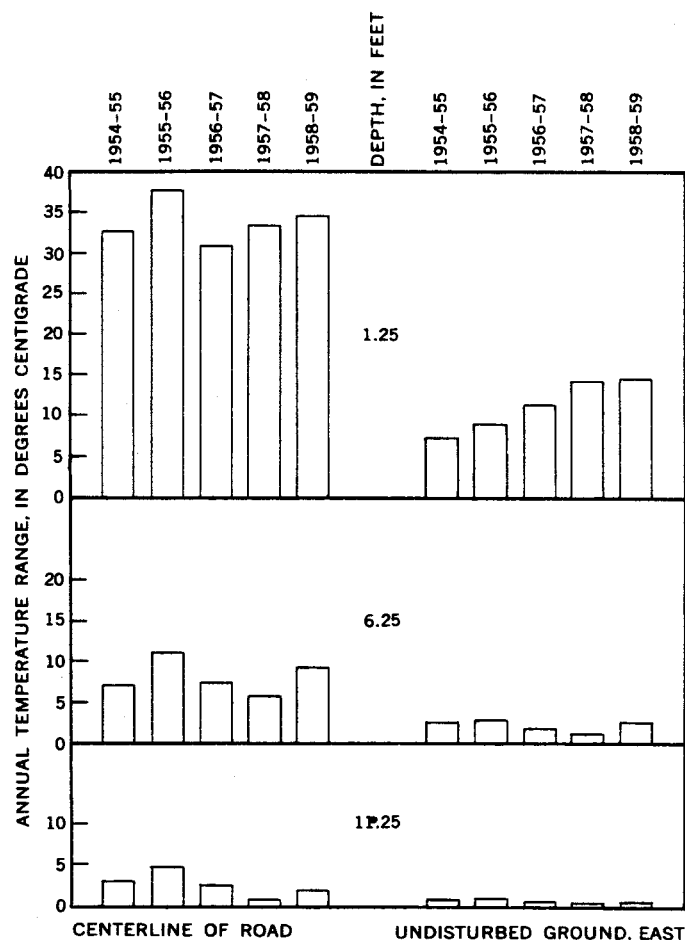


FIGURE 63.1.—Comparison of annual temperature ranges at selected depths beneath the surface of the roadway and nearby undisturbed ground, for the period July 1954 to June 1959, mile 130, Richardson Highway, Alaska.

generally results in a proportionally larger range at depth. Where coarse fill materials are used beneath the road the effect is accentuated as thermal changes are propagated downward with less attenuation in such high-diffusivity, low-moisture-content materials.

Almost as important as the seasonal range of temperature is the change in mean annual temperature beneath a roadway. Inasmuch as a roadway causes increased summer temperatures and decreases winter temperatures its effect on the mean is not obvious. Mean annual temperatures (for years beginning July 1) beneath the roadway and undisturbed ground are compared in figures 63.2 and 63.3. Shown also is the mean annual air temperature as recorded by the Weather Bureau at Gulkana Airfield, approximately 12 miles away. The changes in air temperature from year to year are followed by similar changes beneath the ground surface. Again the roadway shows a greater sensitivity to changing surface conditions. In both environments the temperature changes are attenuated with increasing depth.

Now consider the depth of thaw as illustrated in figure 63.4. We first notice that the thaw depth is consistently greater beneath the centerline of the roadway than at peripheral installations. This is the expected effect of the increased amplitude discussed above. It is interesting to note (figs. 63.2 and 63.3) that during the first three years the more deeply thawing centerline had lower mean temperatures than the undisturbed ground. This illustrates the independent roles played by amplitude and mean.

A striking feature of figure 63.4 is the sudden increase in maximum thaw depth beneath the centerline during the summer of 1957, and the persistence of this deep thawing in subsequent years. Inasmuch as the road was surfaced with asphalt late in the summer of 1956 it seems reasonable to suspect that the deep thawing was caused by an increase in the net radiation absorption by the dark surface during subsequent summers. If this were so, however, we should expect the cumulative thawing index beneath the surface to show an increase commensurate with the increased thaw depth. That it does not is shown by the data presented in table 63.1. The thawing index (maximum cumulative degree centigrade-days above freezing) at a depth of 5 feet is a rough measure of the quantity of heat available to thaw the material below 5 feet. The unusually warm summer of 1957 is associated with a large thawing index at 5 feet (487 degree centigrade-days) and an increase in active layer thickness from 6.9 feet to 10.5 feet. It is significant that roughly the same amount of thawing was accomplished in 1958 with only about half as much heat (258 degree centigrade-days) and in 1959 with less than one-fourth as much (104 degree centigrade-days). Clearly, the deep thawing in 1957, 1958, and 1959 is not the result of sustained increase in summer heat input due to surfacing the road, but the result of a progressive reduction in the amount of heat required to thaw to 10+ feet; that is, a reduction in moisture content. This conclusion is supported by the observation that thawing proceeds rapidly in ground previously thawed, and much more slowly at the degrading permafrost surface.

The effects can now be summarized in fairly general terms as follows. The presence of the road increases

TABLE 63.1.—Thawing index measured at 5 ft below surface of road at the centerline compared with depth of thawing beneath road.

Year (July-June)	Thawing index, degree centigrade-days	Depth of thaw (feet)
1954-55	108	6.1
1955-56	140	6.5
1956-57	172	6.9
1957-58	487	10.5
1958-59	258	10.7
1959-60	104	10.2



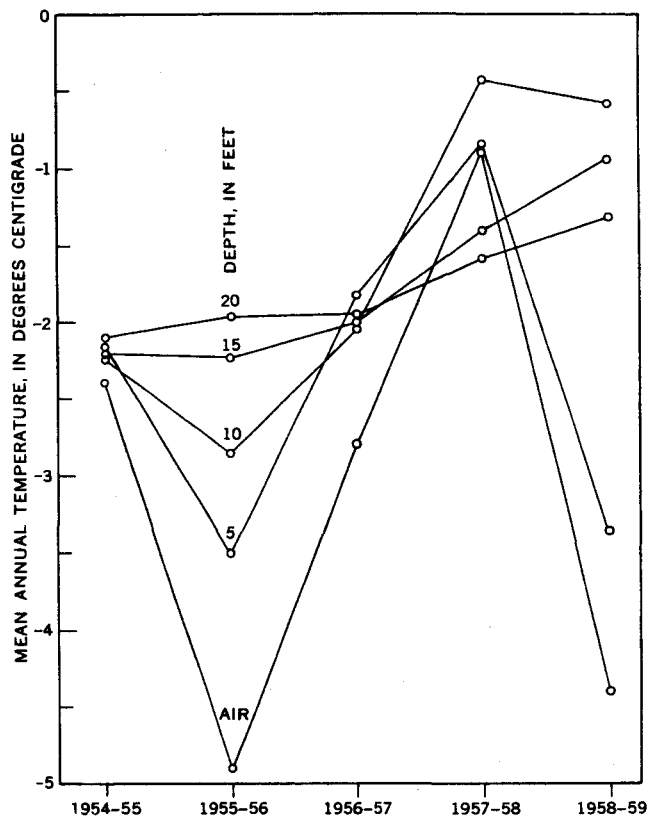


FIGURE 63.2.—Mean annual temperatures, centerline, mile 130, Richardson Highway, Alaska.

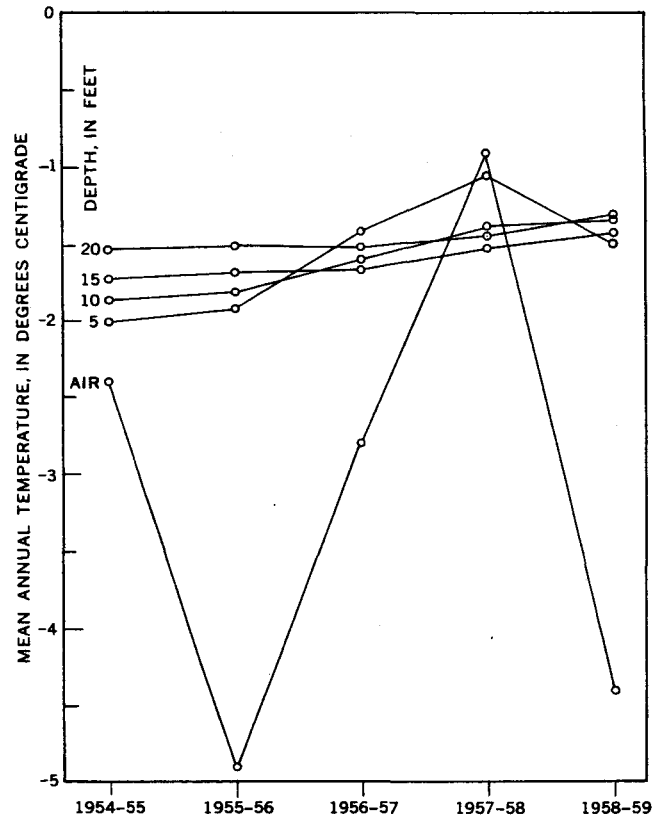


FIGURE 63.3.—Mean annual temperatures, undisturbed ground, east, mile 130, Richardson Highway, Alaska.

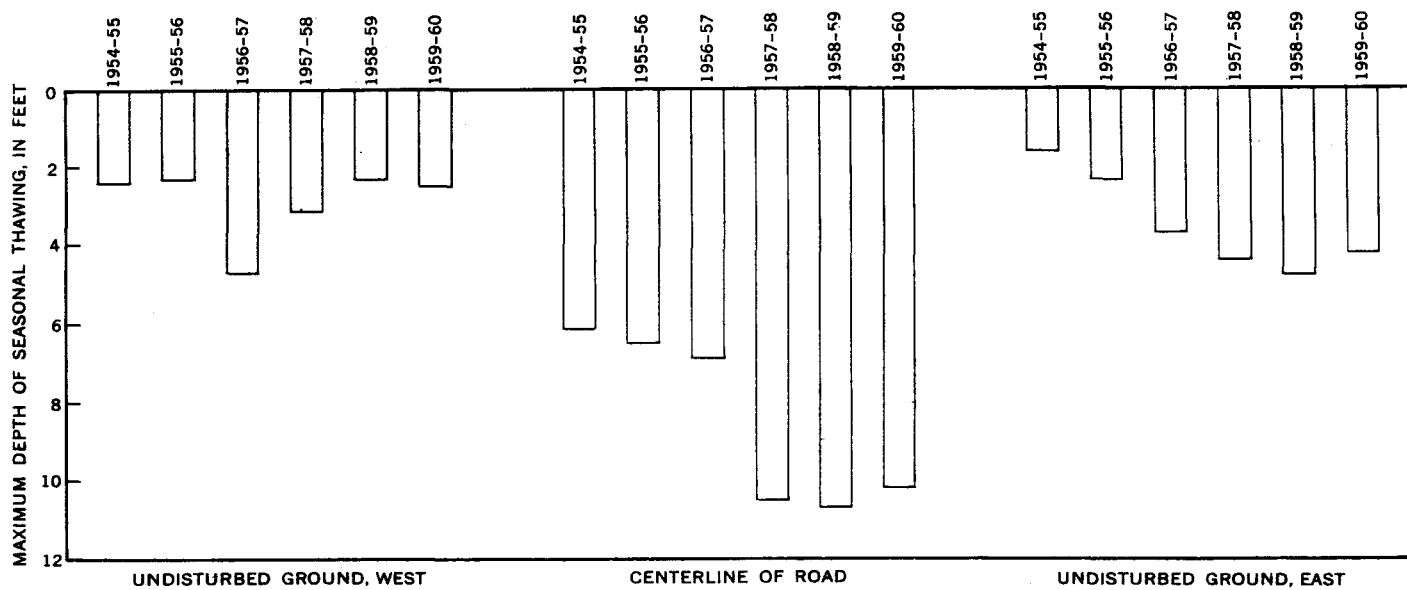


FIGURE 63.4.—Maximum depths of seasonal thawing at mile 130, Richardson Highway, Alaska.

the seasonal range of temperature (fig. 63.1) and hence increases the seasonal depth of thaw, causing the active layer to encroach on permafrost. The roadway is more sensitive to random climatic variation from year to

year (figs. 63.2 and 63.3) and hence the deep thaw is accentuated during an anomalously warm season. If the excess water formed by melting ice in the surficial permafrost layers can drain off, the thickened active

layer will be drier and more easily thawed in subsequent years.

This, of course, will result in a settling of the roadway at the point where this progressive deep thawing occurs. The water would be expected to migrate in the thawed trough beneath the roadway until it is trapped in a basin, or escapes by exterior drainage. When it is trapped in a basin, as when the road crosses a swale or a large culvert, the water is ultimately refrozen and some heaving might be expected. In the case illustrated in figure 63.4, these effects were probably accentuated by the presence of a 3-foot sand layer known to occur between the depths of 8 and 11 feet.

When the thaw depth exceeded 8 feet it is likely that water drained off through this permeable horizon. Transport of heat by the moving water probably aided the thawing process.

The continuing study of the thermal budget of the subgrade is expected to lead to a more detailed elaboration of the thermal and mechanical processes responsible for highway problems in permafrost. A regular unbroken series of field measurements, such as that now being obtained through the cooperation of the Bureau of Public Roads, will permit a more satisfactory quantitative treatment of the problem.



## GEOLOGY OF ALASKA

## 152. CENOZOIC SEDIMENTS BENEATH THE CENTRAL YUKON FLATS, ALASKA

By JOHN R. WILLIAMS, Washington, D.C.

*Work done in cooperation with the Office, Chief of Engineers*

The log of a water well drilled near Fort Yukon by Alaska District, Corps of Engineers, U.S. Army, provides the first stratigraphic information on the upper 440 feet of sediment in the central part of the Yukon Flats Cenozoic Basin. The basin consists of the Yukon Flats, an alluvial plain of about 9,000 square miles, and the bordering marginal upland, an area of dissected high terraces and piedmont slopes flanking the surrounding highlands. Rocks of pre-Cenozoic age do not crop out in the Yukon Flats but are exposed in gullies in the marginal upland and in the 200- to 700-foot escarpment which separates the upland from the Yukon Flats. These rocks are overlain in most places by thin deposits of late Cenozoic gravel and loess and in one area by stratified rocks of early Cenozoic(?) age.

The Corps of Engineers well was drilled August 7 to October 1, 1954, on a stabilized dune approximately 460 feet above sea level and one-half mile east of Fort Yukon. The log of this well appears to contradict an earlier report (Mertie, 1937, p. 16) of bedrock of unspecified type at 237 feet beneath Fort Yukon. The 1954 well penetrated (a) 48 feet of light tan silty eolian sand of Pleistocene or Recent age, (b) 100 feet of gray alluvial sandy gravel of Pleistocene age, and (c) 292 feet of fine sediments (172 feet of blue silt, 70 feet of gray poorly consolidated silt, 35 feet of silty sand, and 15 feet of silt). The base of the fine-grained deposits was not encountered at a depth of 440 feet, the point at which the dry hole was abandoned. Permafrost was logged from 8 to 320 feet, and ice lenses were recorded in gray silt between 320 and 390 feet.

A sample collected from 393 feet by Professor George S. Tulloch of Brooklyn College was examined for pollen by W. S. Benninghoff and for microfossils by Harlan Bergquist of the Geological Survey. The sample lacks Foraminifera but contains pollen. Preliminary studies

(Benninghoff, letter March 7, 1960) show that among the tree pollen pine, spruce, alder, birch, hemlock, and fir are abundant, and that hickory also occurs. Of these, pine, hemlock, fir, and hickory do not grow in the region today.

Information from a single well is insufficient to eliminate alternate hypotheses of origin and age of the fine-grained sediments at depth in the Fort Yukon well and to evaluate the significance of these sediments in terms of the origin and history of the Yukon Flats basin. The thickness and relatively uniform fine texture of these sediments and the topographic form of the basin suggest that they were deposited in a large lake, similar to that postulated by Spurr (1898), but in late Tertiary to early Quaternary time. The upper age limit is fixed by stratigraphic position of the deposits beneath late Quaternary alluvium. The lower limit is late Tertiary, for the incised meanders of the Fort Hamlin-Rampart Canyon which are cut across tilted Eocene rocks (Collier, 1903) are believed to have been inherited from the meandering channel of the lake outlet; and the sediments, lying below the altitude of the lowest known threshold in the pre-Cenozoic rocks that rim the Yukon Flats, were probably deposited in a depression formed by subsidence of the Yukon Flats. Preliminary identification of pollen by Benninghoff (written communication) suggests the possibility of late Tertiary age for the deposits from 393 feet, assuming that the pollen had not been redeposited from older sediments.

## REFERENCES

- Collier, A. J., 1903, The coal resources of the Yukon, Alaska: U.S. Geol. Survey Bull. 218, 71 p.  
 Mertie, J. B., Jr., 1937, The Yukon-Tanana region, Alaska: U.S. Geol. Survey Bull. 872, 276 p.  
 Spurr, J. E., 1898, Geology of the Yukon gold district, Alaska: U.S. Geol. Survey 18th Ann. Rept., pt. III-b, p. 87-392.



## 153. THE COOK INLET, ALASKA, GLACIAL RECORD AND QUATERNARY CLASSIFICATION

By THOR N. V. KARLSTROM, Washington, D.C.

*Work done in cooperation with the Office, Chief of Engineers*

Quaternary deposits in Cook Inlet, Alaska, record five major Pleistocene glaciations and several Recent glacial advances, all separated by intervals of retreat in which alpine glaciers were probably at least as contracted as they are today. Late Pleistocene and Recent glacial oscillations and related depositional changes are now closely dated by more than 50 radiocarbon-dated organic samples. Approximate dates for older events are obtained by extrapolations controlled by roughly quantitative geologic data. Each named glaciation and advance is here defined in terms of moraines and associated deposits, in accord with standard procedures based on Pleistocene type localities.

## RECONSTRUCTED COOK INLET GLACIAL CURVES

The Cook Inlet chronology, as represented by the moraines deposited by the Tustumena glacier on the Kenai Lowland (fig. 153.1, *A* and *C*), is based on geologic information that will be discussed in detail in a manuscript report in preparation. The positions of most named glacial advances are plotted in figure 153.1 according to distance of end moraines from the existing glacier front. The record includes end moraines of Knik age; Naptowne end moraines of the Moosehorn, Killey, Skilak, and Tanya advances; and Alaskan end moraines of the Tustumena and Tunnel advances. Lateral moraines and high-level drift of Mount Susitna, Caribou Hills, and Eklutna age record more extensive glaciations, during which the Cook Inlet trough was filled with ice. No end moraines of these older glaciations were deposited in the region, and their curves are truncated approximately at the position of coalescence of the Tustumena glacier with the Cook Inlet trunk glacier.

The lower boundary of the Naptowne glaciation is dated between 46,000 and 37,000 B.C. (about 45,000 B.C.). This dating is based on an ionium-uranium ratio date of 46,000-31,000 B.C.<sup>1</sup> for marine sediments recording a major glacio-eustatic transgression of late Knik age, and on the radiocarbon date of 37,000 B.C. (Olson and Broecker, 1959) for wood collected from

stratigraphically higher deposits of early Naptowne age. Organic samples from underlying deposits of Knik and Eklutna age are all too old to be finitely dated by the radiocarbon method. The upper boundary of the Naptowne glaciation is placed about 3,500 B.C., coincident with the dated culmination in late Tanya time of a marine transgression to a sea-level stand about 5 or 10 feet above present datum. As bracketed by the two dated higher sea-level stands, the Naptowne glaciation records a major glacial cycle of about 40,000 years.

Roughly estimated dates for the Knik, Eklutna, and Caribou Hills glacial maxima, respectively, are 50,000 to 65,000, 90,000 to 110,000, and 155,000 to 190,000 years ago. These dates are derived from statistical sampling of surface boulder concentrations in carefully selected sites by (a) assuming uniform rates of surface weathering and (b) assuming that the Naptowne maximum occurred 20,000 to 25,000 years ago. The Mount Susitna glaciation has not yet been dated by any direct means, but it probably occurred at least 200,000 or 250,000 years ago.

Subdivision and dating of post-Killey moraines of Skilak age or younger (fig. 153.1, *C*) are based on stratigraphic sections and moraine sequences that record regional depositional changes contemporaneous with glacial oscillations and are cross-dated by radiocarbon measurements. This closely dated part of the chronology expresses a systematic pattern of glacial oscillations, with major retreats occurring every 3,000 to 4,000 years (about 3,500 years) and important but subordinate retreats occurring every 1,000 to 1,200 years (about 1,100 years). Some smaller oscillations of glaciers and sea level that have been recorded are not represented on the reconstructed curve.

Schematic reconstruction of the pre-Skilak part of the Naptowne curve is based on the assumption that pre-Skilak glacial oscillations were produced by the same pulsatory climatic regimen that is recorded by the younger deposits. It gives the following extrapolated dates: about 13,500 B.C. for culmination of the Moosehorn retreat, about 17,000 B.C. for culmination of the retreat just prior to the Moosehorn maximum advance, and about 20,500 B.C., 24,000 B.C., and so on,

<sup>1</sup> Sackett, W. M., 1958, Ionium-uranium ratios in marine deposited calcium carbonates and related materials: Doctoral thesis. Washington University, St. Louis, Mo.

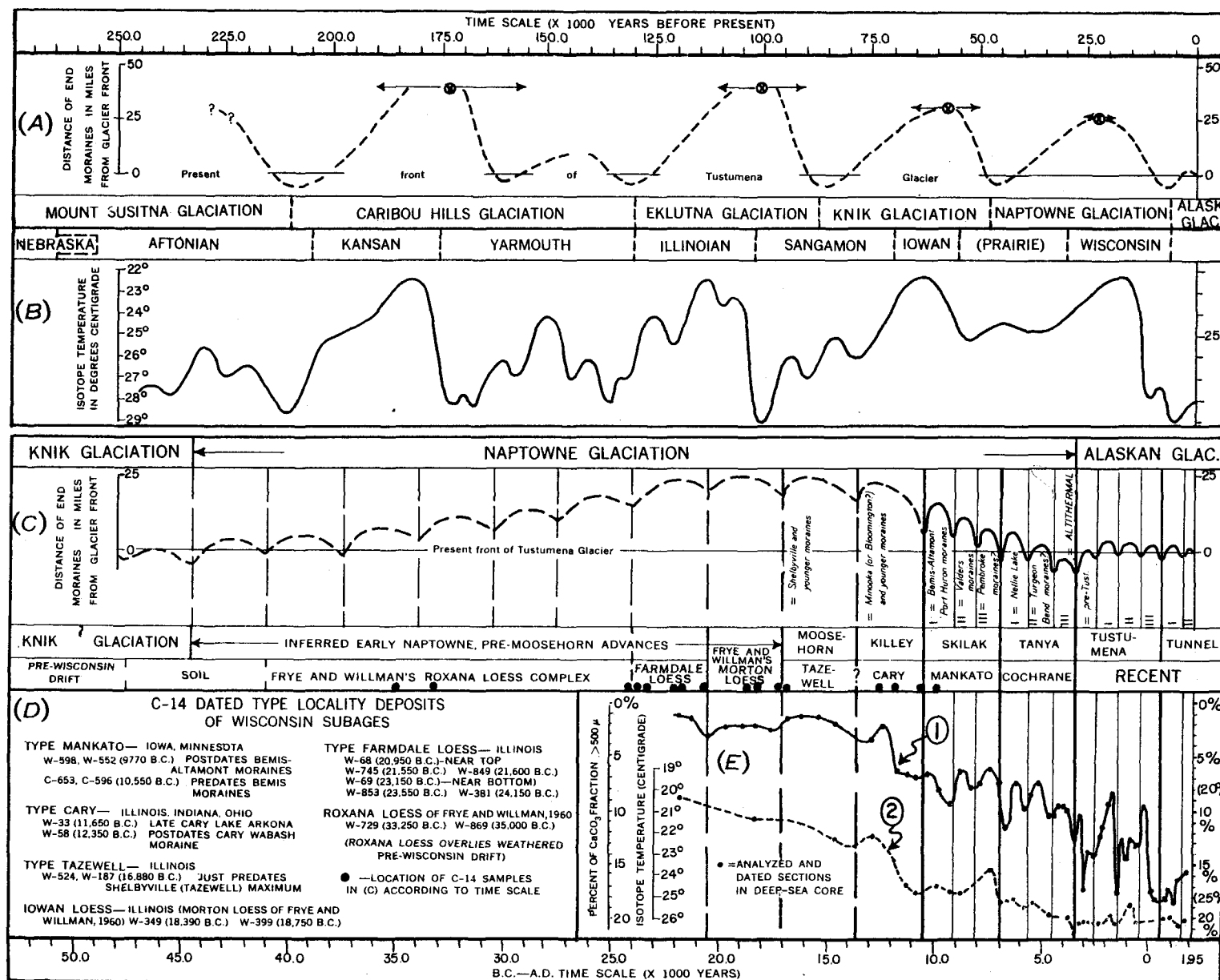


FIGURE 153.1.—Cook Inlet glacial curves and other Quaternary chronologies. A, Generalized curve of Cook Inlet glaciations (Karlstrom, 1955, 1957b). B, Generalized temperature curve for tropical surface waters correlated with midcontinent events (Emiliani and Geiss, 1957). C, Generalized, partly schematic, curve of glacial advances of Naptowne and Alaskan age with midcontinent correlations (Karlstrom 1956, 1957a, 1959). D, C-14 dating of type-locality deposits of Wisconsin substage events by Rubin and Libby from published radiocarbon date lists and from Frye and Willman (1960). E, Secondary temperature oscillations in an equatorial deep-sea core (Wiseman, 1958, 1959): Curve 1, percentage CaCO<sub>3</sub> fraction coarser than 500μ; curve 2, isotope temperatures of *Globigerinoides sacculifera*.

for the earlier intraglacial retreats which presumably interrupted the general advance of the Tustumena glacier to its maximum extension in Moosehorn time. Other Cook Inlet glaciers attained their Naptowne maxima during either pre-Moosehorn or post-Moosehorn advances; in this regard their glacial curves would differ from the reconstructed Tustumena glacier curve.

#### PLEISTOCENE CLASSIFICATION AND CORRELATIONS

The standard North American Pleistocene classification is subdivided on the basis of moraine boundaries, associated stratigraphy, and weathering relations as mapped in the midcontinent drift region. Named stage and substage events are defined in accordance with conventional geologic procedures, from drift deposits in selected areas (Leighton, 1958). Correlation of moraines and related Pleistocene deposits is based on the assumption that glaciers and other geologic processes responded almost immediately, and at about the same time, to widespread paleoclimatic changes.

Important elements of this classical approach to Pleistocene classifications and correlation have been questioned recently (by, among others, Miller, 1958; Frye and Willman, 1960). Some geologists question the use of radiocarbon-dated samples for correlation and dating (Antevs, 1957; Miller, 1958). Many of these criticisms, however, fail to take account of the striking agreement between the reconstructed Cook Inlet glacial sequence and the substage sequence of the midcontinent Wisconsin stage (when these substage events are directly dated from deposits within their defined type localities) (fig. 153.1, *D*), and of other independently dated and detailed Pleistocene chronologies (examples in fig. 153.1, *B* and *D*). These facts, taken together, substantially strengthen the case for: (a) widespread paleoclimatic and glacial synchronism, (b) utility of radiocarbon samples for dating and correlating, and (c) functional validity of the traditional approach to Pleistocene classification, based primarily

on regional mapping of moraines and associated drift units in heavily glaciated areas. Climatic controls on depositional and erosional processes may, in most cases, be more directly inferred from such deposits than from bedded deposits in non-glaciated regions. I therefore believe that relatively minor, rather than drastic, revision of the standard North American Pleistocene classification and nomenclature is in order.

#### REFERENCES

- Antevs, Ernst, 1957, Geologic tests of the varve and radiocarbon chronologies: *Jour. Geology*, v. 65, p. 129-148.
- Emiliani, Cesare, and Geiss, J., 1957, On glaciations and their causes: *Geol. Rundschau*, v. 46, pt. 2, p. 576-601.
- Frye, J. C., and Willman, H. B., 1960, Classification of the Wisconsin stage in the Lake Michigan glacial lobe: *Illinois State Geol. Survey, Circ.* 285, p. 1-15.
- Karlstrom, T. N. V., 1955, Late Pleistocene and Recent glacial chronology of southcentral Alaska [abs.]: *Geol. Soc. America Bull.*, v. 66, p. 1581-1582.
- 1956, The problem of the Cochrane in late Pleistocene chronology: *U. S. Geol. Survey Bull.* 1021-J, p. 303-331.
- 1957a, Tentative correlation of Alaskan glacial sequences: *Science*, v. 125, no. 3237, p. 73-74.
- 1957b, Alaskan evidence in support of a post-Illinoian, pre-Wisconsin glaciation [abs.]: *Geol. Soc. America Bull.*, v. 68, p. 1906.
- 1959, Reassessment of radiocarbon dating and correlations of standard late Pleistocene chronologies [abs.]: *Geol. Soc. America Bull.*, v. 70, no. 12, pt. 2, p. 1627.
- Leighton, M. M., 1958, Important elements in the classification of the Wisconsin glacial stage: *Jour. Geology*, v. 66, no. 3, p. 288-309.
- Miller, J. P., 1958, Problems of the Pleistocene in Cordilleran North America, as related to reconstruction of environmental changes that affected early man: *Univ. Arizona Bull.*, v. 28, no. 4, p. 19-49.
- Olson, E. A., and Broecker, W. S., 1959, Lamont natural radiocarbon measurements V.: *Am. Jour. Sci., Radiocarbon Supplement*, v. 1, p. 506.
- Wiseman, J. D. H., 1958, La topographie et la géologie des profondeurs océaniques: *Colloques Internationaux, Centre National de las Recherche Scientifique*, v. 83, p. 193-208.
- 1959, The relation between paleotemperatures and carbonate in an equatorial Atlantic pilot core: *Jour. Geology*, v. 67, no. 6, p. 685-690.

## 154. SURFICIAL DEPOSITS OF ALASKA

By THOR N. V. KARLSTROM, Washington, D.C.

---

*Work done in cooperation with the Office, Chief of Engineers*

---

The surficial deposits of Alaska map (compilation scale 1:1,584,000) provides for the first time a regional synthesis of geologic information on the surficial deposits of the State. A preliminary copy of the map, on open-file inspection at Washington, D.C., was exhibited by the U.S. Geological Survey at the First International Symposium on Arctic Geology, Calgary, Canada, January 1960. Final compilation is in progress.

The map, a product of over 50 years of geologic mapping in Alaska, incorporates field observations of numerous geologists, and was compiled in coordination with a Survey Committee appointed to compile a glacial map of Alaska. Principal collaborators in compilation are Henry W. Coulter, John R. Williams, Arthur T. Fernald, David M. Hopkins, Troy L. Péwé, and Harald Drewes.

**MAP EXPLANATION**

Density and quality of information on surficial deposits varies appreciably from region to region in Alaska; the map legend is designed to show available information at various levels of completeness. The deposits are classified, where possible, into genetic categories including glacial, glaciofluvial, glaciolacustrine, fluvial, eolian, volcanic, and coastal-type sediments. Where such distinctions are not possible, broader categories are used to show the deposits as sedimentary complexes associated with different types of mountainous and hilly terrain, and as undifferentiated units in unmapped parts of lowlands and broad upland valleys.

The glacial deposits are subdivided, largely on the basis of morainal sequence and morphology, into four map units ranging in age from early Pleistocene to Recent. The age ranges of the nonglacial surficial deposits are placed in reference to the glacial sequence. The moraine units represent the major subdivisions recognized in most regions. More refined subdivisions made in local areas are shown by lines representing significant moraine boundaries within the mapped units. The named glacial deposits of published chronologies included within each map unit are listed in a chart. The chart has been brought up to date by each geologist involved, and represents the latest judgments

on correlations between the moraine sequences of Alaska.

In addition to an areal breakdown of deposits into 23 genetic and age categories, the map shows (a) distribution of present glaciers and ice fields; (b) location of significant stratigraphic sections, high-level glacial drifts, and erratics, with accompanying brief descriptions in an inset; (c) major faults along which surficial deposits have been displaced locally; (d) inferred boundaries of submarine glacial drift in coastal areas; and (e) regions compiled by each principal contributor (presented in an index map and accompanied by a list of principal sources of information).

**SCIENTIFIC RESULTS**

The pattern of surficial deposits in Alaska provides basic geologic information bearing primarily on the State's Quaternary history. As field mapping continues, refinements in the map and in geologic interpretations will follow.

In figure 154.1 the surficial deposits are generalized to show regional units which reflect the major geomorphic environments and dominant geologic processes that affected Quaternary deposition.

The major areas of coastal sediments are restricted to the Arctic coastal plain, the north coast of Seward Peninsula, and the large Bering Sea delta formed at the mouths of the Yukon and Kuskokwim Rivers. Elsewhere emerged coastal sediments are restricted to narrow discontinuous zones commonly interrupted by abrupt rocky shorelines. Where studied, the coastal deposits record complex sea level changes of both tectonic and eustatic origin. The present coastal deposits are much more restricted than in the past, when marine regressions accompanying Pleistocene glaciations exposed vast areas of shallow sea bottom, particularly in the Bering Sea.

Important areas of fluvial deposits occur in the unglaciated interior region where thick alluvium underlies the Yukon and other large valleys. Likewise the main areas of thick eolian deposits lie in unglaciated regions bordering heavily glaciated terrain or along major valleys of the interior. Deposits with high percentages of volcanic material are associated with vol-

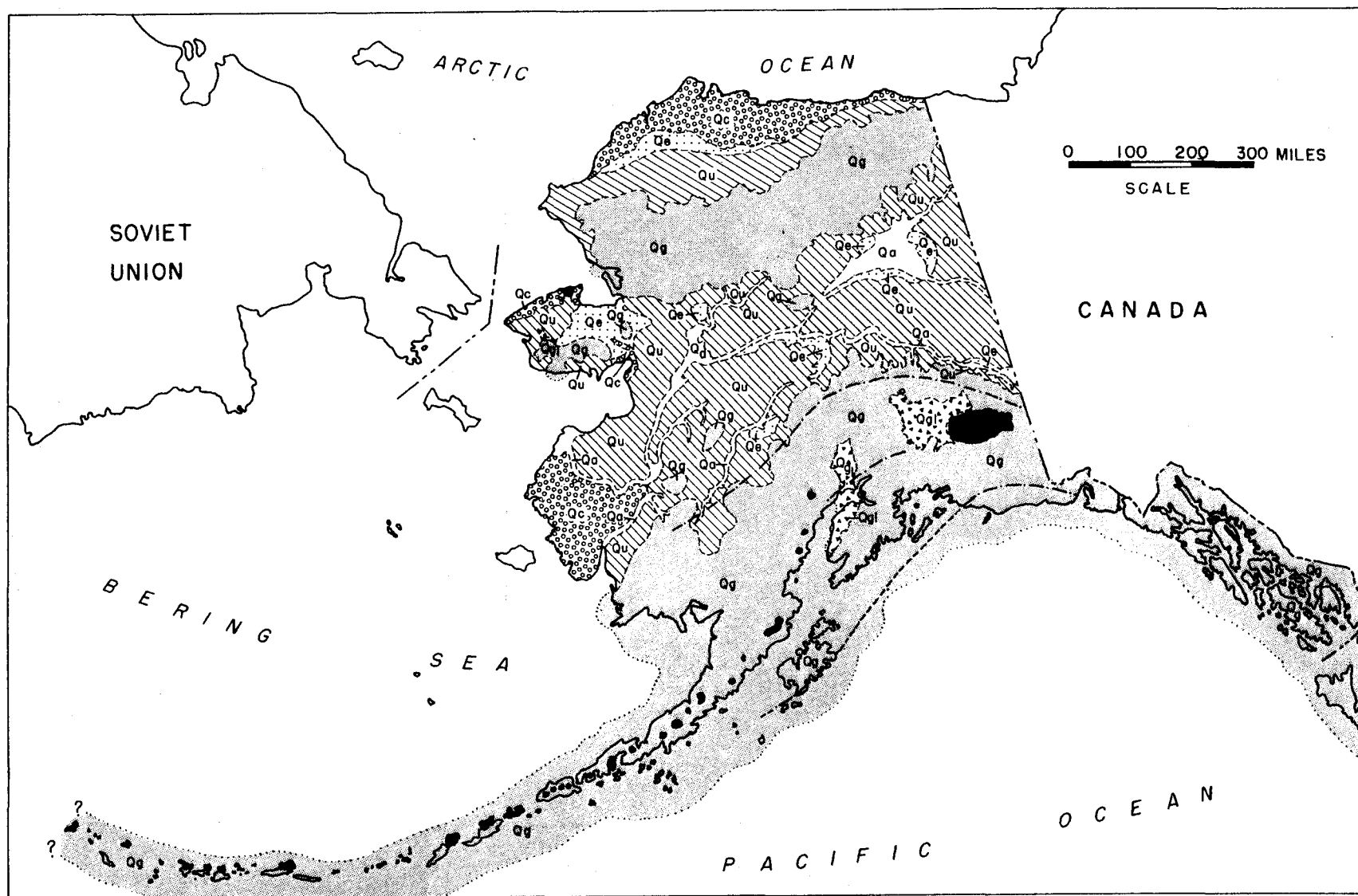


FIGURE 154.1.—Sketch map of major regional groups of surficial deposits in Alaska. Qg—glacial and other deposits associated with heavily glaciated alpine mountains; Ggl—glaciolacustrine deposits of larger Pleistocene proglacial lakes; Qu—undifferentiated deposits associated with generally unglaciated uplands and lowlands of the interior and North Slope; Qa—fluvial deposits; Qe—eolian deposits; and Qc—coastal deposits of interbedded marine and terrestrial sediments. Solid black areas—deposits associated with volcanic peaks and flows of Quaternary and Tertiary age. Heavy dot-dash lines—traces of major pre-Quaternary faults recording local Quaternary displacements (washed lines—inferred trace). Dotted lines—inferred, partly schematic, boundaries of submarine glacial deposits.



canic peaks of Quaternary and Tertiary age along the Aleutian chain and in the Wrangell Mountains, and with cones and flows of Quaternary age on Seward Peninsula. Thick proglacial lake deposits, including "till-like" stony silt, locally underlie basins and trunk valleys in or adjoining the glaciated regions, and record ice damming of regional drainage lines during one or more glaciations.

Quaternary faulting, recorded by minor offsets of surficial deposits, is concentrated along major arcuate pre-Quaternary fault zones cutting underlying bedrock, and assists in delineating these regional fault trends as important linear elements in the tectonic structure and history of the State. Greatest Quaternary movement seemingly was concentrated along the Chugach-St. Elias fault of southern coastal Alaska. Elevated strandlines and marine deposits along the coast south of the fault record notable tectonic displacements during late Quaternary time. In contrast, the evidence along the coast north of the fault indicates essential crustal stability over the same time interval.

The regional pattern of glacial deposits provides significant information on the nature of Quaternary climatic changes in Alaska. The deposits, recording

separate, successively less extensive glaciations, form subparallel belts flanking the alpine mountain ranges. The regional distribution indicates that the Pleistocene glaciers: (a) fed from the same high areas which essentially comprise the modern alpine divides, (b) were largest near the Pacific coast and progressively smaller northward towards the Arctic coast, and (c) were more extensive on the south slopes than on the north slopes of all the alpine ranges. This regional glacial intensity pattern, repeated during each glaciation, conforms with the distribution of existing glaciers, with regional southward inclination of the modern climatic snowline, and with present climatic zonation orographically produced by predominant precipitation supplies from the Pacific Ocean. The pattern reveals neither significant differential uplifts between the coastal mountains north of the Chugach-St. Elias fault and the Alaska and Brooks Ranges nor profound regional atmospheric circulation changes throughout the period of morainal record. The recorded shifts towards more glacial climate thus appear to have been produced primarily from increased precipitation rates resulting from intensification of atmospheric circulation patterns centered, as today, in the North Pacific.



## 155. RECENT EUSTATIC SEA-LEVEL FLUCTUATIONS RECORDED BY ARCTIC BEACH RIDGES

By G. W. MOORE, Menlo Park, Calif.

*Work done in cooperation with the U.S. Atomic Energy Commission*

In the areas near Point Hope and Cape Krusenstern, on the northwestern coast of Alaska, extensive barrier bars composed of numerous beach ridges have been formed since the last major rise of sea level. These areas are about 300 km northwest of Bering Strait and about 190 km apart. The building of gravel beach ridges has prograded the shoreline (moved it seaward) approximately 2 km at Point Hope and 7 km at Cape Krusenstern. Sea level rose nearly to its present position in this area (and throughout the world) about 3000 B.C. (Hopkins, 1959), and the ridges were formed more recently. The age of many of the ridges can be closely estimated from archeological findings. The former inhabitants subsisted principally on marine mammals, and it is safe to assume that they lived close

to the sea (Giddings, 1960); the present-day Eskimos build their houses about 100 m from the shoreline. The dated beach ridges thus provide evidence regarding former positions of sea level.

John Y. Cole, Jr., assisted in the geological work. The estimates of age were made possible by archeological studies, especially those of J. L. Giddings of Brown University, who made some of his results available to us before he had published them.

The barrier bars extend parallel to the shore for about 15 km at both Point Hope and Cape Krusenstern. The individual beach ridges in the barrier bars are remarkably persistent. The highest ridges stand about 3 m above sea level. The amplitudes between crests and swales may be as much as 2 m, and the

crests are, on the average, about 50 m apart. At both localities the broader parts of the barriers partly enclose large lagoons.

The beach ridges were evidently formed either during storms or during periods when persistent onshore winds caused a temporary rise in sea levels. There is some evidence that their growth was mainly due to persistent winds, for whereas the total range of ordinary astronomical tides in this area is only a few tenths of a meter, we have observed that sea level rises more than a meter during some onshore winds. But the beach ridges probably have a broader significance. As the number of beach ridges is only a small fraction of the number of violent storms and abnormally high wind tides that must have occurred while the ridges were being formed, the ridges may record minor world-wide eustatic changes of sea level, or may at least mark the limits of its fluctuations.

There are three reasons for regarding this region as an especially suitable place for finding evidence of former small eustatic changes of sea level: (a) The region was not glaciated during the Wisconsin stage, and therefore did not then undergo isostatic readjustments due to melting of ice; (b) it has not recently been subjected to rapid erosion or sedimentation that would cause isostatic uplift or downwarping; and (c) it does not contain epicenters of any recent earthquakes, which indicates that it is not tectonically active. There is no evidence that any crustal movements have occurred in the region during the last few thousand years. Apart from the minor irregularities associated with the beach ridges, the general altitude of beach sediments is remarkably uniform at both Point Hope and Cape Krusenstern.

In the Cape Krusenstern area, which contains the oldest ridges, the older beach deposits are slightly lower than the younger ones. The oldest dated beach ridge at Cape Krusenstern was formed earlier than 2500 B.C. (Giddings, 1960, p. 127). The highest part of this ridge is about 2 m above sea level, whereas comparable parts of more recent beach ridges in this area are 3 m above sea level. Beaches older than 2500 B. C. and that are farther from the shore and nearer the lagoon are lower; some are submerged in the lagoon behind the cape and are below present sea level, which is here at least 3 m higher than it was when the ridges were formed. The conditions at Cape Krusenstern may be interpreted as follows: Sea level was once considerably lower than it is at present, but rose at some time near 3000 B.C. until it was only about 3 m below its present position. Since then it has been slowly rising, probably at an uneven rate. The late submergence may con-

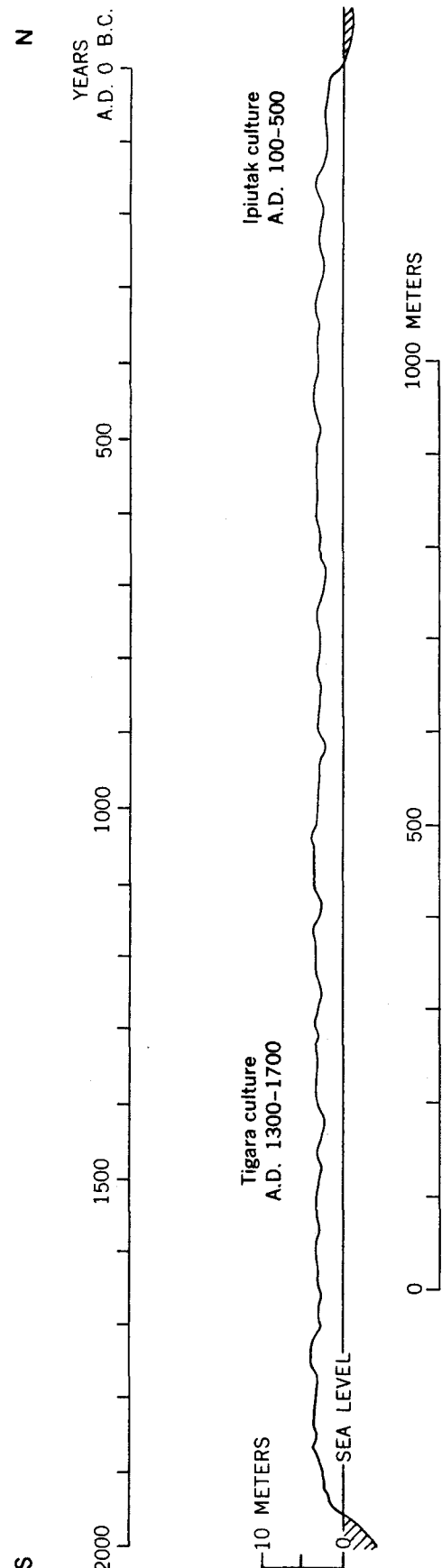


FIGURE 155.1.—Profile through beach ridges at Point Hope, Alaska, with estimated absolute time scale.

ceivably have been due to downwarping, but it appears far more likely, in view of the evidence for the general stability of the coast, that the submergence resulted from eustatic rise of sea level.

At Point Hope the youngest beach ridges have been related to an absolute time scale (fig. 155.1) by the Tigara culture (A. D. 1300–1700) and the Ipiutak culture (A.D. 100–500), which have both been dated by the radiocarbon method (Rainey and Ralph, 1959). The oldest beach ridges now preserved at Point Hope were formed about 200 B. C. Older ridges have been removed by wave erosion cutting inward from the opposite side of the point. The shoreline south of Point Hope is prograding at about 80 m a century, and new ridges have formed at average intervals of about 60 years. Two especially high beach ridges indicate that sea level may have been relatively high from A. D. 1000 to 1100 and from 1700 to 1850, and two especially low

swales indicate that it may have been relatively low from 900 to 1000 and from 1400 to 1500.

Whether these fluctuations are general and accurately dated must remain uncertain until similar studies have been made in other stable parts of the world. As it stands, however, this evidence from Arctic beach ridges indicates that sea level rose about 3 m during the last 5,000 years, and that the rise was characterized by minor fluctuations with an amplitude of 1 to 2 m. The highest stand of sea level since the Wisconsin stage was attained in the 19th century.

#### REFERENCES

- Giddings, J. L., 1960, *The archeology of Bering Strait: Current Anthropology*, v. 1, p. 121–138.  
 Hopkins, D. M., 1959, *Cenozoic history of the Bering land bridge: Science*, v. 129, p. 1519–1528.  
 Rainey, F., and Ralph, E., 1959, *Radiocarbon dating in the Arctic: Am. Antiquity*, v. 24, p. 365–374.



### 156. GENERALIZED STRATIGRAPHIC SECTION OF THE LISBURNE GROUP IN THE POINT HOPE A-2 QUADRANGLE, NORTHWESTERN ALASKA

By RUSSELL H. CAMPBELL, Menlo Park, Calif.

*Work done in cooperation with the U.S. Atomic Energy Commission*

During the summer of 1959 a stratigraphic section of rocks of the Lisburne group, of Early and Late Mississippian age, was measured along continuous sea-cliff exposures southeast of Point Hope, Alaska. Five distinctive lithologic units were recognized in the Lisburne group, which has a total thickness of more than 5,700 feet. The units have been tentatively designated, from oldest to youngest, M<sub>1</sub>, M<sub>2</sub>, M<sub>3</sub>, M<sub>4</sub>, and M<sub>5</sub>.

#### UNIT M<sub>1</sub>

Unit M<sub>1</sub> is about 165 feet thick where measured and is composed of interbedded dark-gray to grayish-black silt-clay shale, medium-gray to dark-gray bioclastic limestone, and grayish-black to black chert. The upper 45 feet consists predominantly of grayish-black shale in beds 0.1 foot to 5 feet thick, composed of fine quartz silt and clay (illite?) with generally minor amounts of disseminated very fine-grained calcite, but it includes a few interbeds of dark-gray limestone. The middle 35 feet consists of grayish-black chert and minor amounts of interbedded dark-gray bioclastic limestone in beds com-

monly about 0.5 foot thick. The lower part of the unit consists chiefly of medium-dark-gray mudstone, in beds 0.1 foot to 8 feet thick, composed of fine quartz silt, clay, and some disseminated fine calcite; but this is interbedded with minor amounts of partly dolomitized bioclastic limestone in beds commonly about 0.5 foot thick. The bioclasts are chiefly crinoid columnals and Bryozoa, but brachiopods and horn corals are locally abundant, and the unit contains a few colonial corals and gastropods.

The upper shaly zone locally intertongues with the overlying unit, M<sub>2</sub>. The contact of M<sub>1</sub> with the sandstone-shale formation that underlies the Lisburne group is gradational.

#### UNIT M<sub>2</sub>

Unit M<sub>2</sub> is about 225 feet thick. It consists wholly of light-gray to light olive-gray bioclastic limestone composed predominantly of sparry calcite fossil fragments ranging from fine sand to very fine pebbles in size, with generally minor amounts of very fine quartz

silt, cemented with sparry calcite and microcrystalline quartz in varying proportions. Microcrystalline quartz also commonly forms rims around fossil fragments and spongy intergrowths with calcite that preserve organic structures within the fragments. In some places fossil fragments have been partly dolomitized. The chief recognizable fossils are crinoid columnals and Bryozoa, but brachiopods and horn corals are also present.

The unit is very thick bedded, locally cropping out as a single thick bed with a few short, discontinuous, uneven bedding planes. Bedding is expressed internally by crinkly uneven laminae at generally regular intervals of 0.5 inch to 1 foot. The contact with the overlying unit Ml<sub>3</sub> is conformable.

#### UNIT Ml<sub>3</sub>

Unit Ml<sub>3</sub> is about 1,650 feet thick and consists predominantly of interbedded dark-gray bioclastic limestone and grayish-black quartz-calcite siltstone. It contains relatively abundant well-preserved fossils. The limestone is composed chiefly of sparry calcite bioclasts of fine-sand to fine pebble size with variable amounts of fine quartz silt, sparry calcite cement, microcrystalline quartz cement, very finely crystalline dolomite cement, and, in a few beds, a small amount of clay (illite?). Replacement of fossils by microcrystalline quartz has occurred, and may be found in all stages from thin rims around bioclasts, through spongy intergrowths preserving organic structure, to complete replacement. The most abundant fossils are crinoid columnals and Bryozoa, but brachiopods, horn corals, and colonial corals are also locally common. Nodular limestone beds containing variable amounts of dark-gray to black chert are common at some horizons. Dark chert is locally abundant in several zones, chiefly as lenticular nodules and irregular angular masses in limestone. The basal 50 feet of unit Ml<sub>3</sub> contains several very thick beds of grayish-black quartz-clay-calcite siltstone containing sparsely scattered small pyrite concretions and a few pyritized fossils.

Rhythmic interbedding of limestone beds 0.2 to 1 foot thick with silt shale laminae 0.01 to 0.1 foot thick is characteristic of the unit. The bedding is generally regular and continuous, although the bedding surfaces are very slightly undulating to very uneven, the uneven surfaces being on nodular beds. The thickness of the silt shale interbeds and the abundance of shaly zones generally decrease upward. The contact between units Ml<sub>3</sub> and Ml<sub>4</sub> was arbitrarily placed at the base of the lowermost thick-bedded dolomitic limestone, but the units grade into each other.

#### UNIT Ml<sub>4</sub>

Unit Ml<sub>4</sub> consists predominantly of light-gray to dark-gray very finely crystalline dolomitic limestone, interbedded with generally minor amounts of dark-gray partly dolomitized bioclastic limestone and a few interbeds and partings apparently consisting largely of calcareous quartz clay siltstone. The bioclastic limestone consists chiefly of sparry calcite fossil fragments ranging in size from fine sand grains to fine pebbles. In some beds the fragments are cemented and in places partly replaced by very finely crystalline dolomite; in other beds they are in a matrix of microcrystalline calcite or dolomite or both. Light-gray and dark-gray chert commonly forms nodules and continuous and discontinuous layers in some limestone beds. The chert content varies greatly from bed to bed, and also along the strike of individual beds. About 140 feet below the top of the unit is a zone of breccia about 400 feet thick, composed of very small to very large fragments of chert and dolomitic limestone in a microcrystalline matrix that is predominantly dolomite. Crinoid columnals and bryozoa predominate in the bioclastic limestone, but horn corals, colonial corals, brachiopods, and a blastoid (*Pentremites?*) were also found. A total of about 3,330 feet of strata was assigned to unit Ml<sub>4</sub> where the section was measured. An unknown thickness has been faulted out of the upper part by three high-angle faults, one of which forms the contact with the unit Ml<sub>5</sub>.

Irregular interbedding of thin, medium, thick, and very thick beds is characteristic of the unit. Very thick beds, one as much as 140 feet thick, of crystalline dolomitic limestone are relatively abundant and commonly show internal horizontal and gently cross-stratified current lamination, brought out by low-contrast color banding. The bedding planes are commonly even but many are discontinuous.

The contact between units Ml<sub>4</sub> and Ml<sub>5</sub> is a high-angle fault where well exposed on the sea cliff, but probably only a few hundred feet of strata are missing.

#### UNIT Ml<sub>5</sub>

Unit Ml<sub>5</sub>, the youngest unit of the Lisburne group, is about 330 feet thick in the incomplete section measured. It consists of interbedded grayish-black chert, dark-gray to medium-dark-gray calcareous and non-calcareous siltstone and mudstone, dark-gray to light medium-gray very finely crystalline to microcrystalline calcitic limestone, and a smaller amount of greenish-black to dark-greenish-gray chert and noncalcareous argillite. Most of the chert is in beds 0.1 foot to

2 feet thick, with slightly uneven but generally continuous bedding surfaces. The limestone beds contain variable but generally small amounts of nodular chert. The siltstone and mudstone beds range from less than 0.1 foot to 3 feet in thickness. The limestone is commonly in beds 0.6 to 1 foot thick. The bedding is generally continuous, regular, and even. Fossils are very rare, but a few gastropods were collected from one siltstone bed.

The contact with the overlying Siksikpuk formation, of Permian(?) age, is a high-angle fault where the rocks are well exposed. Further inland, however, the configuration of the contact, together with the presence in unit M<sub>1</sub> of interbedded greenish-gray chert and argillite resembling rocks in the Siksikpuk formation, suggests that the Siksikpuk grades into the Lisburne group, and that the missing part of the measured section is not more than a few hundred feet thick.



# 157. A MARINE FAUNA PROBABLY OF LATE PLIOCENE AGE NEAR KIVALINA, ALASKA

By D. M. HOPKINS and F. S. MACNEIL, Menlo Park, Calif.

In 1957, the Rev. Milton Swan of Kivalina, Alaska, found a beautifully preserved shell of *Patinopecten* (*Fortipecten*) *hallae* (Dall) near Kivalina, Alaska, on the coast of Chukchi Sea about 200 miles north of Bering Strait (fig. 157.1). Because of the importance of the find (Hopkins, 1959, p. 1521) Hopkins visited the Kivalina locality briefly in 1959 to examine the stratigraphy and to collect additional fossils. This report summarizes the results of field observations by Hopkins, and studies of the mollusks by MacNeil, of the Foraminifera by Ruth Todd, and of the ostracodes by I. G. Sohn.

## GEOLOGIC SETTING

The fossiliferous sediments lie at the inner edge of a coastal plain that fringes the Chukchi Sea coast from 30 miles to the northwest to 150 miles to the southeast of Kivalina. Northwest of Kivalina Lagoon, the coastal plain consists of a nearly horizontal surface less than 25 feet above sea level, terminated at its inner edge by a scarp (fig. 157.1), apparently carved in unconsolidated material, that is similar in appearance and altitude to the ancient wave-cut scarp of Second Beach, of Sangamon age, at Nome (MacNeil, Mertie, and Pilsbry, 1943; Hopkins, MacNeil, and Leopold, in press). Inland from this scarp a smooth surface slopes gently upward, but just north of Kivalina Lagoon and about 50 feet above sea level it is interrupted by a second row of scarps carved in bedrock. The marine fossils were obtained near the projected trend of the second row of scarps, in a small valley that enters the Kivalina River about 1.3 miles above Kivalina Lagoon. The second row of scarps probably represents a wave-cut cliff carved during the maximum landward trans-

gression of Chukchi Sea during late Cenozoic time; it may represent the shoreline at the time that the fossiliferous sediments were deposited.

The marine fauna was obtained from black organic clay, pebbly clay, and silty sand, having a total thickness of 10–15 feet. The sediments rest upon limestone bedrock containing abundant corals of Mississippian age (Helen Duncan, written communication, 1960), and are overlain by 10 to 15 feet of light olive gray sand-free pebble gravel and sandy pebble gravel and 5 to 10 feet of windblown silt (fig. 157.2). The base of the marine clay lies 17.5 feet above the surface of the Kivalina River and probably about 20 feet above sea level; the top lies about 30 feet above the river. Scattered through the basal layers are poorly rounded cobbles and boulders as much as 3 feet across, some consisting of limestone perforated with pholad borings, and others of pebble conglomerate and basalt. The fauna obtained from the marine clay is listed in table 157.1.

The pebble gravel overlying the fossiliferous marine clay is considerably more extensive than the clay itself; it rests directly on the limestone bedrock along the north bank of the Kivalina River downstream from the creek in which the marine clay is exposed, and it may extend throughout the gently sloping area at the inner edge of the coastal plain north of Kivalina Lagoon. Although the gravel is only 10 to 15 feet thick where it overlies the marine clay, it is at least 30 feet thick nearer Kivalina Lagoon.

The gravel consists chiefly of pebbles of chert and limestone a quarter of an inch to an inch in diameter; the small pebbles are well rounded, but the large ones are subrounded to subangular. Limestone pebbles in

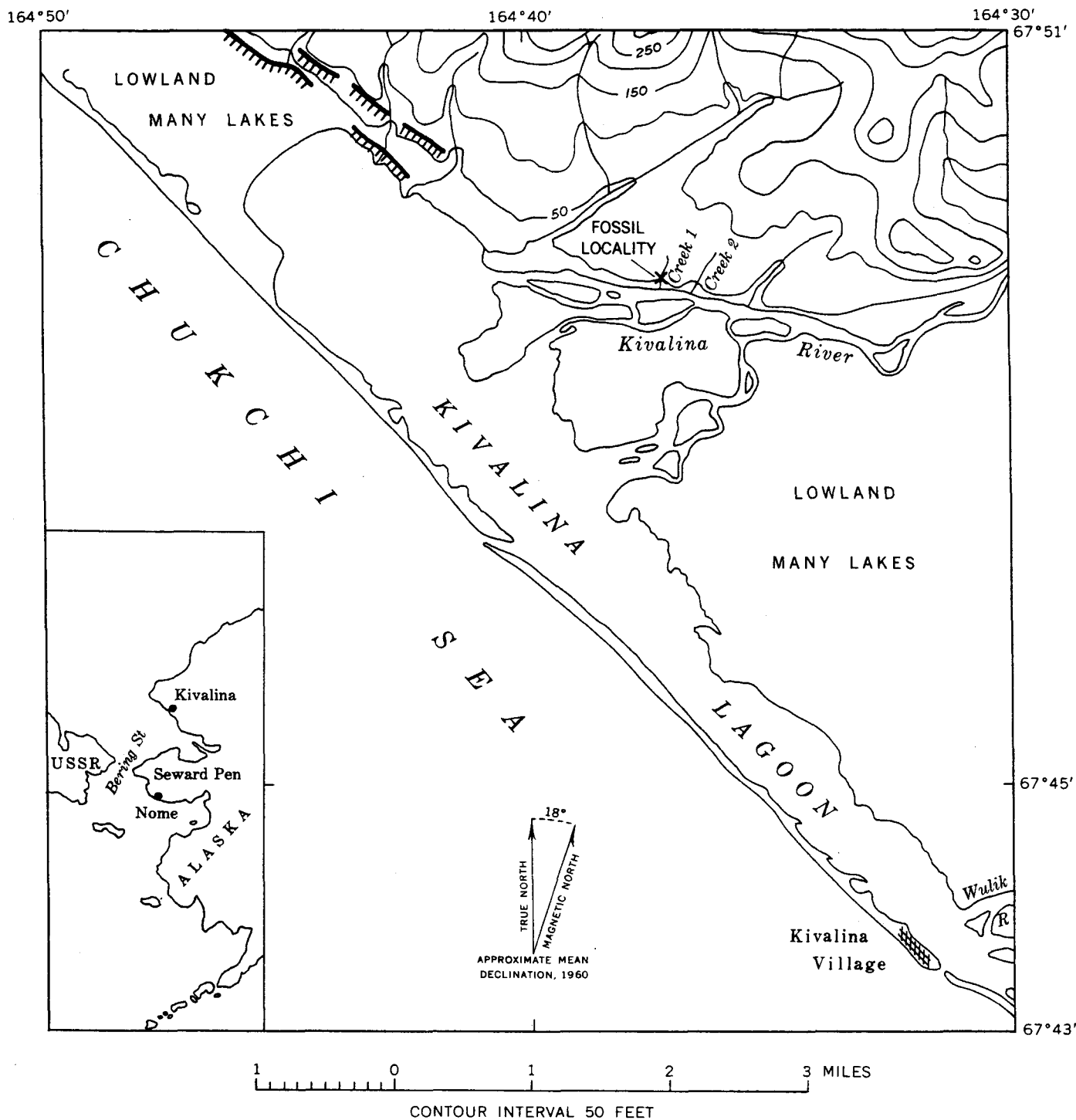


FIGURE 157.1.—Location of fauna probably of Pliocene age near Kivalina, Alaska. Hachures represent scarps believed to be ancient wave-cut cliffs. The lower scarp was probably formed during the last Pleistocene interglacial interval; the upper scarp (between the 50- and 100-foot contours) may have been formed during Pliocene time. Base map adapted from Coast and Geodetic Survey preliminary topographic sheets

the gravel are strongly leached. Where the gravel rests directly on bedrock, the basal layers contain boulders of basalt and limestone one or two feet in diameter, some of which are riddled with pholad borings. No

Cenozoic fossils have been found in the gravel. The fineness of the gravel, the lack of a sandy matrix in some layers, and the pholad-bored boulders in the basal layers suggest that the gravel is a marine sediment, but

TABLE 157.1.—List of fossils from marine clay near Kivalina, Alaska, and their occurrence at Nome, Alaska, and in Bering and Chukchi Seas<sup>1</sup>

	Subma- rine Beach	Third Beach- Int. Beach	Second Beach	Recent in Ber- ing and Chukchi Seas
<b>Pelecypoda:</b>				
<i>Patinopecten (Fortipecten) hallae</i> (Dall).....	?			
<i>Astarte hemicymata</i> Dall.....	×	×		
<i>Astarte nortonensis</i> MacNeil.....	×	×		
<i>Cardita (Cyclocardia) subcras-</i> <i>sidents</i> MacNeil.....	×	×	×	×
<i>Cardita (Cyclocardia) crebico-</i> <i>stata</i> (Krause).....	×	×	×	×
<i>Serripes groenlandicus</i> (Brugi- ère).....	?		×	×
<i>Mya</i> sp. ( <i>truncata</i> or <i>japonica</i> )..	×	×	×	×
<i>Saxicava arctica</i> (Linnè).....	×	×	×	×
<b>Gastropoda:</b>				
<i>Admete</i> or <i>Buccinum</i> .....	×	×		×
<i>Neptunea</i> aff. <i>N. ventricosa</i> (Gmelin).....				×
<i>Colus</i> aff. <i>C. halibrectus</i> Dall.....				?
<i>Boreotrophon</i> sp. cf. <i>B. rotun-</i> <i>datus</i> (Dall).....				?
<i>Polinices pallida</i> Broderip and Sowerby.....				×
<b>Foraminifera:</b>				
<i>Buccella inusitata</i> Andersen.....	×			×
<i>Elphidiella hannai</i> (Cushman and Grant).....	×			
<i>Elphidiella nitida</i> Cushman.....	×	×		
<i>Elphidium clavatum</i> Cushman.....	×	×	×	×
<i>Elphidium orbiculare</i> (Brady).....	×	×		
<i>Elphidium subarcticum</i> Cushman.....	×	×		×
<i>Quinqualoculina seminulum</i> (Linnè).....				×
<b>Ostracoda:</b>				
<i>Clithrocytheridea</i> sp.....	?			?
<i>Haplocytheridea</i> sp.....				?
<i>Cytheridea</i> ? s.l. sp.....				?
<i>Hemicytherura</i> ? sp.....				?
" <i>Cythereis</i> " s.l. sp.....				?
Gen. aff. <i>Trachyleberis</i> sp.....				?
Gen. aff. <i>Loxoconcha</i> sp.....				?

<sup>1</sup> Fossil occurrences at Nome from MacNeil, Mertie, and Pilsbry (1943) and Hopkins, MacNeil, and Leopold (in press). Recent occurrences in Bering and Chukchi Seas from those sources and from MacGinitie (1959), Loeblich and Tappan (1953), and Patsy Smith, table 3 in Scholl and Sainsbury (1960).

the relatively poor rounding of the larger pebbles suggests a fluvial origin.

#### AGE AND AFFINITIES OF THE FAUNA FROM THE MARINE CLAY

The fauna in the marine clay near Kivalina is probably of late Pliocene age but possibly of early Pleistocene age. It is closely similar to both the fauna of

Submarine Beach (probably late Pliocene) and that of Third Beach-Intermediate Beach (middle Pleistocene) at Nome (table 157.1). The stratigraphic relations, however, suggest a correlation with Submarine Beach rather than with Third Beach-Intermediate Beach. The fauna is generally similar to Pliocene and Pleistocene molluscan faunas from the Gubik formation in northern Alaska described by MacNeil (1957), and quite different from Miocene and Pliocene molluscan and foraminiferal faunas from the Nuwok formation of Dall (1919) of northeastern Alaska described by MacNeil (1957) and Todd (1957). One of the ostracode species, *Clithrocytheridea* sp., is present in the Gubik formation, and the others are similar to undescribed species in the Gubik formation (I. G. Sohn, written communication, 1960).

Representatives of all of the mollusks except *Patinopecten (Fortipecten) hallae* and *Astarte hemicymata*, and of all of the Foraminifera except *Elphidiella hannai* and *Elphidiella nitida*, are found in Bering and Chukchi Seas today. *Patinopecten (Fortipecten) hallae* and *Astarte hemicymata* are extinct; *Elphidiella hannai* and *Elphidiella nitida* have been reported as living forms only from the North Pacific Ocean. The presence of *Fortipecten* in the Kivalina fauna constitutes strong evidence for regarding that fauna as Pliocene, because in Japan and Sakhalin that subgenus is confined to beds of Pliocene age (Yabe and Hatai, 1940; K. Kobayashi, written communication, 1959). However, *Fortipecten* could not have reached Kivalina until Bering Strait came into existence, and Hopkins (1959) presents evidence indicating that the first seaway through Bering Strait opened no earlier than late Pliocene time.

A minimum age for the marine clay is established by the stratigraphic relations between the overlying gravel and the windblown silt by which the gravel is itself overlain. Study of air photos suggests that the lowland southeast of the Kivalina River represents an outwash plain mantled within the area of figure 157.1 by marine sediments of Second Beach (Sangamon) age. This plain terminates to the east against moraines resembling those of the Nome River glaciation, of Illinoian age, at Nome. The gravel overlying the fossiliferous marine clay lies above the level of the presumed outwash plain and therefore is probably older. The windblown silt overlying the gravel is probably of the same age as the nearby outwash and therefore largely of Illinoian age. If this reasoning is correct, the marine clay can be no younger than middle Pleistocene.

The physical stratigraphy indicates that the marine clay is the correlative of either Submarine Beach or

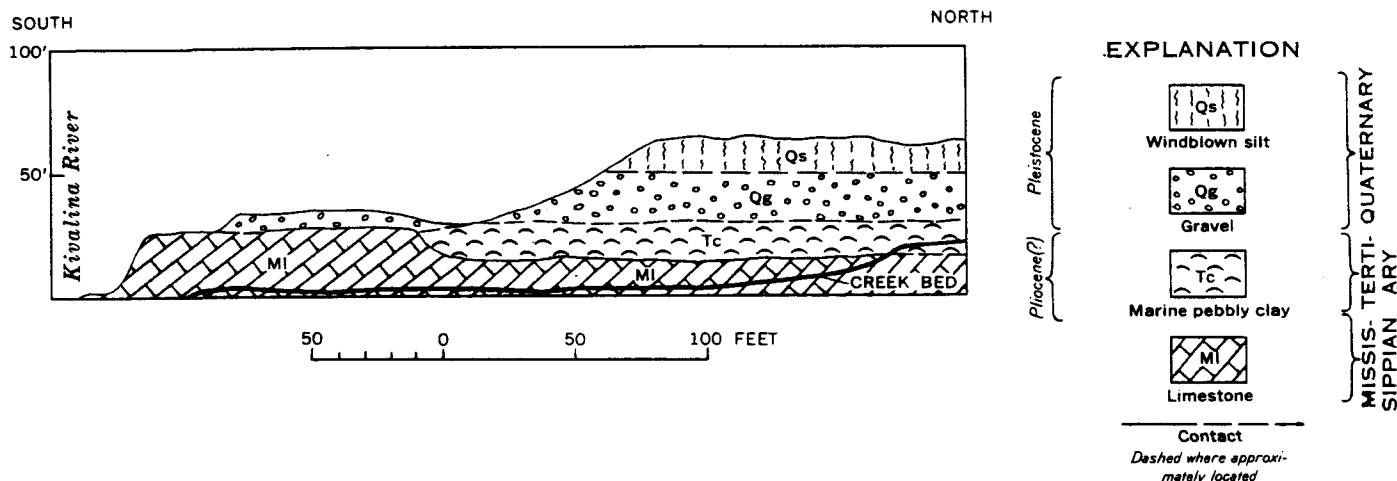


FIGURE 157.2.—Sediments exposed in valley of small tributary entering Kivalina River 1.3 miles above Kivalina Lagoon. Surface of Kivalina River at left is probably less than 5 feet above sea level.

Third Beach-Intermediate Beach at Nome (Hopkins, MacNeil, and Leopold, in press). The fauna is more closely similar to the fauna of Submarine Beach than to that of Third Beach-Intermediate Beach at Nome; and the presence of *Fortipecten* provides strong evidence for a late Pliocene age and for correlation with Submarine Beach at Nome.

#### REFERENCES

- Dall, W. H., 1919, Mollusks, Recent and Pleistocene: Report of the Canadian Arctic Expedition, 1913-1918, v. 8, pt. A, Ottawa.
- Hopkins, D. M., 1959, The Cenozoic history of the Bering land bridge: Science, v. 129, p. 1519-1528.
- Hopkins, D. M., MacNeil, F. S., and Leopold, E. B., in press, The coastal plain at Nome, Alaska: a late Cenozoic type section for the Bering Strait region: Internat. Geol. Cong., 21st, Copenhagen, 1960.
- Loeblich, A. R., Jr., and Tappan, Helen, 1953, Studies of Arctic Foraminifera: Smithsonian Pub. 4105, 150 p.
- MacGinitie, Nettie, 1959, Marine mollusca of Point Barrow, Alaska: U.S. Natl. Museum Proc., v. 109, p. 59-208.
- MacNeil, F. S., 1957, Cenozoic megafossils of northern Alaska: U.S. Geol. Survey Prof. Paper 294-C, p. 99-126.
- MacNeil, F. S., Mertie, J. B., and Pilsbry, H. A., 1943, Marine invertebrate faunas of the buried beaches near Nome, Alaska: Jour. Paleontology, v. 17, p. 69-96.
- Scholl, D. W., and Sainsbury, C. L., 1960, Marine geology and bathymetry of the nearshore shelf of the Chukchi Sea-Ogotoruk Creek area, northwest Alaska: U.S. Geol. Survey TEI-606, issued by U.S. Atomic Energy Comm. Tech. Inf. Service, Oak Ridge, Tenn.; also U.S. Geol. Survey open-file report.
- Todd, Ruth, 1957, Foraminifera from Carter Creek, northeastern Alaska: U.S. Geol. Survey Prof. Paper 294-F, p. 223-234.
- Yabe, Hisakatsu, and Hatai, K. M., 1940, A note on *Pecten* (*Fortipecten* subg. nov.) *takahashii* Yokoyama and its bearing on the Neogene deposits of Japan: Tohoku Imp. Univ. Sci. Rept., ser. 2 (Geology), v. 21, p. 147-160.



#### 158. POSSIBLE SIGNIFICANCE OF BROAD MAGNETIC HIGHS OVER BELTS OF MODERATELY DEFORMED SEDIMENTARY ROCKS IN ALASKA AND CALIFORNIA

By ARTHUR GRANTZ and ISIDORE ZIETZ, Menlo Park, Calif., and Washington, D.C.

Regional aeromagnetic surveys over the Cook Inlet and Copper River Lowlands, Alaska, and the northern and central Great Valley, Calif., record broad total intensity magnetic highs over the belts of Jurassic and Cretaceous marine sedimentary rocks that underlie these areas. These highs are parallel to the major geo-

logic features in each area, and are absent over parallel belts of more severely deformed sedimentary rocks of similar age, which occur in the bordering Chugach Mountains and Alaska Range in Alaska and the Coast Ranges in California. Available magnetic data over the Jurassic slate and greenstone belt in the foothills



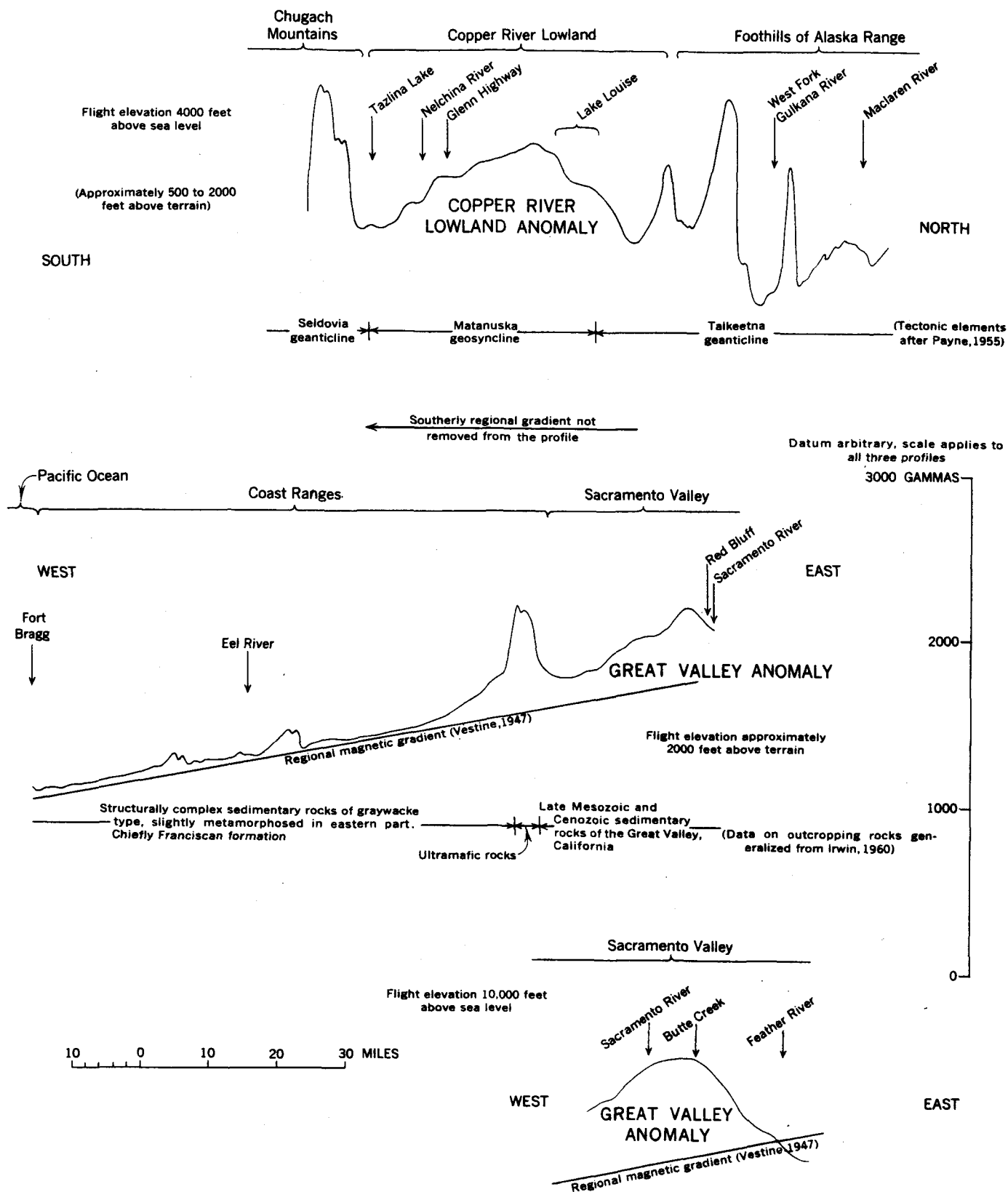


FIGURE 158.1.—Aeromagnetic profiles across Copper River Lowland, Alaska, and Great Valley and Coast Ranges, Calif.

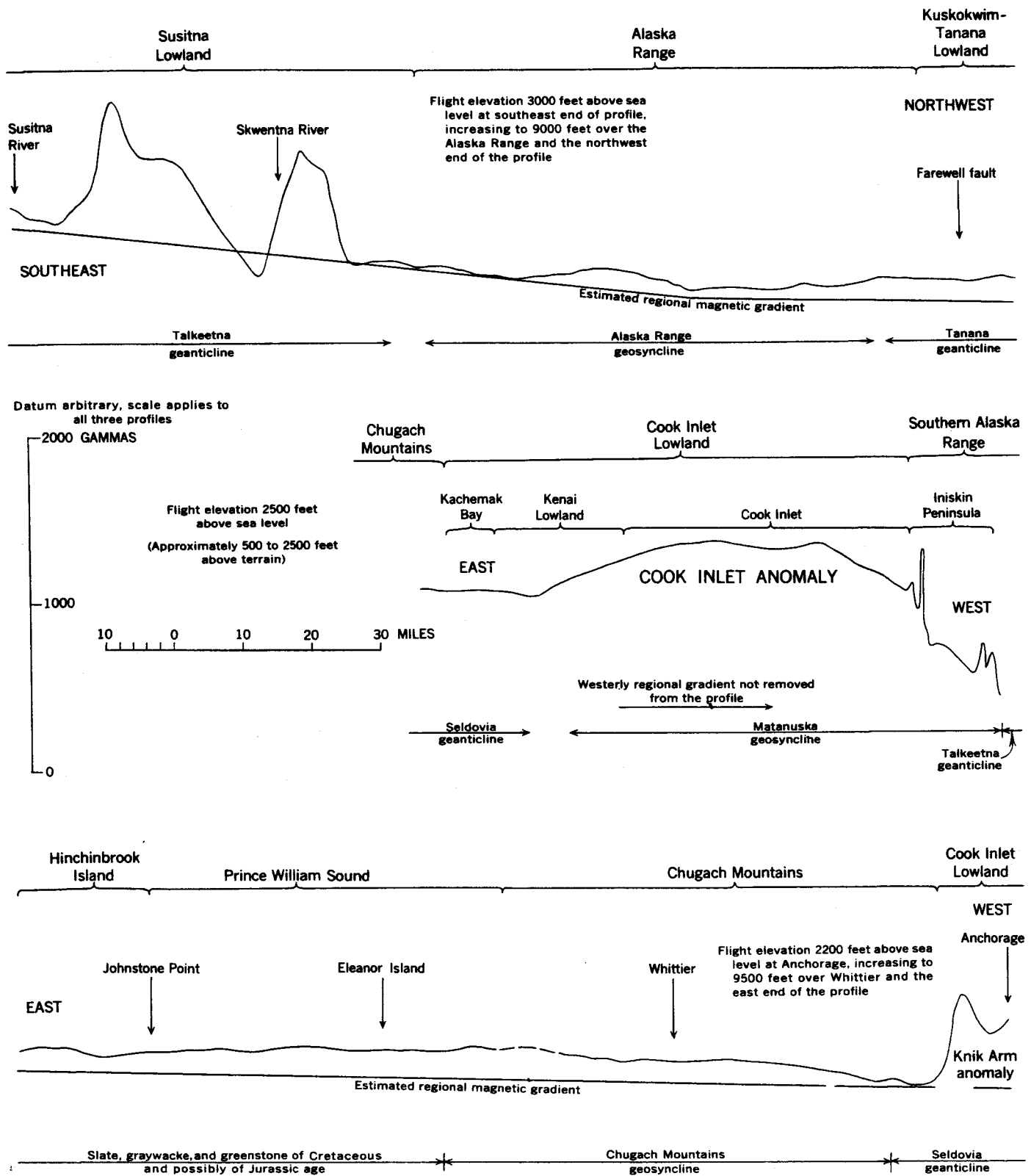


FIGURE 158.2.—Aeromagnetic profiles across Cook Inlet Lowland, Chugach Mountains, and Alaska Range, Alaska.

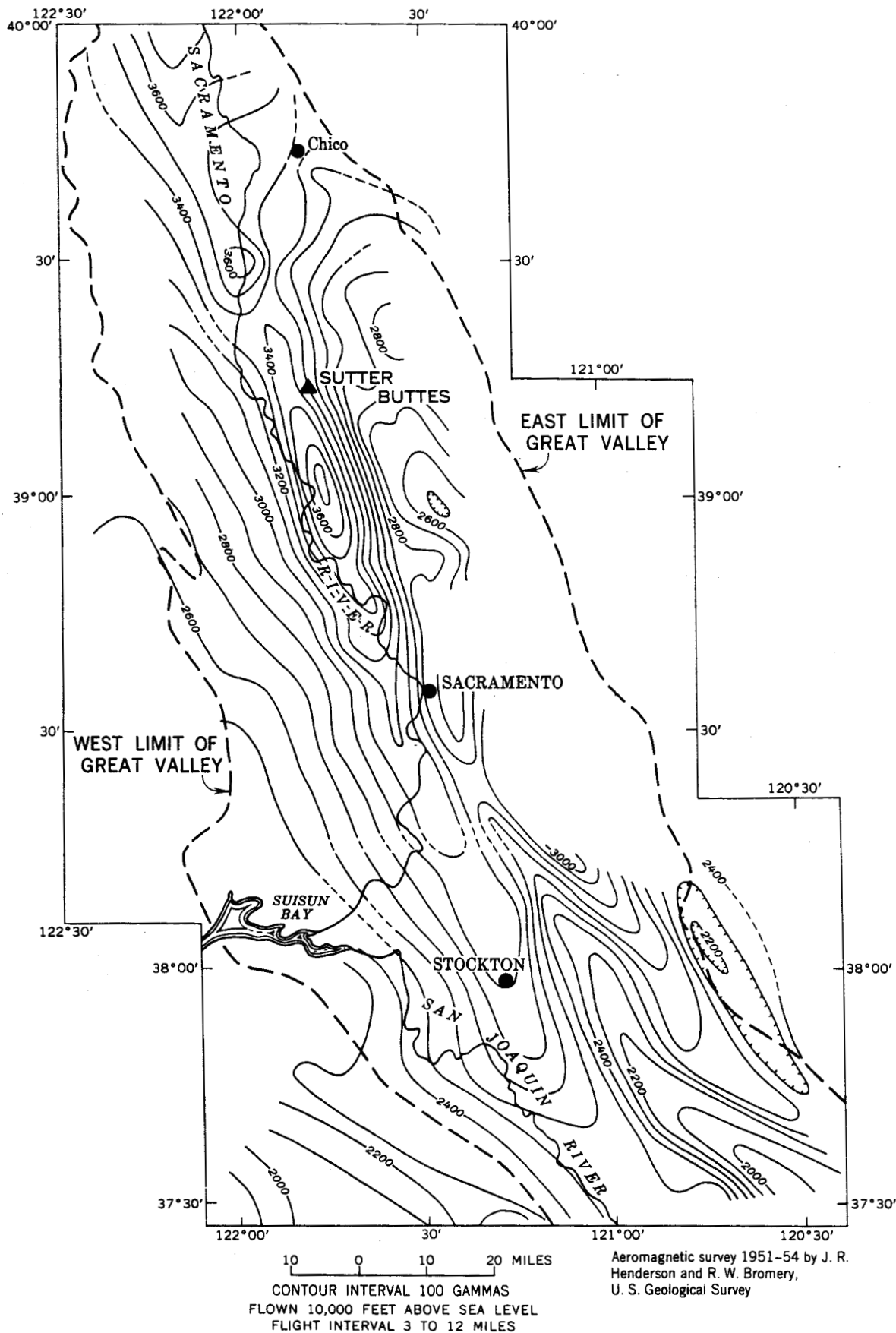


FIGURE 158.3.—Total intensity aeromagnetic map of part of the Great Valley, Calif., relative to arbitrary datum.

of the Sierra Nevada, which borders the Great Valley on the east, record so many magnetic features of shallow origin that it is difficult to determine whether or not broad magnetic highs occur there.

Aeromagnetic profiles across the moderately deformed rocks of the lowland areas and the parallel belts of more severely deformed sedimentary rocks are shown in figures 158.1 and 158.2. The anomalies are seen more clearly if viewed with respect to the sloping regional magnetic gradient. An aeromagnetic map of the northern and central Great Valley is shown in figure 158.3.

The magnetic high over the Cook Inlet Lowland trends northeastward for at least 150 miles, is 50 to 75 miles wide, and has a maximum observed amplitude of about 500 gammas. The magnetic high over the southern Copper River Lowland trends eastward for at least 60 miles, is 35 to 40 miles wide, and has an amplitude of about 400 gammas. The anomaly over the northern and central Great Valley trends northwest along the valley for at least 180 miles, is about 30 miles wide, and ranges in amplitude from a few hundred to more than 1,000 gammas. A broad positive Bouguer gravity anomaly with about the position and width of the magnetic anomaly was found in the Great Valley between the latitudes of Sacramento and Sutter Buttes by George A. Thompson and Manik Talwani (oral communication, March 1960).

The size and gradients of the broad magnetic anomalies suggest that they are produced by areally extensive and thick rock masses that are more magnetic than the surrounding rocks. Depth estimates based on these gradients, patterned after the methods described by Vacquier and others (1951), indicate that a magnetic rock mass may lie 5 to 10 miles beneath Cook Inlet and perhaps as much as 10 miles beneath the southern Copper River Lowland. Depth estimates also indicate that the rocks producing the Great Valley anomaly are buried about 5 to 10 miles, but sharper, superimposed anomalies yield depths that approximate the base of the Mesozoic and Tertiary sedimentary rocks. Because they are magnetic and very large, the rock masses which produce the broad magnetic highs are thought to be igneous.

The Cook Inlet and Copper River Lowland anomalies occur over marine sedimentary rocks deposited in the Matanuska geosyncline (Payne, 1955), which at least in places was a narrow depositional trough. This geosyncline received a thick section of sedimentary rocks of Middle Jurassic to Late Cretaceous age and extended for at least 800 miles from the upper Chitina Valley near the Alaska-Yukon border to a point beyond Herendeen Bay near the tip of the Alaska Peninsula. The

Great Valley anomaly occurs over a belt of marine sedimentary rocks of Late Jurassic to Late Cretaceous age. The crests of the magnetic highs lie several miles north and a few miles east, respectively, of the thickest part of the Mesozoic sedimentary prisms in the Copper River Lowland and the Great Valley, and are probably on the more stable side of the troughs in which the sediments were deposited.

The late Mesozoic sedimentary rocks in the Matanuska geosyncline and the Great Valley are characterized by sandstones that are gradational in lithology between wacke and arenite. They are generally somewhat better sorted than the sandstones in the parallel belts of slate or shale and graywacke in the Chugach Mountains and the Alaska Range in Alaska, and in the Franciscan formation in the Coast Ranges of California.

The sequences of slate or shale and graywacke are apparently very thick, for, although they are intensely folded and faulted, they are the only rocks that crop out over large tracts of mountainous terrain. Their apparent great thickness, poor sorting, and lenticularity, and the presence of interstratified volcanic rocks in some areas, suggest that they were deposited in unstable or tectonically active deep geosynclinal troughs with steep slopes. The sedimentary rocks of the Matanuska geosyncline and the Great Valley are better sorted, probably thinner, and lack interstratified volcanic rocks except thin beds of volcanic ash. They seem to have been deposited in more stable and shallower geosynclinal troughs than the sequences with graywacke.

Structural deformation of the sedimentary rocks of the Matanuska geosyncline and the Great Valley is characteristically gentle to moderate. In contrast, the parallel belts with graywacke are severely deformed. The marked difference in structural deformation between the belts of contrasting lithologic aspect indicates that the area of the Matanuska geosyncline and of the Great Valley continued to be tectonically more stable in latest Mesozoic and Cenozoic time than the belts containing slate or shale and graywacke.

There may be a casual relationship between the existence of the rocks that produce the broad magnetic highs and the structure and lithology of the sedimentary prisms that overlie them. This could be true if the magnetic rock masses are structurally more competent than the rocks under the severely deformed belts, where such broad magnetic highs were not observed. Large competent igneous masses beneath the Matanuska geosyncline and the Great Valley could explain the more stable late Mesozoic depositional environment of these areas and their subsequent greater structural stability.

The suggested contrasts in structural competence be-

tween the rocks underlying the moderately and the severely deformed belts of sedimentary rocks cannot be considered as established by the data at hand, and must be tested by other geophysical methods. For example, it is possible that large, nonmagnetic, structurally competent rock masses underlie the severely deformed belts. Magnetic studies of other areas with analogous structural and stratigraphic conditions are desirable to determine whether the association of the magnetic highs with the tectonically more stable sedimentary belts is more than a local coincidence.



## REFERENCES

- Irwin, W. P., 1960, Geologic reconnaissance of the northern Coast Ranges and Klamath Mountains, California: Calif. Div. Mines Bull. 179 (in press).
- Payne, T. G., 1955, Mesozoic and Cenozoic tectonic elements of Alaska: U. S. Geol. Survey Misc. Geol. Inv. Map I-84.
- Vacquier, Victor, Steenland, N.C., Henderson, R. G., and Zietz, Isidore, 1951, Interpretation of aeromagnetic maps: Geol. Soc. America Mem. 47.
- Vestine, E. H., and others, 1947, Description of the earth's main magnetic field and its secular change, 1905-1945: Carnegie Inst. Washington Pub. 578.

## 159. STRATIGRAPHY AND AGE OF THE MATANUSKA FORMATION, SOUTH-CENTRAL ALASKA

By ARTHUR GRANTZ and DAVID L. JONES, Menlo Park, Calif.

A thick sequence of dark-gray siltstones and shales and light-colored sandstones and conglomerates, all of marine origin, is well exposed in the narrow Matanuska Valley, which extends westward from the southwest Copper River lowland to the town of Palmer (see inset map, fig. 159.1). Martin and Katz (1912, p. 34-39) measured a section of these rocks and were the first to show that they were of Cretaceous age. Martin (1926, p. 317) stated that these rocks " \* \* \* have a broad extent and attain a great thickness in the Matanuska Valley, but they apparently constitute only a single formation \* \* \*", and he proposed that they be named the Matanuska formation.

Mapping by Grantz in the Nelchina area in 1952-57, followed by a stratigraphic reconnaissance by Grantz and Jones farther west in the Matanuska Valley in 1959, demonstrated that several lithologic units within the formation can be mapped in the Nelchina area, and that at least two units can be distinguished by reconnaissance methods in the structurally and stratigraphically complex Matanuska Valley. The difference in the number of units that can be distinguished in the two areas arises from the fact that the structure is simpler, and the exposures more complete, in the Nelchina area than in the Matanuska Valley. The units recognized in the Nelchina area are designated in the schematic columnar sections of figure 159.2. Many of these units are limited at the top by unconformities that record deep erosion. The number indicates that the Matanuska formation was deposited in an unstable seaway.

In the Nelchina area the Matanuska formation unconformably overlies beds of Sinemurian to Neocomian age and is succeeded by coal-bearing rocks of Paleocene or early Eocene age, but the contact at the top of the Matanuska has not been observed. In the Matanuska Valley the Matanuska formation probably rests directly on Lower Jurassic rocks in most places, and regional relations indicate that it is unconformably overlain by the Chickaloon formation, of Paleocene or early Eocene age. As it is here more indurated and more deformed than the Chickaloon formation, it was probably involved in tectonic events that occurred before the Chickaloon formation was deposited.

Study of the numerous collections of mollusks obtained from the formation, and determination of their ages, was begun by Ralph W. Imlay and completed by David L. Jones. These mollusks can be grouped into assemblages of Albian, Cenomanian, Turonian, Campanian, and Upper Campanian and Maestrichtian(?) ages. The critical fossils of these assemblages are listed in table 159.1. Their position in the lithogenetic units is shown in figure 159.2, and the locations of those collected in the Matanuska Valley are shown in figure 159.1.

Albian fossils occur in hard siltstones with sandstone interbeds along the north front of the Chugach Mountains from Palmer to Tazlina Lake, and in distinctly different soft coaly sandstone and abundantly fossiliferous claystone that crop out in the northern part of the Nelchina area. The difference between these rocks is due in part to structural deformation, which was ac-

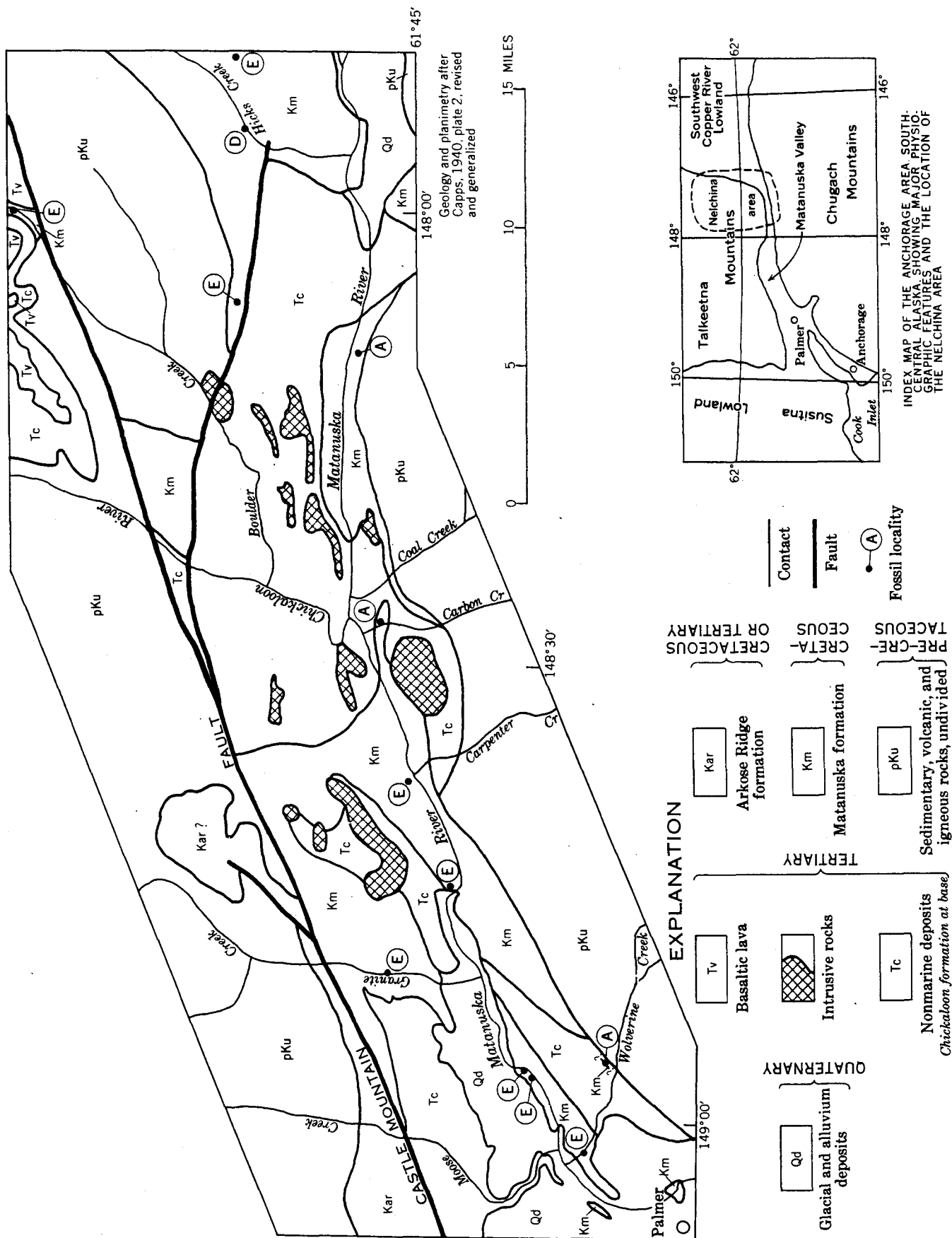


Figure 159.1.—Generalized geologic map of the Matanuska Valley, Alaska, showing Cretaceous fossil localities; these are indicated by letters which correspond with fossil assemblages listed in table 159.1.

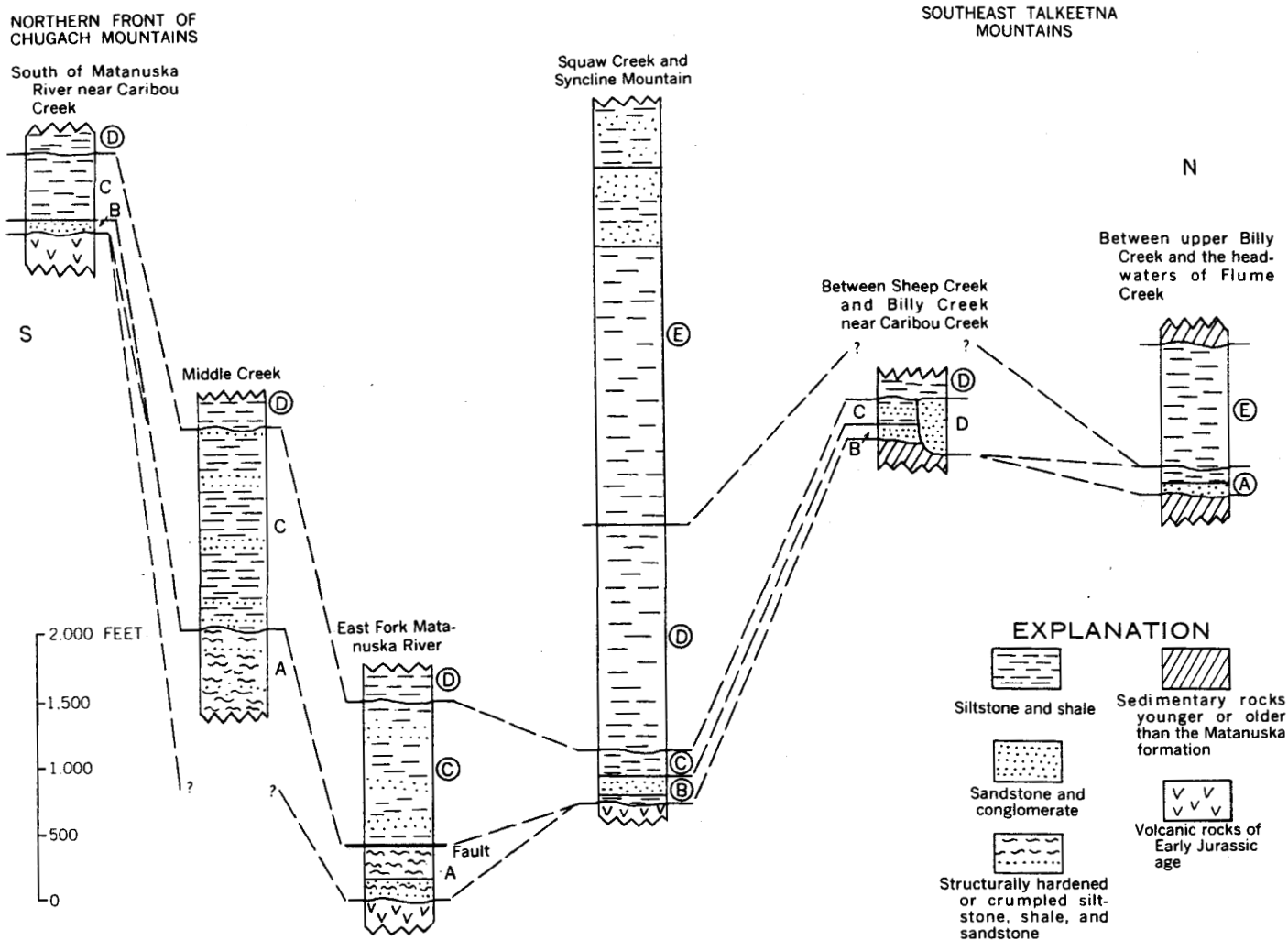


FIGURE 159.2.—Schematic columnar sections of the Matanuska formation, Nelchina area, Alaska. Letters correspond with fossil assemblages listed in table 159.1. Circled letters indicate lithogenetic units from which critical fossils were collected. Uncircled letters indicate lithogenetic units correlated on the basis of lithology.

tive along the Chugach Mountains but not in the northern Nelchina area. This deformation occurred before the overlying Cenomanian to Maestrichtian rocks were deposited.

The structural contrasts in the Albian sedimentary rocks, the rapid coarsening and other changes in the lithology of Cenomanian and Turonian sedimentary rocks in approaching the north front of the Chugach Mountains, and the absence of Bajocian to Valanginian beds in the south part of the Nelchina area suggest that during post-Valanginian Cretaceous time and much of Matanuska time the area of the northern Chugach Mountains was positive and contributed sediment to the Matanuska formation. A more important source of sediment, however, and probably a larger landmass, lay to the north of the Nelchina area.

TABLE 159.1.—Fossil assemblages and critical fossils found in the Matanuska formation

Lithologic unit	Age and fossils
E	Upper Campanian and Maestrichtian (?)
	<i>Pachydiscus</i> ( <i>Neodesmoceras</i> ) n. sp.
	<i>Pachydiscus ootacodensis</i> (Stoliczka)
	<i>Pachydiscus</i> n. sp.
	<i>Pseudophyllites indra</i> (Forbes)
	<i>Baculites occidentalis</i> Meek
	<i>Baculites</i> n. sp.
	<i>Didymoceras hornbyense</i> (Whiteaves)
	<i>Diplomoceras notabile</i> Whiteaves
	<i>Inoceramus subundatus</i> Meek
D	Campanian
	<i>Inoceramus schmidt</i> Michael
	<i>Anapachydiscus</i> sp.
	<i>Helcion</i> cf. <i>H. giganteus</i> Schmidt

TABLE 159.7.—Fossil assemblages and critical fossils found in the Matanuska formation—Continued

Lithologic unit	Age and fossils
C	Turonian
	<i>Inoceramus</i> aff. <i>I. corpulentus</i> McLearn
	<i>Sciponoceras</i> aff. <i>S. bohemicus</i> (Fritsch)
	<i>Inoceramus woodsi</i> Boehm (= <i>Inoceramus costellatus</i> Woods)
	<i>Mesopuzosia indopacifica</i> (Kossmat)
	<i>Tetragonites</i> aff. <i>T. glabrus</i> (Jimbo)
	<i>Inoceramus</i> aff. <i>I. cuvierii</i> Sowerby
	<i>Otoscaphtes puerculus</i> (Yabe)
B	Cenomanian
	<i>Calycoceras</i> sp. indeter.
	<i>Desmoceras</i> ( <i>Pseudouhligella</i> ) <i>japonicum</i> Yabe
	<i>Inoceramus</i> n. sp. aff. <i>I. yabei</i> Nagao and Matsumoto
A	Albian
	<i>Brewericeras hulenense</i> (Anderson)
	<i>Freboidiceras singulare</i> Imlay
	<i>Beudanticeras glabrum</i> (Whiteaves)
	<i>Lemuroceras</i> sp.

Because of the northward coarsening in some units, the northward thinning and overlapping of others, and the beach deposits and coal in the basal Albian deposits of the northern Nelchina area, it seems likely that the

north edge of the Matanuska seaway was not far beyond the present northern limit of the Matanuska formation in the Nelchina area.

The Matanuska formation underlies a part of the Cook Inlet lowland and much of the southern Copper River lowland. Since the formation is very thick (see fig. 159.2), consists predominantly of dark-gray marine siltstone and shale, and contains abundant mollusks, foraminifers, and radiolaria in many beds, it may be a source of petroleum in the Cook Inlet and Copper River lowlands. In the Nelchina area, however, preliminary tests of porosity and permeability based on a few samples collected at the surface suggest that reservoir rocks may not be abundant even among the beds of sandstone and conglomerate which occur in the formation there at many levels.

## REFERENCES

- Capps, S. R., 1940, Geology of the Alaska Railroad region: U.S. Geol. Survey Bull. 907, 201 p.
- Martin, G. C., 1926, The Mesozoic stratigraphy of Alaska: U.S. Geol. Survey Bull. 776, 493 p.
- Martin, G. C., and Katz, F. J., 1912, Geology and coal fields of the lower Matanuska Valley, Alaska: U.S. Geol. Survey Bull. 500, 98 p.



## 160. RADIOCARBON DATES RELATING TO THE GUBIK FORMATION, NORTHERN ALASKA

By HENRY W. COULTER, KEITH M. HUSSEY, and JOHN B O'SULLIVAN, Washington, D.C., Iowa State University, Ames, Iowa, and Iowa State University, Ames, Iowa

Radiocarbon dates indicate that deposition of the upper member of the Gubik formation near Barrow was initiated prior to 38,000 years B.P. and was terminated prior to 9,100 years B.P. In the eastern part of the Arctic coastal plain province the Quaternary Gubik formation, consisting of as much as 150 feet of unconsolidated marine and nonmarine gravel, sand, silt, and clay, unconformably overlies the Upper Cretaceous Colville group (Miller, Payne and Gryc, 1959, p. 106). Near Barrow the upper member of the formation comprises 15 to 25 feet of tan, fine-grained sand with cross-bedded gravel lenses and contains an extensive marine fauna.

A log (sample W-380) from the base of the upper member of the Gubik formation has been dated at greater than 38,000 years. Although not found in

growth position the log showed no evidence of the degree of abrasion which would be expected if it had been successively buried, uncovered, and redeposited. Furthermore, the unweathered condition of the wood suggests that it did not remain long at the surface prior to burial. Consequently, the log cannot predate the enclosing deposits by more than a relatively short period and deposition of the basal sediments must have begun more than 38,000 years ago.

Bedded lacustrine silt, deposited in thaw-lake basins, overlies the upper member of the Gubik formation in many localities near Barrow. Pits dug in the bottom of an artificially drained lake basin 4 miles south of Barrow show two peat-bearing beds in lacustrine silt, one 12 inches and the other one 44 inches below the top of the lake deposits. Radiocarbon age determinations



on samples from these two beds give dates of  $3,540 \pm 300$  years (W-432) and  $9,100 \pm 260$  years (W-847) respectively. Therefore, the uppermost beds of the Gubik formation were deposited more than 9,100 years ago.



# 161. METASEDIMENTARY ROCKS IN THE SOUTH-CENTRAL BROOKS RANGE, ALASKA

By WILLIAM P. BROSGÉ, Menlo Park, Calif.

Devonian and older metasedimentary rocks and post-Devonian mafic intrusive rocks form most of the southern Brooks Range in the John River-Wiseman area (fig. 161.1). The Lisburne group and Kayak shale of Mississippian age and the Kanayut conglomerate, in contact with the underlying sandstone of Late Devonian age, occur only near the crest of the range. The Kanayut conglomerate wedges out southward beneath Mississippian rocks. South of the crest a thick unit of black slate and phyllite lies beneath the Upper Devonian sandstone and rests with apparent conformity on the Skajit limestone and with apparent unconformity on Middle(?) Devonian and older chloritic to calcareous schists, chloritic phyllites, black siltstones and limestones.

Although the Skajit limestone has been referred to the Silurian (Schrader; Smith and Mertie), in the type area on the John River it seems related to limestone that is locally interbedded in the basal part of the black slate and phyllite unit and that contains fossils of Middle(?) Devonian age. Furthermore, fossils of Middle or Late Devonian age were collected by I. L. Tailleux (personal communication, 1955) in the Western Brooks Range from limestone which had been mapped as Skajit by Smith and Mertie (1930). The black slate-phyllite unit that overlies the Skajit limestone is correlated tentatively with black mica schist that overlies interbedded marble and calcareous schist in a belt south of the outcrop belt of typical Skajit limestone. A previously unmapped thick silty limestone may be the youngest unit beneath the unconformity.

The metamorphic grade of the rocks near the crest of the range increases southward, from slate to schist of the greenschist facies. Farther south the metamorphic

grade decreases sharply to slate and phyllite in the south front of the range.

A belt of Jurassic(?) and Cretaceous graywacke, conglomerate, shale, chert, and mafic igneous rocks lies south of the range and pinches out eastward. Schist pebbles in the graywackes show pre-middle Cretaceous metamorphism.

Granite, granodiorite, and granite gneiss intrude the northern part of the schist belt in the Chandalar Lake area (fig. 161.1). Most of the known metal prospects and zones of silicification lie in the schist belt near the granite and along a line between the granite near Chandalar Lake and an uninvestigated granite on the Alatna River to the west. Lode gold occurs near Chandalar Lake, stibnite and some copper sulfides occur near Wiseman, and small amounts of copper sulfides are common in breccia beneath the Skajit limestone from Wild Lake to the John River.

In addition, copper sulfides occur on the West Fork of Chandalar River in mafic igneous bodies in the Mesozoic rocks. Analyses of stream sediments show a slight concentration of copper around the mafic intrusive rocks at Mount Doonerak and Boreal Mountain, and a marked concentration of zinc at Cladonia Creek.

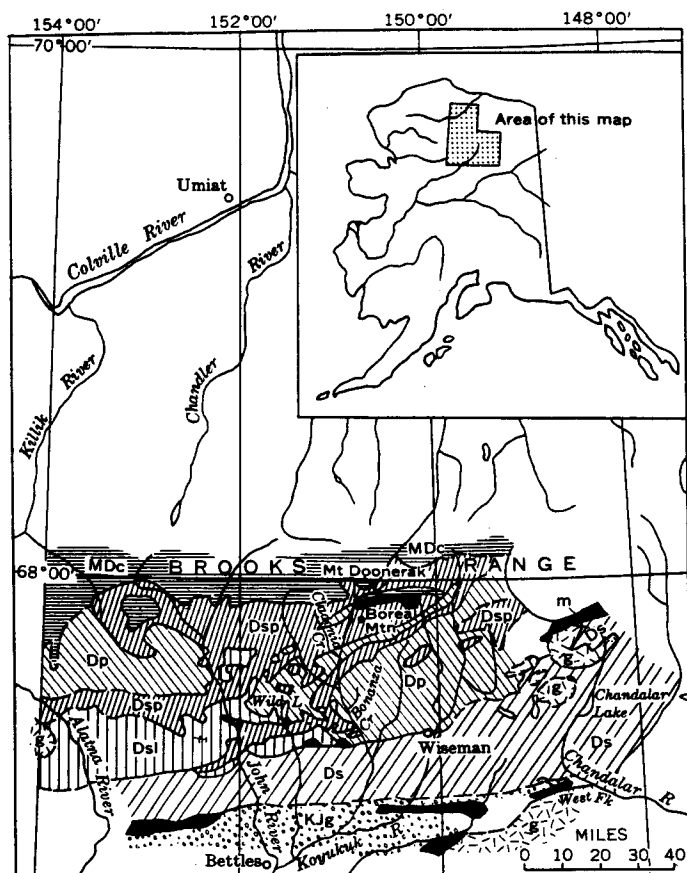
Cymrite was identified by X-ray diffraction analysis in samples collected from a pyritized zone near the head of Bonanza Creek in the Wiseman quadrangle. This is the first known United States occurrence of that rare barium silicate mineral.

## REFERENCES

- Schrader, F. C., 1902, A reconnaissance in Northern Alaska: U.S. Geol. Survey Prof. Paper 20, 139 p.  
 Smith, P. S., and Mertie, J. B., Jr., 1930, Geology and mineral resources of northwestern Alaska: U.S. Geol. Survey Bull. 815, 351 p.

## REFERENCE

- Miller, D. J., Payne, T. G., and Gryc, George, 1959, Geology of possible petroleum provinces in Alaska: U.S. Geol. Survey Bull. 1094, 131 p.



## EXPLANATION

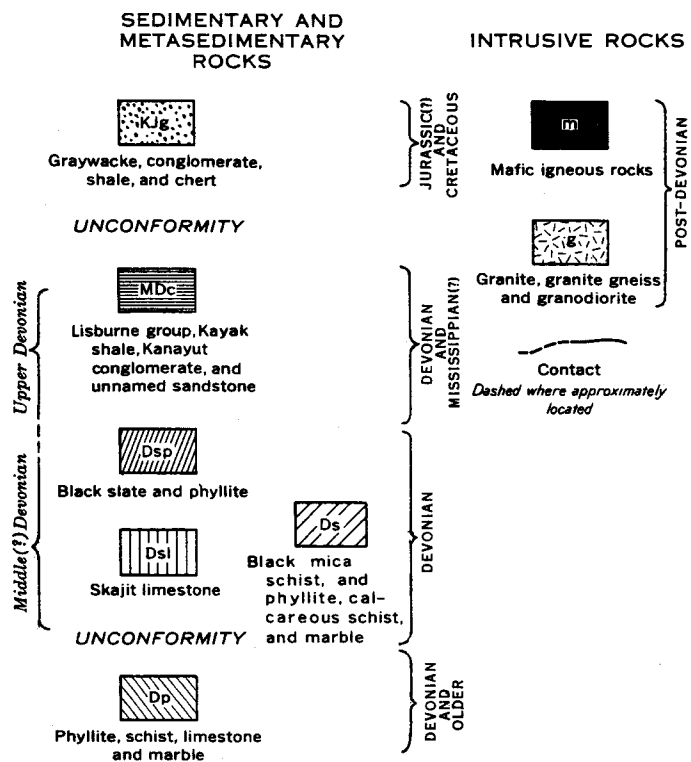


FIGURE 161.1.—Generalized geologic map of the south-central Brooks Range. Inset map shows location in Alaska.

## 162. SLUMP STRUCTURES IN PLEISTOCENE LAKE SEDIMENTS, COPPER RIVER BASIN, ALASKA

By DONALD R. NICHOLS, Washington, D.C.

*Work done in cooperation with Office, Chief of Engineers*

Various types of contorted bedding occur in horizontal zones in thin-bedded Pleistocene lake deposits in the Copper River Basin, Alaska. The zones are generally 1 to 5 feet thick and contain folded and sometimes faulted beds of sand, silt, clay, and locally one or more thin beds of volcanic ash that have been faulted and folded. A zone may persist throughout an exposure, but none can be identified in more than one exposure. Two types of contortion, described below, are attributed to slumping generated by earthquakes.

Highly deformed beds lying between undisturbed lake sediments are exposed on the east bank of the Tonsina River, 2 miles south of the Upper Tonsina bridge (fig. 162.1). Both disturbed and undisturbed beds consist mainly of finely laminated, rhythmically bedded sand, silt, and clay, and each bed includes thin layers of white volcanic ash. Intensity of deformation is uniform throughout any vertical section of the contorted zone, which has sharp upper and lower boundaries. Folds generally are tight, commonly are recumbent, and in places are fanshaped. Most of the faults

are normal, but some are low-angle thrusts; displacement generally is along the axial plane of folds, which dip in random directions.

The excellent preservation of bedding in the lake sediments at this locality indicates considerable compaction. Subsequent deformation either broke the beds into tabular fragments or crinkled them by plastic-fluid flow (fig. 162.1); graded bedding or other evidence of density currents in these materials is lacking. The abrupt termination of folds and faults at the base and top of the zone, together with a lack of soil horizons, excludes glacier overriding, iceberg drag, and frost action as causes of deformation. The contorted beds probably were not transported far; their character suggests that they had the same depositional environment as the undisturbed beds. It seems probable, from the character and composition of the contorted beds, that the deformation was caused by subaqueous sliding of a discrete upper zone of coherent sediment over a gently sloping bed of "fatty" clay that served as a lubricant.

Mendenhall (1905, pl. 9-B and p. 66) described laminated and folded lake silt exposed in a bluff on the Tazlina River, 1 mile above its mouth. He attributed these structures to drag of floating icebergs on the lake bottom or to overriding of glacier ice. The deformed silt and overlying deposits were observed by the author to terminate upstream in a newly exposed, nearly vertical contact with a mass of till. The till, which rises 60 feet above river level, probably formed a subaqueous or subaerial escarpment. The character of the contact suggests that the folds, which gradually diminish in intensity downward and downstream, were developed by subaqueous sliding generated by lateral compression of silt that was displaced when some of the till slumped to the base of the bluff—perhaps during an earthquake. Till blocks in the troughs of some of the folds were probably dislodged contemporaneously to form load casts.

Seismic activity presumably accompanied widespread volcanism to the east, which produced andesite flows, volcanic mud flows, and ash deposits interbedded with Pleistocene glacial and lacustrine deposits in the Copper

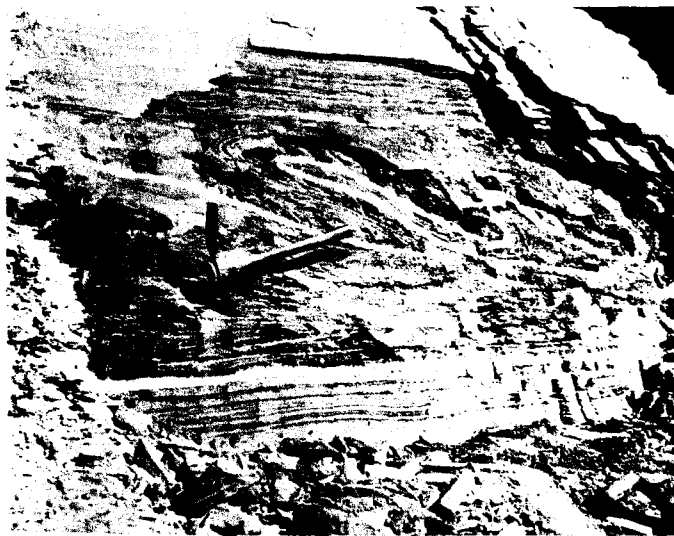


FIGURE 162.1.—Compacted strength of lake sediments and included white ash beds is shown by the excellent preservation of bedding after strong folding and faulting. Contorted zone lies between undisturbed varvelike beds.

River Basin (summarized by Nichols and Yehle, 1960).

Earthquakes as far distant as the Yakutat disturbance of July 1958 have caused bluff debris to cascade onto flood plains. Earthquakes provide an ideal mechanism for triggering subaqueous slides, and they probably were the cause of many types of slump structures.

#### REFERENCES

- Mendenhall, W. C., 1905, *Geology of the Copper River region, Alaska*: U.S. Geol. Survey Prof. Paper 41, 133 p., 20 pls., 11 figs.
- Nichols, D. R., and Yehle, L. A., 1960, *Mud volcanoes in the Copper River Basin, Alaska*: Proc. 1st Internat. Symposium on Arctic Geology, Calgary, Alberta. (in press)



## GEOPHYSICS

## 181. RATE OF MELTING AT THE BOTTOM OF FLOATING ICE

By DAVID F. BARNES and JOHN E. HOBBIE, Menlo Park, Calif., and Arctic Institute of North America, Bloomington, Ind.

*Work done in cooperation with the Arctic Institute of North America, the Air Force Cambridge Research Center, and the Office of Naval Research*

The ice sheets covering Arctic lakes and seas have an important influence on both the surficial geology and the climate of their environment. Yet the influence of the underlying water on the thickness and duration of these ice sheets has received little attention, although important effects are sometimes attributed to small changes in water temperature. Research on the thermal regimen and physical properties of a melting ice sheet at Lake Peters, Alaska, provided an opportunity to study the effect of a deep, current-free body of fresh water on an overlying sheet of ice.

At Lake Peters a nearly continuous record was maintained of the micrometeorological and limnological factors influencing ice melt. The study began early in May, when the temperature of the 6-foot-thick ice cover was still below freezing, and ended in the last week of July, when the last ice melted off the lake. The rate of melting at the bottom of the ice sheet was obtained by freezing translucent plastic horizon markers into the ice early in the season and measuring their distances from the top and bottom of the ice sheet at 4-day intervals during the melting season. Many of these markers were originally attached to white wooden poles, but these poles absorbed so much solar radiation that they became loose midway in the season. Another marker, however, attached to a white wire, persisted nearly throughout the melting season. Because of the loosening of the markers and the unevenness of the top and bottom ice surfaces, there is considerable scatter in the measurements. Nevertheless the data indicate that not more than a few centimeters melted from the bottom of the ice sheet during the entire melting season.

This small amount of melting is consistent with the thermal gradients measured in the water beneath the ice. Water temperatures at various depths in the lake were determined at frequent intervals with a small thermistor probe lowered into the lake. Four curves obtained at the middle of Lake Peters during the melting season are shown in figure 181.1. The three early-sea-

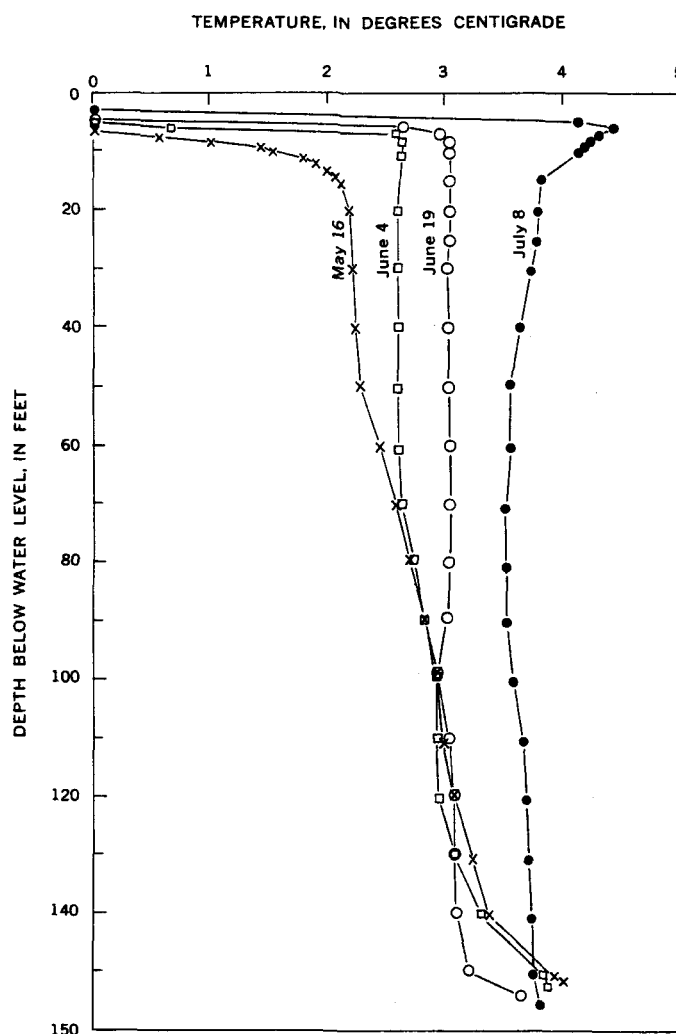


FIGURE 181.1.—Water temperature versus depth curves from Lake Peters, 1959.

son curves show a well-mixed constant-temperature layer which grows warmer and thicker as the season progresses. The temperature gradient beneath the ice may be computed for the early part of the melting season, during which this constant-temperature layer is

developing, but the proposed theory does not give the gradient in the later part of the melting season.

The water temperature is below the maximum-density point, and the well-mixed layer can be created by warming the water just beneath the ice so that it sinks and creates convection. Solar radiation penetrating the ice is the major source of heat for the lake water before mid-June, when rivers begin to flow and a shoreline moat develops. The heat radiated into the well-mixed layer is transferred downward by convection. Above the well-mixed layer is a thin, stably stratified boundary layer where the absorbed radiant heat is transferred upward by conduction. This is the heat that causes melting at the bottom of the ice, and its source is solar radiation.

Because the convective processes in the well-mixed layer are very slow, we may assume that almost no heat is transferred from this layer to the boundary layer. The thermal processes in the stable boundary layer may then be expressed mathematically for steady-state conditions by the equation:

$$(1) \quad Lm = K \frac{\partial v}{\partial x} \bigg|_{x=0} = I_0(1 - e^{-\eta h})$$

where  $L$  is the latent heat of ice,  $m$  the mass of ice melted per unit time and area,  $K$  the thermal-conductivity of water,  $v$  the temperature at depth  $x$  below the bottom of the ice,  $I_0$  the solar radiation that enters the water,  $\eta$  the extinction coefficient of water, and  $l$  the thickness of the stable boundary layer. This equation does not take into account the heat transferred upward by a thermal gradient within the ice. Measurements reveal, however, that during the melting season such gradients are negligible. During the winter and before the melting condition is established the right-hand side of equation (1) gives the heat which is supplied to the ice by the water and which tends to reduce the amount of new ice formed by a thermal gradient in the ice. It thus furnishes a correction for Stefan's (1889) formula for ice growth.

Equation (1) shows that in the absence of currents the heat available for melting ice cannot exceed the radiation reaching the lake water. At Lake Peters the solar radiation at the top of the ice was about 700 cal per cm<sup>2</sup> per day, but less than  $\frac{1}{10}$  of this passed through the ice. In the following paragraphs we show that only about  $\frac{1}{5}$  of the radiation reaching the water was absorbed in the stable boundary layer and caused melting of the ice.

The thickness of the boundary layer,  $l$ , may be obtained by integrating

$$(2) \quad \frac{\partial^2 v}{\partial x^2} = -\frac{\eta I_0}{K} e^{-\eta x}$$

Using the boundary conditions  $x=l$ ,  $\frac{\partial v}{\partial x}=0$  and  $x=0$ ,  $v=0$  we get:

$$(3) \quad v = \frac{I_0}{\eta K} - \frac{I_0}{\eta K} e^{-\eta x} - \frac{I_0 x}{K} e^{-\eta l}$$

which gives the water temperature at any depth in the boundary layer. Since the temperature at the base of the boundary layer ( $x=h$ ) is  $v=T$ , the temperature of the mixed layer, we get:

$$(4) \quad (1 + \eta h) e^{-\eta l} = 1 - \frac{\eta K T}{I_0}$$

which defines  $\eta l$  as a function of  $\frac{\eta K T}{I_0}$ . Figure 181.2 shows the relation between  $\frac{\eta K T}{I_0}$  and both  $\eta h$  and  $(1 - e^{-\eta h})$ . The latter gives from equation (1) the proportion of radiation that goes into melting ice. The dashed line in figure 181.2 shows an approximation that leads to:

$$(5) \quad Lm \approx 1.4 \sqrt{\eta K T I_0}$$

which shows that  $T$ , and  $I_0$  all have an equal effect on the rate of melting. However, solar radiation and water transparency are more variable and cause greater variations in melting rate.

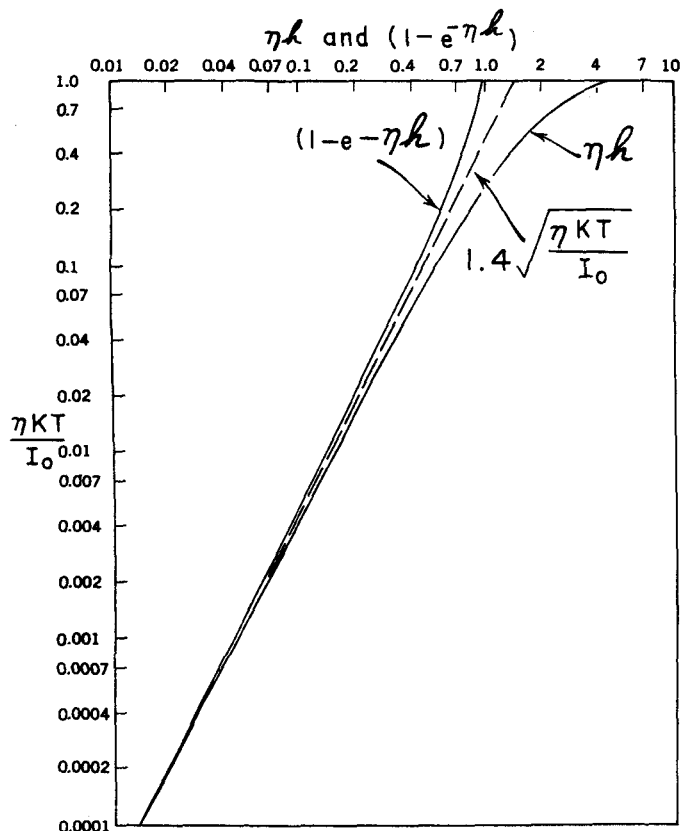


FIGURE 181. 2.—Relationship between  $\frac{\eta K T}{I_0}$  and both  $\eta h$  and  $(1 - e^{-\eta h})$ .

Sufficient data were obtained at Lake Peters to check the reliability of these formulas. The values of  $L$  and  $K$  are well known; they are about 80 cal/gm and 0.0013 cal °C<sup>-1</sup> cm<sup>-1</sup> sec<sup>-1</sup> respectively. The values of  $T$  and  $h$  may be obtained by plotting water temperature against depth. The extinction coefficient  $\eta$  and solar radiation  $I_0$  were measured with a submarine photometer. Some uncertainty is involved in the photocell calibration, which depends on both the spectral distribution and the angular incidence of radiation at the point of measurement. However, an analysis of data obtained from Moon (1940), Lyons and Stoiber (1959), and the photocell manufacturer has provided a calibration factor which is also supported by computations of water-heat increments from the temperature-depth curves. The extinction coefficient varied from 0.002 cm<sup>-1</sup> to 0.005 cm<sup>-1</sup>, and we used an average value of 0.003 cm<sup>-1</sup>.

In the early part of June the radiation penetrating the ice was about 63 cal/cm<sup>2</sup>/day, or 0.0007 cal/cm<sup>2</sup>/sec, and the temperature of the mixed layer was about 3° C. From figure 181.2 these values give a boundary-layer thickness of about 67 cm, which is very close to the measured value of a little more than 60 cm. The calculated heat flow to the overlying ice is about 10 cal per day, which implies an ablation rate of about one centimeter per week. This agrees well with the measured ablation data.

The variation of temperature with depth in the boundary layer may best be measured early in the season, when the boundary layer is thicker than it is later on when there is no snow cover to absorb radiation. The May 16 temperature curve in figure 181.1 was obtained under snow-covered ice, and figure 181.3 shows how well the data from the upper part of this curve agree with a theoretical curve obtained by using an  $I_0$  of 0.00004 in equation (3). No radiation measurements were made on May 16, but a value of 0.00004 is consistent with a value measured a few days later.

These formulas seem to provide a reliable method for estimating the steady-state, under-ice thermal gradient during the freeze-up, winter, and early melting season. They do not take account of turbulent heat transfers resulting from water currents or ice drift. Later in the melting season (after mid-June at Lake Peters in 1959 when the ice was about four feet thick) such turbulent transfers may become important. Furthermore, when

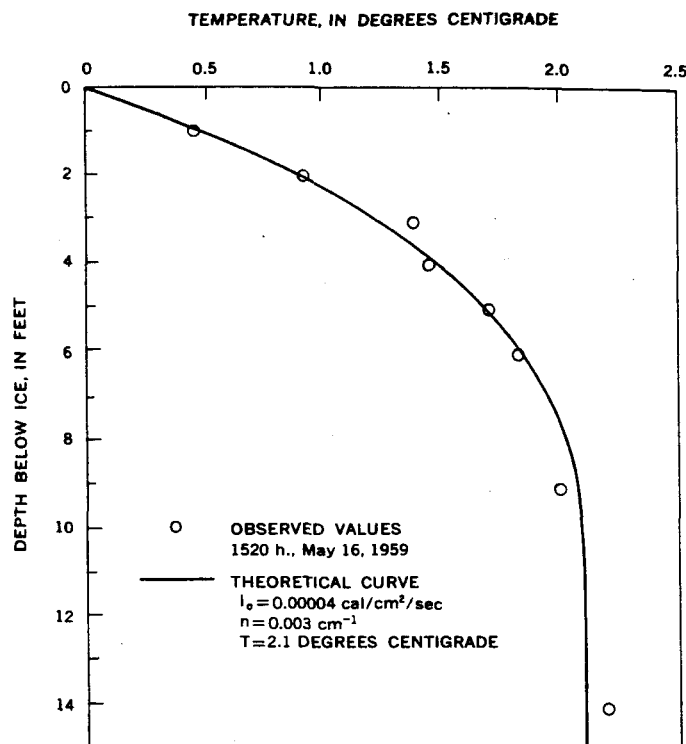


FIGURE 181.3.—Comparison of observed and theoretical water temperatures beneath Lake Peters ice on May 16, 1959.

the water temperature approaches the maximum density value of 4°C small variations in salinity become important, and layers of warmer, fresher water (Birge, 1910) may develop beneath the ice, as shown in the July 8 curve of figure 181.1. Analyses of the Lake Peters thermal data for this portion of the melting season are not complete, but the ablation-marker data show that the rate of melting at the bottom of the ice did not exceed 1 cm per week before the last week of the melting season.

#### REFERENCES

- Birge, E. A., 1910, The apparent sinking of ice in lakes: *Science*, v. 32, p. 81-82.
- Lyons, J. B., and Stoiber, R. E., 1959, The absorptivity of ice: A critical review: Scientific Report No. 3, Dartmouth College, Contract AF 19(604)-2159, Oct. 31, 1959, AFRCR-TN-59-656.
- Moon, Parry, 1940, Proposed standard solar-radiation curves for engineering use: *Jour. Franklin Inst.*, v. 230, no. 5, p. 583-618.
- Stefan, Julius, 1889, Über die Theorien des Eisbildung insbesondere über die Eisbildung in Polarmeere: *Wien Sitzungsber. Akad. Wiss., A*, v. 42, pt. 2, p. 965-83.